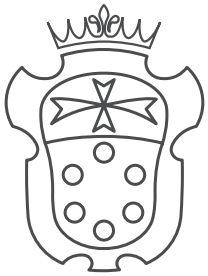

SCUOLA
NORMALE
SUPERIORE

Classe di Scienze

Corso di perfezionamento in Matematica

XXXV ciclo

L-spaces and taut foliations on 3-manifolds

Settore Scientifico Disciplinare **MAT/03**

Candidato
dr. Diego Santoro

Relatori

Prof. Paolo Lisca
Prof. Bruno Martelli

Supervisione interna

Prof. Angelo Vistoli

Anno accademico 2022–2023

Contents

Introduction

This thesis can be roughly divided in two parts. The first part takes up most of the thesis. It comprises Chapters $1-2-3$ and concerns the study of the so-called L-space conjecture for manifolds that arise as surgeries on fibered hyperbolic two-bridge links. The material there presented is based on the papers [98] and [99].

The second part of the thesis is the content of Chapter 4. It is based on a joint work with Ludovico Battista and Leonardo Ferrari [3] where, addressing a conjecture by LeBrun [69] on Seiberg-Witten invariants of hyperbolic 4-manifolds, we studied L-spaces among some hyperbolic 3-manifolds with particularly nice geometric properties.

We now proceed to a more detailed introduction to the thesis and to the mathematical concepts contained therein.

The L-space conjecture

The L-space conjecture is a conjecture in 3-manifolds theory and is a driving force in modern research within low-dimensional topology. It predicts a way to organise closed, connected, oriented 3-manifolds according to their "complexity", which can be measured in three, conjecturally equivalent, ways. The three properties that should formalise the notion of complexity belong to areas of low-dimensional topology that, at least apparently, seem to have very little in common. We now introduce the properties involved in the conjecture.

Taut foliations

The idea of using codimension one objects to study the topology of a 3-manifold is classical: for instance, Alexander proved the irreducibility of $\mathbb{R}^3$ by exploiting the decomposition of $\mathbb{R}^3 = \mathbb{R}^2 \times \mathbb{R}$ in horizontal planes $\cup_{t\in\mathbb{R}}\mathbb{R}^2 \times \{t\}$. This decomposition provides the easiest example of foliation and we denote it by $\mathcal{F}_{std}$. A (codimension-1) foliation $\mathcal{F}$ of a closed orientable 3-manifold M is a decomposition of M into disjoint, injectively immersed, connected surfaces (called leaves) so that the pair $(M, \mathcal{F})$ is locally isomorphic to $(\mathbb{R}^3, \mathcal{F}_{std})$. It is of course possible to require various degrees of regularity of these local isomorphisms; we will be mainly working with the class of $C^{\infty,0}$-foliations.

This roughly means that the leaves are smoothly immersed and that the tangent planes to the leaves define a continuous subbundle $T\mathcal{F}$ of TM. We will give more details on this in Chapter 2. We consider coorientable foliations, i.e. those that have orientable normal line bundle $TM/T\mathcal{F}$. Since M is orientable, this is equivalent to asking that $T\mathcal{F}$ is orientable as a plane bundle.

From now on, unless otherwise stated, manifolds are connected and orientable, and foliations are coorientable.

Of course the definition of foliation can be extended to every dimension and codimension, and in general it is not true that every n-manifold admits a codimension-k foliation. For example, it is not difficult to show that if an orientable surface admits a coorientable foliation by lines, then it must be diffeomorphic to the 2-dimensional torus. From this point of view, dimension 3 is quite special, since we have the following theorem by Lickorish:

Theorem 0.0.1 ([74])**.** *Every closed orientable* 3*-manifold* M *supports a coorientable (codimension-*1*) foliation.*

Therefore, asking for a coorientable foliation on a 3-manifold M does not impose any restriction on the topology of M. Nevertheless, the foliations provided by the proof of Theorem 0.0.1 all contain *Reeb components*.

Example 0.0.2. (Reeb component, see [15, Example 1.1.12]) Consider the submersion

$$f : \mathbb{R}^2 \times \mathbb{R} \to \mathbb{R}$$
$$f(r, z, t) = (r^2 - 1)e^t$$

where (r, z) are polar coordinates on $\mathbb{R}^2$ and the t-coordinate parametrises the third $\mathbb{R}$-factor. Since f is a smooth submersion, the implicit function theorem implies that by considering the fibers of f we obtain a (C^∞) codimension-1 foliation of $\mathbb{R}^2 \times \mathbb{R}$. We restrict this foliation to a foliation $\hat{\mathcal{F}}$ of $\mathbb{D}^2 \times \mathbb{R}$, where $\mathbb{D}^2 \subset \mathbb{R}^2$ is the set of points with norm less than or equal to one. Observe that the boundary of $\mathbb{D}^2 \times \mathbb{R}$ is a leaf of this foliation and that translations along the t-component permute the leaves of $\hat{\mathcal{F}}$. Therefore this foliation projects to a foliation $\mathcal{F}$ of the solid torus with the property that the boundary is a leaf and all the leaves in the interior are planes, that wind out asymptotically toward the boundary. A solid torus foliated in this way is a Reeb component. See Figure 1 for a picture.

Hence, the first step toward a definition of "complexity" from the point of view of foliation theory can be that of asking for *Reebless foliations*, i.e. foliations without Reeb components.

Indeed, supporting a (coorientable) Reebless foliation forces topological restrictions on M.

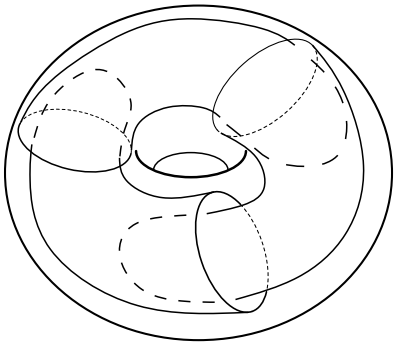

Figure 1: A Reeb component.

Theorem 0.0.3 ([83, 97, 90])**.** *Let M be a closed manifold not diffeomorphic to $S^2 \times S^1$ and suppose that M supports a Reebless foliation $\mathcal{F}$. Then*

- *the leaves of $\mathcal{F}$ are π_1-injective;*
- *M is irreducible (i.e. every embedded 2-sphere in M bounds an embedded ball);*
- *the universal cover of M is diffeomorphic to $\mathbb{R}^3$*

The definition of taut foliation generalises that of Reebless foliation.

Definition 0.0.4. A foliation $\mathcal{F}$ on M is taut if every leaf intersects a closed transversal.

In this definition, by closed transversal we refer to a smooth simple closed curve in M that is everywhere transverse to the leaves of $\mathcal{F}$.

Remark 0.0.5. If a foliation $\mathcal{F}$ contains a Reeb component, then it cannot be taut. In fact it is not difficult to see that there exist no closed transversals intersecting the boundary of the Reeb component.

We point out that as a consequence of the Theorem 0.0.3, a closed orientable 3-manifold with finite fundamental group cannot support a coorientable taut foliation.

Corollary 0.0.6. *The 3-sphere, lens spaces, and more generally any M with finite fundamental group, do not support coorientable taut foliations.*

Taut foliations have been extensively studied and they can be used to deduce important topological properties of the ambient manifold. Notably, Thurston [111] proved that compact leaves of taut foliations are genus minimising in their homology classes, and Gabai [38] proved that the converse holds: if S represents a non-trivial element in $H_2(M, \mathbb{R})$, where M is irreducible, and it is genus minimising in its homology class, then S is the leaf of a coorientable taut foliation. In particular Gabai's result implies:

Theorem 0.0.7 ([38])**.** *Every closed irreducible M with $b_1(M) > 0$ supports a taut foliation.*

This theorem of Gabai implies that in some sense taut foliations are quite common. In fact a lot of work had to be done to prove the existence of hyperbolic 3-manifolds not supporting taut foliations. The first examples are due to Roberts-Shareshian-Stein [96].

Some years later, many other examples were found by using techniques coming from Heegaard Floer homology.

Heegaard Floer homology

Heegaard Floer homology was introduced by Ozsváth and Szabó in [87] . It consists of a package of topological invariants associated to closed oriented 3-manifolds and in its simplest form it associates to a 3-manifold M an abelian group of finite rank denoted by $\widehat{HF}(M)$.

The definition of the Heegaard Floer homologies is very complicated and uses ideas coming from symplectic topology and the study of lagrangians submanifolds in symplectic manifolds. Roughly speaking, $\widehat{HF}(M)$ is the Lagrangian Floer homology associated to a pair of lagrangian tori in the g-fold symmetric product of the surface of genus g. These tori are obtained from the attaching circles of a Heegaard decomposition of M of genus g, i.e. a decomposition of M into two handlebodies of genus g. For the purposes of this thesis, no knowledge of all this machinery is needed. What we want to stress is that the setting in which these invariants are defined is analytic: elliptic operators and indices of Fredholm operators are involved. This theory has now found many important and profound applications in low dimensional topology (see [52] and [50] for some examples) and so it is intriguing to give new interpretations to these invariant in topological, geometrical or algebraic terms.

In [86, Proposition 5.1] Ozsváth and Szabó observed the following

Proposition 0.0.8. *Let M be a rational homology sphere. Then* $\mathrm{rk}\widehat{HF}(M) \geq |H_1(M,\mathbb{Z})|$.

Definition 0.0.9. A rational homology sphere M is an L-space if $\widehat{HF}(M)$ is a free abelian group with $\mathrm{rk}\widehat{HF}(M) = |H_1(M,\mathbb{Z})|$.

Therefore L-spaces are rational homology spheres with minimal Heegaard Floer homology. Examples of L-spaces are S^3, lens spaces or more generally:

Proposition 0.0.10. ([88, Proposition 2.2]). *Every M with finite fundamental group is an L-space.*

By comparing this proposition with Corollary 0.0.6, we see that manifolds with finite fundamental groups are "simple" both from the point of view of Heegaard Floer homology and foliation theory. This analogy is not a coincidence:

Theorem 0.0.11 ([85])**.** *If M is an L-space, then M does not support coorientable taut foliations.*

Remark 0.0.12. We point out that the previous theorem is based on a result by Eliashberg-Thurston [33] whose proof assumes the foliation to be at least of regularity C^2. Later, the result by Eliashberg-Thurston was generalised independently by Bowden [5] and Kazez-Roberts [54] to $C^{\infty,0}$- and $C^{1,0}$-foliations, respectively. Since every C^0 *topologically* taut foliation is isotopic to a taut $C^{\infty,0}$-foliation, Theorem 0.0.11 holds for this more general class of foliations. See [23], [54] for more details.

Remark 0.0.13. It was already known that manifolds that are *monopole Floer homology L-spaces* do not support coorientable taut foliations [62], see also [60]. Monopole Floer homologies are another package of invariants of 3-manifolds defined by Kronheimer and Mrowka, see [59]. It is now known that these invariants are isomorphic to the Heegaard Floer homologies, [63, 64, 65, 66, 67].

The strength of Theorem 0.0.11 is due to the fact that the class of L-spaces is larger than the class of manifolds with finite fundamental group. One instance of this fact is the following theorem:

Theorem 0.0.14 ([89])**.** *Let K be a non-trivial knot in S^3 and suppose that there exists a rational $r > 0$ such that the r-surgery on K is an L-space. Then the s-surgery on K is an L-space if and only if $s \in [2g(K) - 1, \infty]$.*

In the previous theorem $g(K)$ denotes the genus of K, i.e. the minimal genus of a Seifert surface for K.

Example 0.0.15. Let K be the Pretzel knot $P(-2, 3, 7)$. It has genus 5 and it was shown by Fintushel and Stern [36] that K has positive lens space surgeries; therefore the r-surgery on K is an L-space, for $r \in [9, \infty]$. Since K is hyperbolic, by virtue of the hyperbolic Dehn filling theorem by Thurston [110], all but finitely many of these surgeries on K provide examples of hyperbolic manifolds that do not support coorientable taut foliations.

Left-orderability

The last property involved in the L-space conjecture is stated in terms of fundamental groups. As we have already seen in the previous sections, manifolds with finite fundamental groups are simple from the point of view of Heegaard Floer homology and foliation theory. On the other hand, we have also seen that there are examples of hyperbolic manifolds that are simple from these points of view, thus if the fundamental group has to play a role in this conjecture then it has be involved in a subtler way. The candidate notion of "complexity" is the following:

Definition 0.0.16. A group G is left-orderable if there exists a total order on G that is invariant by left multiplication, i.e. such that $g < h$ if and only if $kg < kh$ for all $k, g, h \in G$.

By convention, the trivial group is *not* left-orderable.

Example 0.0.17. It is not difficult to see that if G is a finite group then G is not left-orderable. Suppose in fact by contradiction that there exists a left-order on G and let $g \neq 1$ be any element in G. Without loss of generality we can suppose that $g > 1$. Then by the definition of left-order we deduce that $g^2 = gg > g > 1$ and by induction we deduce that $g^n > 1$ for all natural n. Since G is finite, there exists n_0 such that $g^{n_0} = 1$ and this leads to a contradiction. More generally, we have just proved that if G has torsion then it is not left-orderable.

Despite the definition of left-orderability of a group G being purely algebraic, this notion can be interpreted in terms of dynamical properties of G:

Theorem 0.0.18. *Let G be a countable group. Then G is left-orderable if and only if there exists an embedding $G \to \mathrm{Homeo}^+(\mathbb{R})$.*

For a proof of the previous theorem, see [19].

When G is the fundamental group of an irreducible 3-manifold this theorem was improved by Boyer, Rolfsen and Wiest.

Theorem 0.0.19 ([9])**.** *Let G be the fundamental group of a closed, orientable, irreducible 3-manifold. Then G is left-orderable if and only if there exists a non-trivial homomorphism $G \to \mathrm{Homeo}^+(\mathbb{R})$.*

The previous theorem is very powerful and gives a very practical way to prove that many 3-manifolds group are left-orderable and we will make use of it in Chapter 3.

The conjecture and some evidences

We are now ready to state the L-space conjecture.

L-space conjecture. ([52, 7]) *For an irreducible oriented rational homology 3-sphere M, the following are equivalent:*

1) M supports a cooriented taut foliation;

2) M is not an L-space, i.e. its Heegaard Floer homology is not minimal;

3) M is left-orderable, i.e. $\pi_1(M)$ is left-orderable.

The equivalence between (1) and (2) was conjectured by Juhász in [52], while the equivalence between (2) and (3) was conjectured by Boyer, Gordon and Watson in [7]. This conjecture predicts strong connections among geometric, dynamical, Floer homological, and algebraic properties of 3-manifolds. Despite its boldness, as a result of the work by many researchers [6, 7, 10, 18, 32, 47, 76] it is now known that the conjecture

holds for graph manifolds, i.e. manifolds whose JSJ decomposition includes only Seifert fibered pieces. Moreover, as we have pointed out in the previous sections, results by Oszváth-Szabó [85], Bowden [5] and Kazez-Roberts [54] imply that in general manifolds supporting coorientable taut foliations are not L-spaces.

Regarding left-orderability, recently Tao Li proved that if M has Heegaard genus two and is left-orderable, then it supports a coorientable taut foliation [72]. On the other hand, if M supports a coorientable taut foliation, there are two natural ways of trying to produce a left-order on $\pi_1(M)$. In fact, there are two actions of $\pi_1(M)$ associated to a coorientable taut foliation. The first one comes from the action on the leaf space $\mathscr{L} = \widetilde{M}/\widetilde{\mathcal{F}}$ of the pullback foliation on the universal cover $\widetilde{M}$ of M.

Theorem 0.0.20 ([46, 90])**.** *Let $\mathcal{F}$ be a coorientable taut foliation on M. Then the leaf space $\mathscr{L}$ of the pullback foliation on $\widetilde{M}$ is a simply-connected, non necessarily Haussdorff,* 1*-manifold.*

Of course the action of the fundamental group of M by deck transformations on $\widetilde{M}$ induces a non-trivial action on $\mathscr{L}$. Since $\mathcal{F}$ is coorientable, $\mathscr{L}$ is orientable and this action is by orientation preserving homeomorphisms. If the leaf space is Haussdorff, then by virtue of Theorem 0.0.19 we can deduce that M is left-orderable. Also in the case when $\mathscr{L}$ is not Haussdorff one can make use of this action: for example, in [117] Zung collapses $\mathscr{L}$ in a $\pi_1(M)$-equivariant way to construct an action on the real line.

The second action follows from a construction of Thurston, see [14], and is an action on S^1. One can then try to lift this action to an action on the real line. This was done, for example, by Hu in [51]. We will also use this method in Chapter 3, where we will add more details to this discussion.

Since the conjecture has been proved for graph manifolds, it is interesting to study the conjecture in the case of hyperbolic manifolds. In this direction, in [117] the conjecture is proved for some manifolds obtained by considering mapping tori of pseudo-Anosov diffeomorphisms of closed surfaces and then by surgering on some collections of closed orbits.

In addition, in [30], the conjecture is tested on a census of more than $300,000$ hyperbolic rational homology spheres and proved for more than 60% of these manifolds.

My contributions

A natural way to investigate this conjecture is by using Dehn surgery descriptions of 3-manifolds. For instance, it is known that if a non-trivial knot K has a positive surgery that is an L-space, then K is prime [57], fibered [42, 82] and strongly quasipositive [48]. Moreover, the r-framed surgery on such a knot K is an L-space if and only if $r \in [2g(K) - 1, \infty]$, where $g(K)$ denotes the genus of K [89]. Taut foliations on manifolds obtained as surgery on knots in S^3 are constructed for example in [94, 95, 29, 28, 58]

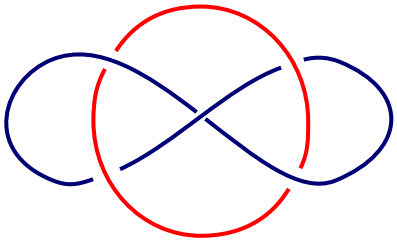

Figure 2: The Whitehead link

and it is possible to prove the left-orderability of some of these manifolds by determining which of these foliations have vanishing Euler class, as done in [51]. Another approach to study the left-orderability of surgeries on knots is via representation theoretic methods, as in [25] and [31].

When it comes to investigate surgeries on links, the story becomes more mysterious. For instance, there is no generalisation of the result of [89] we cited in the previous paragraph – even if it holds in some cases, as we will see in Section 1.2 and Section 1.3. Moreover, links admitting L-space surgeries need not be fibered [78, Example 3.9] nor quasipositive [16, Proposition 1.5]. Concerning foliations, in [53] Kalelkar and Roberts construct coorientable taut foliations on some fillings of 3-manifolds that fiber over the circle and their methods can be applied to surgeries on fibered links as well.

In this thesis we focus our attention on manifolds that can be obtained as surgery on hyperbolic links (recall that the L-space conjecture holds for graph manifolds). A link is said to be hyperbolic if its exterior admits a complete finite volume hyperbolic metric and by virtue of Thurston's hyperbolic Dehn surgery theorem [110], almost every Dehn surgery on a hyperbolic link is hyperbolic.

Fibered hyperbolic two-bridge links.

Our main contribution is the study of the conjecture for fibered hyperbolic two-bridge links. This is an infinite family of two-component links that contains the Whitehead link, the hyperbolic link with two components depicted in Figure 2. This study was carried out in [98] and [99]. Our main result is the following:

Theorem A ([98, 99])**.** *Let L be a fibered hyperbolic two-bridge link and let M be a manifold obtained as Dehn surgery on L. Then M admits a coorientable taut foliation if and only if M is not an L-space.*

Remark 0.0.21. In contrast to the case of knots, the property of being fibered for a link depends on the choice of an orientation of the components of the link. This happens for

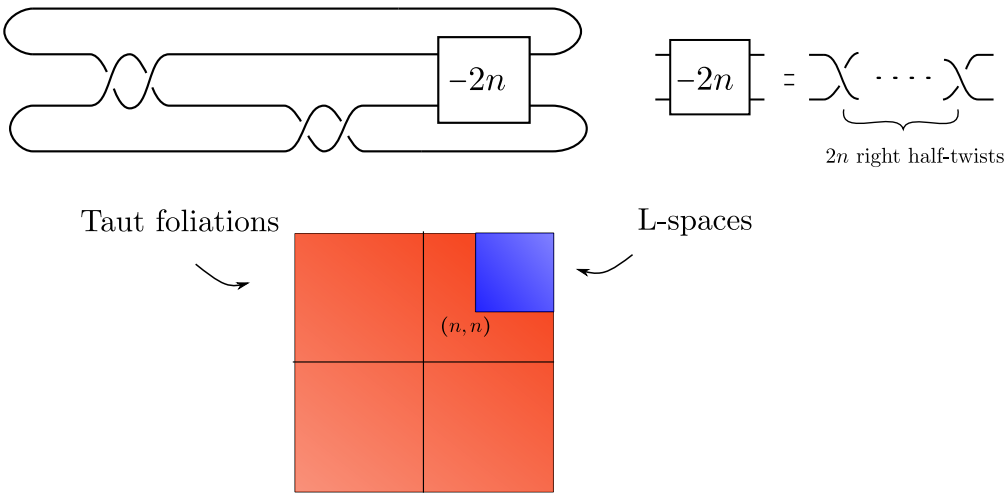

Figure 3: The link L_n. The figure also describes the slopes on the exterior of L_n yielding manifolds that are L-spaces (in blue) and manifolds with coorientable taut foliations (in red).

instance in the case of the $(2, 2n)$ torus link for $n > 1$, see for example [2, Example 3.1]. On the other hand, changing orientations of the components of L has no effects on the study of the L-space conjecture for the surgeries on L. For this reason we will consider links as unoriented and say that a link is fibered if there exists an orientation for which it is a fibered link.

To the best of the author's knowledge, Theorem A provides the first example of the equivalence between conditions 1) and 2) of the conjecture for all manifolds obtained via Dehn surgery on hyperbolic links with at least 2 components.

More precisely, we are able to determine exactly, for each fibered hyperbolic two-bridge link L, the set of surgeries on L that are L-spaces and the set of surgeries that contains coorientable taut foliations. We denote with $\mathcal{L}(L)$ the set of slopes on L that produce L-spaces, and we denote by $\{L_n\}_{n\geq 1}$ the links shown in Figure 3. We point out that L_1 is the Whitehead link.

Recall that by choosing the canonical meridian and longitude for each component we obtain a canonical parametrisation of Dehn surgeries on a two-component link in S^3 by elements in $\overline{\mathbb{Q}} \times \overline{\mathbb{Q}}$, where $\overline{\mathbb{Q}} = \mathbb{Q} \cup \{\infty\}$.

Theorem B ([98, 99])**.** *Let L be a fibered hyperbolic two-bridge link. Then*

- *if L is isotopic to L_n, then $\mathcal{L}(L) \cap \mathbb{Q}^2 = [n, \infty) \times [n, \infty)$;*
- *if L is isotopic to the mirror of L_n, then $\mathcal{L}(L) \cap \mathbb{Q}^2 = (\infty, -n] \times (\infty, -n]$;*
- *if L is not isotopic to any of the links L_n or their mirrors, then $\mathcal{L}(L) \cap \mathbb{Q}^2 = \emptyset$.*

This implies the following Dehn surgery characterisation of the Whitehead link:

Corollary 0.0.22. *Let L be a fibered hyperbolic two-bridge link and suppose that the $(1,1)$-surgery on L is an L-space. Then L is isotopic to the Whitehead link.*

We observe that all the links $\{L_n\}_{n\geq 1}$ can be obtained as surgery on a 3-component link, see Figure 1.4. On the other hand we have the following:

Proposition 0.0.23. *It is not possible to obtain the exteriors of all the hyperbolic fibered 2-bridge links as Dehn filling on a fixed cusped hyperbolic manifold N. In particular there exists no hyperbolic link L such that every hyperbolic fibered two-bridge link is surgery on L.*

Proof. By using the main result of [68], it is easy to see that there exists a family of fibered hyperbolic 2-bridge links whose volumes grow to infinity. This is the family of links associated to $L(a_1,\dots,a_n) = L(2,2,\dots,2)$ in the notation introduced in Section 1. Since volume decreases under hyperbolic Dehn filling [110], we obtain the result. □

As two-bridge links have tunnel number one, all surgeries on these links have at most Heegaard genus two and therefore as a consequence of the main result of [72] and Theorem B we have:

Corollary 0.0.24. *Let M be obtained as (r_1,r_2)-surgery on the link L_n, with $(r_1,r_2) \in [n,\infty)\times[n,\infty)$ and suppose that M is irreducible. Then M is not left-orderable. In particular, for all these manifolds the L-space conjecture holds.*

For the case of the Whitehead link, in [98], we were also able to determine which taut foliations constructed in the proof of Theorem A have zero Euler class, by adapting the ideas of Hu in [51] to this case. This implies that manifolds supporting such taut foliations have left-orderable fundamental group. We denote the Whitehead link by WL.

Theorem C ([98])**.** *Let p_1,q_1 and p_2,q_2 be two pairs of non vanishing coprime integers. Let $S^3_{\frac{p_1}{q_1},\frac{p_2}{q_2}}(\mathrm{WL})$ be the $\left(\frac{p_1}{q_1},\frac{p_2}{q_2}\right)$-surgery on the Whitehead link, with $q_1,q_2 \neq 0$ and $p_1,p_2>0$.*

Then the foliations constructed in the proof of the Theorem A have vanishing Euler class if and only if $|q_i| \equiv 1 \pmod{p_i}$ for $i=1,2$.

In particular, for all these manifolds the L-space conjecture holds.

We record the following corollary of Theorem A, Theorem C and Corollary 0.0.24:

Corollary 0.0.25. *All rational homology spheres obtained by integer surgery on* WL *satisfy the L-space conjecture.*

This corollary can also be obtained by using the result from [117]. We refer to Chapter 3 for a more detailed statement of Corollary 0.0.25, which also combines results from [117].

Applications to satellite knots and links.

The proof of Theorem A can be used to construct taut foliations on surgeries on some particular types of satellite knots and links. In [99] we introduce a satellite operation called *two-bridge replacement*, see Section 2.4, and prove the following:

Theorem D ([99])**.** *Let $\mathcal{L}$ be a fibered link with positive genus or any non-trivial knot and let $\mathcal{L}'$ denote the link obtained by performing two-bridge replacement on every component of $\mathcal{L}$. Then all manifolds obtained by doing surgery on each component of $\mathcal{L}'$ along a non-meridional slope support a coorientable taut foliation.*

Since two-bridge replacement generalises Whitehead doubling we deduce the following corollary.

Corollary 0.0.26. *Let $\mathcal{L}$ be a fibered link with positive genus or any non-trivial knot and let $\mathcal{L}'$ denote the link obtained by replacing each component of L with one of its Whitehead doubles. Then the manifolds obtained by doing surgery on each component of $\mathcal{L}'$ along a non-meridional slope support a coorientable taut foliation.*

Dodecahedral L-spaces and hyperbolic 4-manifolds

The last part of the thesis will focus on a slightly different topic, and will be about a joint work with Ludovico Battista and Leonardo Ferrari [3], where we study and classify the L-spaces among some hyperbolic 3-manifolds with particularly nice geometric properties.

Definition 0.0.27. A hyperbolic 3-manifold is *dodecahedral* if it can be tessellated by regular right-angled hyperbolic dodecahedra.

The dodecahedral manifolds tessellated with four or less dodecahedra were classified in [43]. Using this, we fix the following notation:

Notation 0.0.28. We denote by $\mathscr{D}$ the set of the 29 dodecahedral hyperbolic rational homology spheres tessellated with four or less dodecahedra.

To identify the L-spaces in $\mathscr{D}$, we elaborate on some ideas presented by Dunfield in [30], and we introduce an algorithm that can be used to prove that a hyperbolic rational homology sphere is an L-space. With the help of the code provided by Dunfield in [30], we show that the remaining 3-manifolds are not L-spaces, so we can conclude:

Theorem E ([3])**.** *Among the 29 manifolds in $\mathscr{D}$, 6 are L-spaces and 23 are not.*

The information given by Theorem E is very little compared with, for example, the one from [30], where L-spaces among more than $300,000$ hyperbolic manifolds are classified. Nevertheless, the geometric properties of the manifolds in $\mathscr{D}$ can be used to

answer a question asked by Agol and Lin in [1]. Before stating the question, we give a brief introduction to the problem.

Seiberg-Witten invariants are smooth invariants for 4-manifolds with $b_2^+ \geq 2$ and were defined in [101, 102, 116] by Seiberg and Witten. These invariants, coming from gauge theory, soon established surprising connections between the topology and the geometry of smooth 4-manifolds. For example, if a 4-manifold with $b_2^+ \geq 2$ supports a metric with positive scalar curvature then these invariants all vanish [116], while on the other hand Taubes [103] proved that any symplectic 4-manifold with $b_2^+ \geq 2$ has a non-zero Seiberg-Witten invariant. Putting together these results, we have that any symplectic 4-manifold with $b_2^+ \geq 2$ does not support a metric with positive scalar curvature.

In [69] LeBrun conjectured that the Seiberg-Witten invariants of a closed hyperbolic 4-manifold are all zero. In [1] Agol and Lin showed the existence of infinitely many commensurability classes of hyperbolic 4-manifolds containing representatives with vanishing Seiberg-Witten invariants. This is shown by proving that there exist hyperbolic 4-manifolds that contain separating L-spaces. Part of their proof was based on a result regarding the embeddings of arithmetic hyperbolic manifolds proved by Kolpakov-Reid-Slavich [56]. However, as a consequence of the techniques employed in [56], the hyperbolic 4-manifolds of [1] are not explicitly constructed. Therefore they ask the following:

Question 1 ([1, Conclusions (1)])**.** Can one find an explicit hyperbolic 4-manifold N such that $N = N_1 \cup_{M'} N_2$, where the separating hypersurface M' is an L-space and such that $b_2^+(N_i) \geq 1$ for $i = 1, 2$?

The separating hypersurfaces that we will use are built from the ones in $\mathscr{D}$ and to build the 4-manifold we will follow the construction presented in [79]. The methods used in [79] allow to construct the 4-manifold in an explicit way. In fact, if M is a dodecahedral manifold tessellated into n dodecahedra, the result of [79] yields, under certain hypotheses, a 4-manifold N tessellated into at most $2^{44} \cdot n$ hyperbolic right-angled 120-cell [79, Proof of Theorem 3] in which M geodesically embeds. Notice that this gives a bound on the volume of N that depends only on the number of dodecahedra that tessellate M. This bound on the number of 120-cells is in general not sharp and in practice our examples are tessellated by less 120-cells than predicted by this bound.

Using this construction, the manifold M is non-separating inside N. However, inside N it is easy to find a certain number of copies of M that, all together, separate. At this point if M is an L-space one can use an argument as in [1, Corollary 2.5] to obtain a separating L-space M' that is diffeomorphic to the connected sum of several copies of M. There is also a natural way to ensure that $b_2^+(N_i) \geq 1$.

With the help of Theorem E, we prove the following:

Theorem F ([3])**.** *There are two hyperbolic 4-manifolds $\mathcal{N}_{11}$ and $\mathcal{N}_{28}$ tessellated with*

2^9 right-angled 120-cells that can be obtained as $N_1 \cup_{M'} N_2$, where the separating hypersurface M' is an L-space and such that $b_2^+(N_i) \geq 1$ for $i = 1, 2$.

The manifolds in the statement are built by colouring 4-manifolds with right-angled corners tessellated in 120-cells and are explicitly described in Chapter 4. The Betti numbers with coefficients in $\mathbb{R}$ and $\mathbb{Z}_2$ of the explicit examples that we build are collected in some tables that can be found in Section 4.3.2.

We point out that dodecahedral manifolds satisfy the hypotheses of [56, Theorem 1.1] and therefore their theorem can be used to prove that they embed in hyperbolic 4-manifolds, but the use of the construction of [79] allows us to describe the 4-manifolds explicitly.

The proof of Theorem E is achieved by rigorous computer-assisted computations. In particular, we make use of the code written by Nathan Dunfield [30] and SnapPy [26] in a Sage [109] environment. All the code used is available at [21], and it can be used to check if a given manifold is an L-space.

The proof of Theorem F is also computer-assisted. We make use of Regina [13] in a Sage [109] environment, and in particular of modules written by Tom Boothby, Nathann Cohen, Jeroen Demeyer, Jason Grout, Carlo Hamalainen, and William Stein. All the code used is available at [21].

Structure of the thesis

The thesis is organised as follows.

- Chapter 1 is devoted to the study of L-space surgeries on fibered hyperbolic two-bridge links. In Section 1.1 we recall some useful notions on two-bridge links that we will need in the second chapter. In Section 1.2 we present the main result of [93] and use this to study surgeries on the links $\{L_n\}_{n\geq 1}$. In Section 1.3 we present some results, that can be of independent interest, regarding the structure of the set of L-space surgeries on links with two unknotted components and linking number zero.

- Chapter 2 is devoted to the construction of the foliations. In Section 2.1 we introduce branched surfaces and recall some of their basic properties, together with the main result of [71]. In Section 2.2 we recall a general method of constructing branched surfaces in fibered manifolds with boundary and in Section 2.3 we focus our attention on surgeries on fibered hyperbolic two-bridge links, proving Theorem A and Theorem B. We conclude the chapter by showing how these results can be applied to construct taut foliations on surgeries on some satellite knots and links. In particular these results apply to all Whitehead doubles of non-trivial knots. This is described in Section 2.4.

This chapter also contains an appendix, where we study fillings of 3-manifolds that fiber over the circle with fiber a k-holed torus and with some prescribed monodromy. The content of the appendix is not needed in the proof of the other theorems in the thesis, but it can be of independent interest.

- In Chapter 3 we address the left-orderability–side of the conjecture. In Section 3.1 we describe how group cohomology can be used to study the existence of lifts of certain homomorphisms. In Section 3.2 we study the Euler classes of the foliations constructed in Chapter 2 on the surgeries on the Whitehead link, and prove Theorem C.

- Chapter 4 is devoted to the study of dodecahedral L-spaces and the construction of some hyperbolic 4-manifolds with vanishing Seiberg-Witten invariants. In Section 4.2, we recall the techniques used by Dunfield to classify the L-spaces in [30]. We then elaborate on these techniques and describe an algorithm that can be used to prove that a hyperbolic rational homology sphere is an L-space and prove Theorem E. Section 4.3 contains the details of the construction necessary for the proof of Theorem F. In Section 4.3.1 we recall the general theory of manifolds with right-angled corners and colourings; then, in Section 4.3.2, we move to the explicit construction.

  Appendices 4.A-4.B contain a detailed description of the algorithm used in Section 4.2, with some examples.

Acknowledgments

I warmly thank my advisors Paolo Lisca and Bruno Martelli for proposing me to work on the L-space conjecture, for carefully reading the drafts of my papers and for their constructive comments about math and how to present it. I also extend my gratitude to the referees for accepting to review my thesis and for contributing significantly to the mathematics I have used during my years as a Ph.D. student. I am very happy to have spent the last nine years of my life in Pisa. I benefited greatly from the vibrant mathematical environment that is present at the math department and from the friendships I established there. While I won't list any names, I want to express my appreciation to all my friends who have shared their time, and often their mathematical insights, with me over these years. I thank Ludovico and Leonardo for collaborating with me in a paper that is included in this thesis. Finally, I thank my family for their constant support and Alice for helping me face many mathematical (and non-mathematical) challenges.

Chapter 1

L-spaces

The aim of this chapter is to prove that the (r_1, r_2)-surgery on the two-bridge link L_n (depicted in Figure 3) is an L-space for $r_1 \geq n$, $r_2 \geq n$. This is the content of Proposition 1.2.7 and will be proved in Section 1.2. We first recall some basic notions on two-bridge links and the main result of [93]. The last section is devoted to prove some additional results for two-component links with unknotted components and linking number zero.

1.1 Basic notions on two-bridge links

In this first section we briefly recall some facts about two-bridge links that will be useful for us, especially in Chapter 2. We refer to [11] for proofs and details. A two-bridge link (with one or two components) can be described by a rational number $\frac{p}{q}$, where p and q are coprime integers, $p > 0$, q is odd and $0 < |q| < p$, in the following way. We fix a sequence of integers $(a_1, \dots, a_n)$ such that

$$\frac{p}{q} = a_1 + \cfrac{1}{a_2 + \cfrac{1}{\ddots + \cfrac{1}{a_n}}} \qquad (*)$$

and consider the link defined by the diagram in Figure 1.1. We denote this link by $L(a_1, \dots, a_n)$.

We are interested in the case when $L(a_1, \dots, a_n)$ has two components. This happens exactly when p is even. When $L(a_1, \dots, a_n)$ is a link we can consider it as oriented link by orienting the components as in Figure 1.2.

A priori it could happen that the isotopy class of the two-bridge link associated to $\frac{p}{q}$ depends on the choice of the continued fraction representation of $\frac{p}{q}$. This is not the case, by the following theorem by Schubert [100], see also [11].

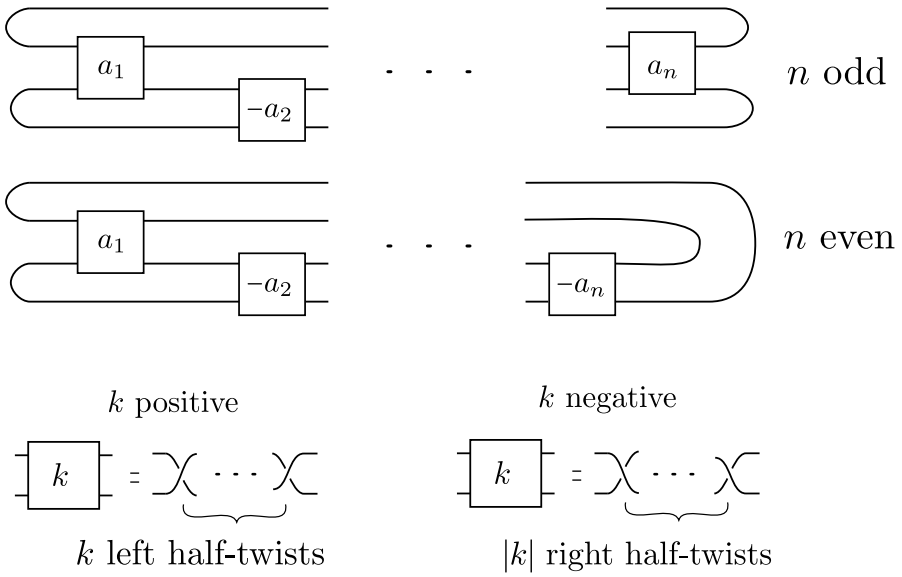

Figure 1.1: The two-bridge knot or link $L(a_1, \dots, a_n)$.

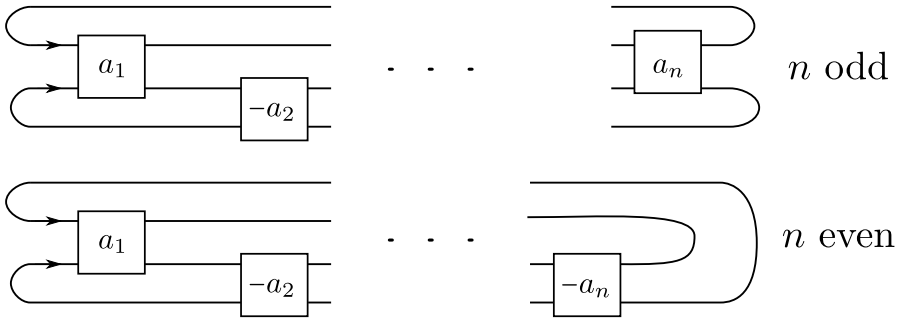

Figure 1.2: The oriented two-bridge link $L(a_1, \dots, a_n)$.

Theorem 1.1.1. *Let $L = L(a_1 \dots, a_n)$ and $L' = L(b_1, \dots, b_m)$ be two oriented two-bridge links and let $\frac{p}{q}$ and $\frac{p'}{q'}$ be the rational numbers defined as in (*). Then the links L and L' are isotopic as oriented links if and only if $p = p'$ and $q' \equiv q^{\pm 1} \mod 2p$. If $p = p'$ and $q' \equiv q + p \mod 2p$ or $qq' \equiv 1 + p \mod 2p$, then L and L' are isotopic after reversing the orientation of one of the components.*

We denote by $b(p, q)$ the two-bridge link associated to the rational number $\frac{p}{q}$.

For convenience we also recall some facts on hyperbolic fibered two-bridge links that we will use in the next chapter. Given a two-bridge link with two components L we can write $L = L(2b_1, \dots, 2b_n)$ as unoriented link, where b_i is a nonzero integer and n is odd. Moreover L is fibered if and only if we can find such a description with $|b_i| = 1$ for all i [40, Proposition 2][1] and by using Theorem 1.1.1 one can see that L is a torus link if and only

[1]The result presented there is for knots, but the same proof works also for links.

if any such description with all $|b_i| = 1$ satisfies $(b_1, \dots, b_n) = \pm(1, -1, 1, \dots, (-1)^{n-1})$. Two-bridge links are non-split, prime, alternating links (see [11]) and as a consequence of [81, Corollary 2], a two-bridge link is hyperbolic if and only if is it not a torus link. Therefore hyperbolic fibered two-bridge links are those that can be written as $L(2b_1, \dots, 2b_n)$ where $|b_i| = 1$ for all i's and at least two consecutives b_i's are equal. Recall that we will consider links as unoriented and say that a link is fibered if there exists an orientation for which it is a fibered link.

1.2 L-space surgeries on the links L_n

The aim of this section is to study L-space surgeries on the links $\{L_n\}_{n\geq 1}$, depicted in Figure 3. Notice that when $n > 1$ it is not evident from the diagrams of Figure 3 that these links are fibered. This will follow from Lemma 2.3.10, that allows us to find diagrams for these links of the form $L(2b_1, \dots, 2b_n)$ where $|b_i| = 1$ for all i's and at least two consecutives b_i's are equal.

We start by recalling some definitions and the main result of [93]. Let Y be a rational homology solid torus, i.e. a compact oriented 3-manifold with toroidal boundary such that $H_*(Y; \mathbb{Q}) \cong H_*(\mathbb{D}^2 \times S^1; \mathbb{Q})$.

We are interested in the study of Dehn fillings on Y. We define the *set of slopes in* Y as

$$Sl(Y) = \{\alpha \in H_1(\partial Y; \mathbb{Z}) |\, \alpha \text{ is primitive}\}/ \pm 1.$$

It is a well known fact that each element $[\alpha] \in Sl(Y)$ determines a Dehn filling on Y, that we will denote by $Y(\alpha)$.

Notice that since Y is a rational homology solid torus, there is a distinguished slope in $Sl(Y)$ that we call the *homological longitude* of Y and that is defined in the following way. We denote by $i : H_1(\partial Y; \mathbb{Z}) \to H_1(Y; \mathbb{Z})$ the map induced by the inclusion $\partial Y \subset Y$ and we consider a primitive element $l \in H_1(\partial Y; \mathbb{Z})$ such that $i(l)$ is torsion in $H_1(Y; \mathbb{Z})$. The element l is unique up to sign, and its equivalence class $[l] \in Sl(Y)$ is the homological longitude of Y. This definition, that may seem to be counterintuitive, is given so that when Y is the complement of a knot in S^3, the homological longitude of Y coincides with the slope defined by the canonical longitude of the knot.

We want to study the fillings on Y that are L-spaces. For this reason we define the set of the *L-space filling slopes*:

$$L(Y) = \{[\alpha] \in Sl(Y) |\, Y(\alpha) \text{ is an L-space}\}$$

and we say that Y is *Floer simple* if Y admits multiple L-space filling slopes, i.e. if $|L(Y)| > 1$.

It turns out that if Y is Floer simple then the set $L(Y)$ has a simple structure, and this can be computed by knowing the *Turaev torsion* of Y. We only recall some properties of the Turaev torsion and we refer the reader to [113] for the precise definitions.

Fix an identification $H_1(Y;\mathbb{Z}) = \mathbb{Z} \oplus T$, where T is the torsion subgroup, and denote by $\phi : H_1(Y;\mathbb{Z}) \to \mathbb{Z}$ the projection induced by this identification. Then the Turaev torsion of Y can be normalised to be written as a formal sum

$$\tau(Y) = \sum_{\substack{h \in H_1(Y;\mathbb{Z}) \\ \phi(h) \geq 0}} a_h h$$

where a_h is an integer for each h, $a_0 \neq 0$ and $a_h = 1$ for all but finitely many h with $\phi(h) \geq 0$. We understand that when $\phi(h) < 0$ the coefficient a_h is zero.

For example (see [113, Section II.5]) if $H_1(Y;\mathbb{Z}) = \mathbb{Z}$ the Turaev torsion of Y can be written as

$$\tau(Y) = \frac{\Delta(Y)}{1-t} \in \mathbb{Z}[[t]]$$

where $(1-t)^{-1}$ is expanded as an infinite sum in positive powers of t and $\Delta(Y)$ is the Alexander polynomial of Y normalised so that $\Delta(Y) \in \mathbb{Z}[t]$, $\Delta(Y)(0) \neq 0$ and $\Delta(Y)(1) = 1$. In fact, in this case the coefficients of $\tau(Y)$ are eventually constant and equal to the sum of all the coefficients of $\Delta(Y)$, and this value is exactly $\Delta(Y)(1) = 1$.

We define $S[\tau(Y)] = \{h \in H_1(Y;\mathbb{Z}) |\ a_h \neq 0\}$ to be the *support of* $\tau(Y)$.

We also define the following subset of $H_1(Y;\mathbb{Z})$:

$$D^{\tau}_{>0}(Y) = \left\{x - y \,|\, x \notin S[\tau(Y)], y \in S[\tau(Y)] \text{ and } \phi(x) > \phi(y)\right\} \cap i(H_1(\partial Y;\mathbb{Z}))$$

where $i : H_1(\partial Y;\mathbb{Z}) \to H_1(Y;\mathbb{Z})$ is induced by the inclusion.

We prove here the following lemma, that we will use in the next section.

Lemma 1.2.1. *The set $D^{\tau}_{>0}$ is always finite.*

Proof. Recall that we fixed an identification $H_1(Y,\mathbb{Z}) = \mathbb{Z} \oplus T$, where T is the torsion subgroup, and we denoted by $\phi : H_1(Y,\mathbb{Z}) \to \mathbb{Z}$ the projection induced by this identification. Also recall that the Turaev torsion of Y is normalised so to be written as

$$\tau(Y) = \sum_{\substack{h \in H_1(Y;\mathbb{Z}) \\ \phi(h) \geq 0}} a_h h$$

where a_h is an integer for each h, $a_0 \neq 0$ and $a_h = 1$ for all but finitely many h with $\phi(h) \geq 0$. This implies in particular that if $h \in S[\tau(Y)]$ then $\phi(h) \geq 0$. Moreover since $a_h = 1$ for all but finitely many h with $\phi(h) \geq 0$ we also deduce that there exists a positive constant $c \in \mathbb{Z}$ such that if $h' \notin S[\tau(Y)]$ then $\phi(h') \leq c$.

We now prove that $D^\tau_{>0}$ is finite. To do this, we define for each $x \notin S[\tau(Y)]$ the set

$$\mathcal{S}^\tau_x = \{y \in S[\tau(Y)] \,|\, \phi(x) > \phi(y)\}.$$

We show that $\mathcal{S}^\tau_x$ is always finite and that it is non-empty only for finitely many $x \notin S[\tau(Y)]$. It follows from the definition of $D^\tau_{>0}(Y)$ that this implies that $D^\tau_{>0}(Y)$ is finite. We fix $x \notin S[\tau(Y)]$ and we have two cases:

- $\phi(x) \leq 0$*:* in this case, since all the $y \in S[\tau(Y)]$ satisfy $\phi(y) \geq 0$, we have that $\mathcal{S}^\tau_x$ is empty.
- $\phi(x) > 0$*:* we use again the fact that all the $y \in S[\tau(Y)]$ satisfy $\phi(y) \geq 0$ to deduce that
$$\mathcal{S}^\tau_x \subset \{0, 1, \dots, \phi(x) - 1\} \oplus T \subset \mathbb{Z} \oplus T = H_1(Y, \mathbb{Z}).$$
Since the torsion subgroup T is finite we have that S^τ_x is finite.

To conclude the proof we show that the latter case occurs only for finitely many $x \notin S[\tau(Y)]$. In fact since there exists a positive constant $c \in \mathbb{Z}$ such that if $x \notin S[\tau(Y)]$ then $\phi(x) \leq c$ we have that the set $\{x \notin S[\tau(Y)] \,|\, \phi(x) > 0\}$ is contained in $\{0, 1, \dots, c\} \oplus T$, and this is a finite set. □

We are now ready to state the main result of [93]:

Theorem 1.2.2 ([93])**.** *If Y is Floer simple, then either*

- $D^\tau_{>0}(Y) = \emptyset$ *and* $L(Y) = Sl(Y) \setminus [l]$*, or*
- $D^\tau_{>0}(Y) \neq \emptyset$ *and $L(Y)$ is a closed interval whose endpoints are consecutive elements in $i^{-1}(D^\tau_{>0}(Y))$.*

We explain more precisely the second part of the statement of this theorem. Once we fix a basis (μ, λ) for $H_1(\partial Y; \mathbb{Z})$ we can associate to each element $a\mu + b\lambda \in H_1(\partial Y; \mathbb{Z})$ the element $\frac{a}{b} \in \overline{\mathbb{Q}} = \mathbb{Q} \cup \{\infty\} \subset S^1$. This association defines a map onto $\overline{\mathbb{Q}}$ that yields an identification between $Sl(Y)$ and $\overline{\mathbb{Q}}$.

If the set $D^\tau_{>0}$ is not empty, then we can apply this map to the set $i^{-1}(D^\tau_{>0}) \subset H_1(\partial Y; \mathbb{Z})$ and Theorem 1.2.2 states that if Y is Floer simple then $L(Y)$ is a closed interval in $Sl(Y) = \overline{\mathbb{Q}}$ whose endpoints are consecutive elements in the image of $i^{-1}(D^\tau_{>0})$ in $\overline{\mathbb{Q}}$.

We point out the following corollary of Theorem 1.2.2:

Corollary 1.2.3. *Let Y be a rational homology solid torus and let $[\alpha] \neq [\beta]$ be two slopes in $L(Y)$. Then $L(Y)$ contains the interval in $Sl(Y)$ between $[\alpha]$ and $[\beta]$ that does not contain the homological longitude $[l]$.*

In the case of our interest we consider links $\mathcal{L} = K_1 \sqcup K_2 \subset S^3$ with unknotted components.

By analogy with the definition given for rational homology solid tori we denote by $Sl(\mathcal{L}) = Sl(E_{K_1}) \times Sl(E_{K_2})$ the set of slopes of the exterior of $\mathcal{L}$, where E_{K_i} denotes the exterior of the knot K_i, for $i = 1, 2$. Notice that this set parametrises all Dehn surgeries on $\mathcal{L}$. We also denote by $L(\mathcal{L})$ the set of L-space filling slopes of the exterior of $\mathcal{L}$.

We fix an orientation of the components of $\mathcal{L}$ and in this way we obtain canonical meridian-longitude bases $(\mu_i, \lambda_i)_{i=1,2}$ of the first homology groups of the boundary tori of its exterior. The choice of these bases also determines an identification $Sl(\mathcal{L}) = \overline{\mathbb{Q}} \times \overline{\mathbb{Q}}$. Given $(r_1, r_2) \in \overline{\mathbb{Q}}^2$, we denote by

- $S^3_{r_1,r_2}(\mathcal{L})$ the (r_1, r_2)-surgery on $\mathcal{L}$;
- $S^3_{r_1,\bullet}(\mathcal{L})$ the manifold obtained by drilling K_2 and performing r_1-surgery on K_1;
- $S^3_{\bullet,r_2}(\mathcal{L})$ the manifold obtained by drilling K_1 and performing r_2-surgery on K_2.

Recall that if $\mathcal{L}$ has two components by using Mayer-Vietoris one can see that the manifold $S^3_{r_1,r_2}(\mathcal{L})$ is not a rational homology sphere if and only if $\{r_1, r_2\} = \{0, \infty\}$ or $r_1 r_2 = \mathrm{lk}(\mathcal{L})^2$, where $\mathrm{lk}(\mathcal{L})$ denotes the linking number of the components of $\mathcal{L}$. Hence if $r_1 \neq 0$ the manifold $S^3_{r_1,\bullet}(\mathcal{L})$ is a rational homology solid torus with homological longitude given by $\frac{\mathrm{lk}(\mathcal{L})^2}{r_1} \in \mathbb{Q}$. Analogously, if $r_2 \neq 0$ the manifold $S^3_{\bullet,r_2}(\mathcal{L})$ is a rational homology solid torus with homological longitude given by $\frac{\mathrm{lk}(\mathcal{L})^2}{r_2} \in \mathbb{Q}$.

We recall the definition of L-space link from [45]. We give this definition for links with two components, but it generalises in the obvious way to links with more components.

Definition 1.2.4. ([45]) A link $\mathcal{L} \subset S^3$ is an *L-space link* if all sufficiently large integer surgeries are L-spaces, i.e. if there exist integers p_1, p_2 such that $S^3_{d_1,d_2}(\mathcal{L})$ is an L-space for all integers $d_1 > p_1$ and $d_2 > p_2$.

Recall that Theorem 0.0.14 implies that if a knot has a positive L-space surgery then it is an L-space knot. This is no longer true in the case of links, as Example 2.4 in [78] shows.

Nevertheless, the following proposition shows that under mild hypotheses Theorem 0.0.14 extends to links with two unknotted components.

Proposition 1.2.5. *Let $\mathcal{L}$ be a link with two unknotted components. Suppose that $(r_1, r_2) \in L(\mathcal{L})$ with $r_1 r_2 > \mathrm{lk}(\mathcal{L})^2$ and $r_1 > 0, r_2 > 0$. Then $\big([r_1, \infty] \times [r_2, \infty]\big) \cap \overline{\mathbb{Q}}^2$ is contained in $L(\mathcal{L})$. Analogously, if $r_1 r_2 > \mathrm{lk}(\mathcal{L})^2$ and $r_1 < 0, r_2 < 0$ then $\big([\infty, r_1] \times [\infty, r_2]\big) \cap \overline{\mathbb{Q}}^2$ is contained in $L(\mathcal{L})$.*

Proof. We prove the proposition in the case $r_1 r_2 > \mathrm{lk}(K)^2$ and $r_1 > 0, r_2 > 0$. The other case is analogous. We consider the manifold $Y = S^3_{r_1,\bullet}$. We have that $r_2 \in L(Y)$

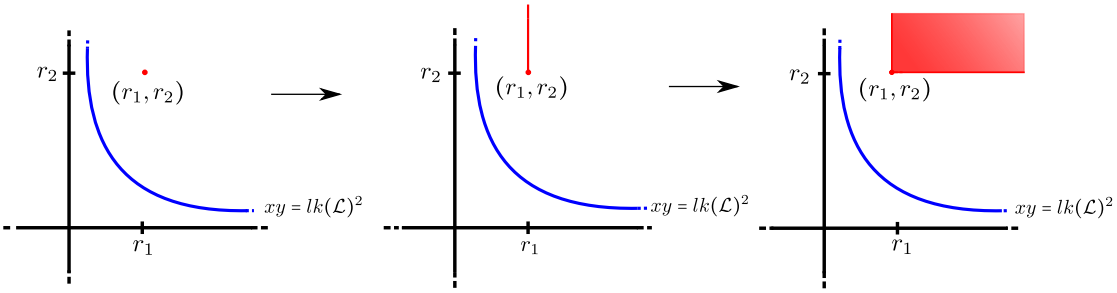

Figure 1.3: A pictorial sketch of the proof.

and since the components of $\mathcal{L}$ are unknotted it follows that also $\{\infty\} \in L(\mathcal{L})$. In fact $S^3_{r_1,\infty}(\mathcal{L})$ is a lens space, and hence an L-space. Thus we can deduce, by virtue of Corollary 1.2.3, that the interval between r_2 and ∞ that does not contain the homological longitude is contained in $L(Y)$. By hypothesis, the homological longitude $\frac{\mathrm{lk}(\mathcal{L})^2}{r_1}$ is smaller than r_2, so we deduce that $[r_2, \infty] \cap \overline{\mathbb{Q}} \subset L(Y)$. In other words we have proved that $S^3_{r_1,s}(\mathcal{L})$ is an L-space for all $s \geq r_2$. Now we fix $s \geq r_2$ and consider the manifold $Y_s = S^3_{\bullet,s}$. As a consequence of r_1 and ∞ belonging to $L(Y_s)$, we can apply again Corollary 1.2.3 and deduce that the interval between r_1 and ∞ that does not contain the homological longitude is contained in $L(Y_s)$. Since $r_1 \geq \frac{\mathrm{lk}(\mathcal{L})^2}{r_2} \geq \frac{\mathrm{lk}(\mathcal{L})^2}{s}$ and the latter is the homological longitude of Y_s, we conclude that $[r_1, \infty] \cap \overline{\mathbb{Q}} \subset L(Y_s)$ for all $s \geq r_2$. This is exactly equivalent to saying that $\big([r_1, \infty] \times [r_2, \infty]\big) \cap \overline{\mathbb{Q}}^2 \subset L(\mathcal{L})$. A pictorial sketch of the proof is described in Figure 1.3. □

In case of links with linking number zero, the previous proposition implies that the property of being an L-space link is determined by a single positive L-space surgery, as in the case of knots:

Corollary 1.2.6. *If $\mathcal{L}$ is a link with linking number zero and two unknotted components and the (r_1, r_2)-surgery on $\mathcal{L}$ is an L-space, for some positive r_1, r_2, then $\mathcal{L}$ is an L-space link.*

Indeed, the previous corollary can be improved and it can be generalised to *Brunnian links*. Since we do not need this for the aims of this section, we postpone the discussion to the next section.

We are now ready to study L-space surgeries on the links $\{L_n\}_{n\geq 1}$.

Proposition 1.2.7. *Let L_n be the link described in Figure 3. Then $\big([n, \infty] \times [n, \infty]\big) \cap \overline{\mathbb{Q}}^2 \subset L(L_n)$.*

Proof. The link L_n satisfies $\mathrm{lk}(L_n)^2 = (n-1)^2$ and its components are unknotted, hence by Proposition 1.2.5 it is enough to prove that $(n, n) \in L(L_n)$. We can see the links L_n

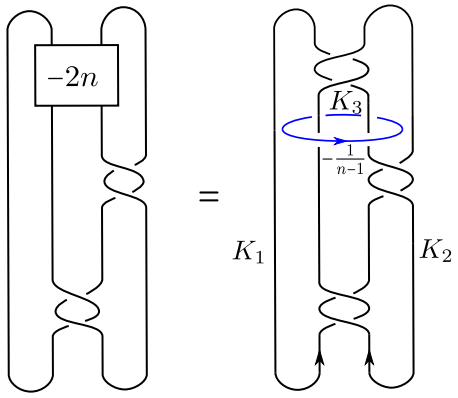

Figure 1.4: How to obtain the links $\{L_n\}_{n\geq 1}$ as surgeries on a 3-component link $\mathscr{L}$.

as surgeries on a three-component link $\mathscr{L}$, as represented in Figure 1.4. We have also fixed an orientation of this link, that we will use later in the proof.

More precisely we have that $S^3_{a,b,-\frac{1}{n-1}}(\mathscr{L}) = S^3_{a+n-1,b+n-1}(L_n)$. This implies that the statement is equivalent to proving that $S^3_{1,1,-\frac{1}{n-1}}(\mathscr{L})$ is an L-space for all $n \geq 1$ and to prove this we will apply Corollary 1.2.3 to the rational homology solid torus $S^3_{1,1,\bullet}(\mathscr{L})$. Denoting this manifold by Y, we have:

- $\infty \in L(Y)$*:* in fact $S^3_{1,1,\infty}(\mathscr{L})$ is $(1,1)$-surgery on the Whitehead link. This is the Poincaré homology sphere, which has finite fundamental group and is therefore an L-space [88, Proposition 2.2];

- $1 \in L(Y)$*:* in fact $S^3_{1,1,1}(\mathscr{L})$ is $(0,0)$-surgery on the Hopf link, see Figure 1.5. This manifold is S^3 and therefore an L-space;

- *the homological longitude of Y is the slope* 2*:* to prove this we have to do a simple computation. We fix an orientation for the link and we denote the components of $\mathscr{L}$ with K_1, K_2 and K_3 as in Figure 1.4.

  We have that $\mathrm{lk}(K_1, K_3) = \mathrm{lk}(K_2, K_3) = 1$ and $\mathrm{lk}(K_1, K_2) = 0$. Consequently, a presentation matrix for $H_1(S^3_{1,1,\frac{p}{q}}(\mathscr{L}), \mathbb{Z})$ is given by

$$A = \begin{pmatrix} 1 & 0 & q \\ 0 & 1 & q \\ 1 & 1 & p \end{pmatrix}$$

  and in particular $S^3_{1,1,\frac{p}{q}}(\mathscr{L})$ is not a rational homology sphere if and only if the determinant of A is zero. This happens if and only if $p = 2q$ and therefore 2 is the homological longitude of the manifold $S^3_{1,1,\bullet}(\mathscr{L})$.

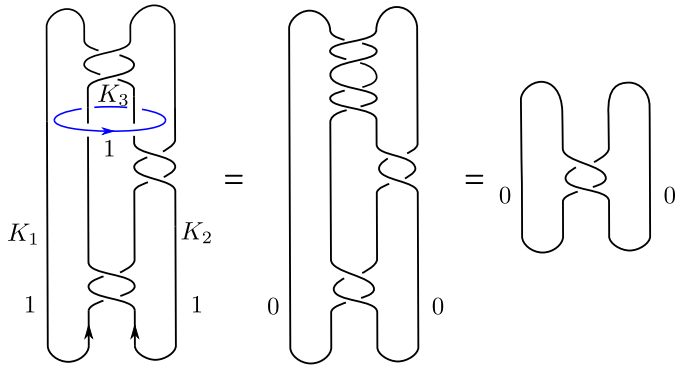

Figure 1.5: The $(1,1,1)$-surgery on $\mathscr{L}$ is $(0,0)$-surgery on the Hopf link

What we have just proved implies by Corollary 1.2.3 that $[\infty,1]\cap\overline{\mathbb{Q}}\subset L(Y)$. In particular $S^3_{1,1,-\frac{1}{n-1}}(\mathscr{L})$ is an L-space for all $n\geq 1$ and this manifold is exactly the (n,n)-surgery on L_n. □

Remark 1.2.8. In [77, 78], Liu conjectured that a two-bridge link is an L-space link if and only if it is of the form $b(pq-1,-q)$, where p and q are odd positive integers. This conjecture was proved by Dawra in [27]. It is not difficult to prove that the link L_n, as unoriented link, is isotopic to $b(6n+2,-3)$. It will follow from the results of Chapter 2, that these are the only fibered nontorus two-bridge L-space links.

1.3 Some general results for links with linking number zero

In this section we focus on the case when $\mathcal{L}$ has unknotted components and linking number zero, and we provide an improvement of Proposition 1.2.5.

Notice that since $\mathcal{L}$ has linking number zero, we have an isomorphism

$$H_1\left(S^3_{\frac{p_1}{q_1},\bullet}(\mathcal{L});\mathbb{Z}\right)\cong\mathbb{Z}_{p_1}\oplus\mathbb{Z}$$

where the image of the meridian μ_1 in $H_1\left(S^3_{\frac{p_1}{q_1},\bullet}(\mathcal{L});\mathbb{Z}\right)$ is mapped to $(1,0)$ and the image of the meridian μ_2 in $H_1\left(S^3_{\frac{p_1}{q_1},\bullet}(\mathcal{L});\mathbb{Z}\right)$ is mapped to $(0,1)$. Moreover, by fixing the canonical meridian and longitude for the component K_1 of $\mathcal{L}$ we have an identification $Sl(S^3_{\frac{p_1}{q_1},\bullet})=\overline{\mathbb{Q}}$. An analogous result holds for $S^3_{\bullet,\frac{p_2}{q_2}}(\mathcal{L})$.

Lemma 1.3.1. *Fix $p\neq 0$ and q coprime integers. Let $S^3_{\frac{p}{q}}(\mathcal{L})$ denote either one of $S^3_{\frac{p}{q},\bullet}(\mathcal{L})$ or $S^3_{\bullet,\frac{p}{q}}(\mathcal{L})$ and suppose that $S^3_{\frac{p}{q}}(\mathcal{L})$ is Floer simple. Then the set $L\left(S^3_{\frac{p}{q}}(\mathcal{L})\right)$ has one of the following forms:*

- $L\left(S^3_{\frac{p}{q}}(\mathcal{L})\right) = \overline{\mathbb{Q}} \setminus \{0\}$, *or*
- *there exists a natural number* $k > 0$ *such that either* $L\left(S^3_{\frac{p}{q}}(\mathcal{L})\right) = [k, \infty]$ *or* $L\left(S^3_{\frac{p}{q}}(\mathcal{L})\right) = [\infty, -k]$.

Proof. We suppose that $S^3_{\frac{p}{q}}(\mathcal{L}) = S^3_{\bullet,\frac{p}{q}}(\mathcal{L})$, the case $S^3_{\frac{p}{q}}(\mathcal{L}) = S^3_{\frac{p}{q},\bullet}(\mathcal{L})$ being analogous. We denote $S^3_{\frac{p}{q}}(\mathcal{L})$ with M.

The lemma follows from Theorem 1.2.2 together with a simple inspection on the possible forms of the set $D^\tau_{>0}(M)$:

- $D^\tau_{>0}(M)$ *is empty:* in this case we have that $L(M) = \overline{\mathbb{Q}} \setminus \{0\}$.
- $D^\tau_{>0}(M)$ *is not empty:* recall that by definition $D^\tau_{>0}(M)$ is the subset of $H_1(M;\mathbb{Z})$ defined as

$$D^\tau_{>0}(M) = \left\{x - y \,|\, x \notin S[\tau(M)], y \in S[\tau(M)] \text{ and } \phi(x) > \phi(y)\right\} \cap i(H_1(\partial M;\mathbb{Z})).$$

In our case the projection ϕ associated to the identification

$$H_1(M;\mathbb{Z}) = \mathbb{Z} \oplus \mathbb{Z}_p$$

is simply the map $\phi(x_1, x_2) = x_1$ and therefore the condition $\phi(x) > \phi(y)$ in the definition of $D^\tau_{>0}(M)$ implies that

$$D^\tau_{>0}(M) \subset (\mathbb{Z}_{>0} \times \mathbb{Z}_p) \cap i(H_1(\partial M;\mathbb{Z})).$$

Since the components of $\mathcal{L}$ have linking number zero, $i(H_1(\partial M;\mathbb{Z})) = \mathbb{Z} \times \{0\}$ and we denote by $S = \{n_1, \dots, n_h\} \subset \mathbb{Z}_{>0}$ the first coordinates of the elements of $D^\tau_{>0}(M) \subset \mathbb{Z}_{>0} \times \{0\}$, listed in ascending order. Recall from Lemma 1.2.1 that $D^\tau_{>0}(M)$ is always a finite set.

We have that

$$i^{-1}(D^\tau_{>0}(M)) = \{(n_i, m) \in \mathbb{Z} \times \mathbb{Z} \,|\, n_i \in S \text{ and } m \in \mathbb{Z}\}$$

and we know by Theorem 1.2.2 that $L(M)$ is a closed interval in $\overline{\mathbb{Q}}$ whose endpoints are consecutive elements in the set $\left\{\frac{n_i}{m} |\, n_i \in S \text{ and } m \in \mathbb{Z}\right\}$. Since the components of $\mathcal{L}$ are unknotted we know that $S^3_{\infty,\frac{p}{q}}(\mathcal{L})$ is an L-space (it is indeed a lens space) and therefore that ∞ belongs to $L(M)$. Hence we can conclude that either $L(M) = [n_h, \infty]$ or $L(M) = [\infty, -n_h]$.

This concludes the proof. □

We will use the symbols $\lfloor x \rfloor$ and $\lceil x \rceil$, where x is a rational number, to denote the integers

$$\lfloor x \rfloor = \max\{k \in \mathbb{Z} | k \leq x\}$$
$$\lceil x \rceil = \min\{k \in \mathbb{Z} | k \geq x\}.$$

Recall that a link $\mathcal{L}$ with three or more components is Brunnian if all of its sublinks are unlinks. This in particular implies that all the components of $\mathcal{L}$ have pairwise linking number zero. A link with two components is Brunnian when its components are unknotted and have linking number zero.

Proposition 1.3.2. *Let $\mathcal{L}$ be an n-components Brunnian link and suppose that there exist rationals $r_1 > 0, r_2 > 0, \cdots, r_n > 0$ such that $S^3_{r_1,\dots,r_n}(\mathcal{L})$ is an L-space. Then $S^3_{s_1,\dots,s_n}(\mathcal{L})$ is an L-space for all $(s_1, \dots, s_n)$ satisfying*

$$\begin{cases} s_i \geq \lfloor r_i \rfloor & \text{if } r_i \geq 1 \\ s_i > \lfloor r_i \rfloor = 0 & \text{if } 0 < r_i < 1. \end{cases}$$

In particular $\mathcal{L}$ is an L-space link.

Proof. We suppose that $\mathcal{L}$ has two components, the proof being analogous in the general case. The proof follows the same lines as the one of Proposition 1.2.5.

We consider $Y = S^3_{r_1,\bullet}$ and we denote by I the set $L(Y)$. We know by hypothesis that $r_2 \in I$ and that $\infty \in I$, the components of $\mathcal{L}$ being unknotted. This implies, by virtue of Lemma 1.3.1, that $[\lfloor r_2 \rfloor, \infty] \subset I$ when $r_2 \geq 1$ and that $\overline{\mathbb{Q}} \setminus \{0\} \subset I$ (and in particular $(0, \infty] \subset I$) when $0 < r_2 < 1$.

We now fix any $s \in I \cap (0, \infty]$ and consider $Y_s = S^3_{\bullet,s}$ with the associated set of L-space surgery slopes $I_s := L(Y_s)$. By repeating the same argument as before, we deduce that $[\lfloor r_1 \rfloor, \infty] \subset I_s$ when $r_1 \geq 1$ and $(0, \infty] \subset I_s$ when $0 < r_2 < 1$. This concludes the proof. The case when $\mathcal{L}$ has more than two components is completely analogous and one only has to observe that any surgery on an unlink that is a rational homology sphere is an L-space, since it has to be a connected sum of lens spaces, and the set of L-spaces is closed under connected sums [86, Proposition 6.1]. □

Remark 1.3.3. It will follow from Theorem 1.3.5 that if $\mathcal{L}$ has two components and is not the unlink, then in the previous proposition the case $0 < r_1 < 1$ or $0 < r_2 < 1$ cannot occur.

The previous proposition allows us to generalise the following theorem from [44].

Theorem 1.3.4 ([44])**.** *Assume that $\mathcal{L}$ is a non-trivial L–space link with two unknotted components and linking number zero. Then there exist non-negative integers b_1, b_2 such that for $p_1, p_2 \in \mathbb{Z}$ we have that $S^3_{p_1,p_2}(\mathcal{L})$ is an L–space if and only if $p_1 > 2b_1$ and $p_2 > 2b_2$.*

More precisely, the theorem we are going to state generalises Theorem 1.3.4 in two directions:

1. we only ask that (r_1, r_2)-surgery on $\mathcal{L}$ is an L-space, for some positive r_1, r_2, instead of requiring $\mathcal{L}$ to be an L-space link;

2. we give a complete description of all the L-space surgeries on $\mathcal{L}$, and not only of the integer ones.

We use the symbol $\mathbb{Q}^*$ to denote the set $\mathbb{Q} \setminus \{0\}$.

Theorem 1.3.5 ([98])**.** *Suppose that $\mathcal{L}$ is a non-trivial link with two unknotted components and linking number zero. Suppose that there exist rationals $r_1 > 0$ and $r_2 > 0$ such that $S^3_{r_1,r_2}(\mathcal{L})$ is an L-space. Then there exist non-negative integer numbers b_1, b_2 such that*

$$L(\mathcal{L}) = \big([2b_1+1, \infty] \times [2b_2+1, \infty]\big) \cup \big(\{\infty\} \times \mathbb{Q}^*\big) \cup \big(\mathbb{Q}^* \times \{\infty\}\big).$$

Proof. We know from Proposition 1.3.2 that $\mathcal{L}$ is an L-space link. Therefore we can apply Theorem 1.3.4 and deduce that there exist non-negative integers b_1, b_2 such that

$$L(\mathcal{L}) \cap \mathbb{Z}^2 = \big([2b_1+1, \infty) \times [2b_2+1, \infty)\big) \cap \mathbb{Z}^2$$

Exactly as in the proof of Proposition 1.3.2, we can use Lemma 1.3.1 to deduce that

$$L(\mathcal{L}) \supset \big([2b_1+1, \infty] \times [2b_2+1, \infty]\big) \cup \big(\{\infty\} \times \mathbb{Q}^*\big) \cup \big(\mathbb{Q}^* \times \{\infty\}\big).$$

and therefore we only have to prove that this inclusion is an equality.

Suppose on the contrary that there exists an L-space surgery slope (r_1, r_2), with r_1, r_2 rationals, such that

$$(r_1, r_2) \notin \big([2b_1+1, \infty] \times [2b_2+1, \infty]\big) \cup \big(\{\infty\} \times \mathbb{Q}^*\big) \cup \big(\mathbb{Q}^* \times \{\infty\}\big).$$

We suppose that $r_1 < 2b_1 + 1$. The case $r_2 < 2b_2 + 1$ can be solved in the same way. We have the following cases:

- $1 \leq r_1 < 2b_1 + 1$.

  By virtue of Lemma 1.3.1 we have that $[\lfloor r_1 \rfloor, \infty]$ is contained in $L(S^3_{\bullet,r_2})$. This implies that $S^3_{\lfloor r_1 \rfloor,\bullet}$ is Floer simple and therefore, by applying again Lemma 1.3.1, we deduce that it admits integral L-space filling slopes. In this way we produce a point in

  $$(L(\mathcal{L}) \cap \mathbb{Z}^2)) \setminus \Big(\big([2b_1+1, \infty) \times [2b_2+1, \infty)\big) \cap \mathbb{Z}^2\Big)$$

  contradicting Theorem 1.3.4.

- $r_1 \in (-1, 1)$.

  As a consequence of Lemma 1.3.1 we have that $L(S^3_{\bullet,r_2}) = \overline{\mathbb{Q}} \setminus \{0\}$. Therefore if we fix any negative integer $-m < 0$ we have that $r_2 \in L(S^3_{-m,\bullet})$ and by applying again Lemma 1.3.1 we deduce that there exist integral L-space filling slopes on $S^3_{-m,\bullet}$, contradicting Theorem 1.3.4.

- $r_1 \leq -1$.

  By applying the same argument used in the first case we have that $L(S^3_{\bullet,r_2})$ contains $[\infty, \lceil r_1 \rceil]$. Therefore $S^3_{\lceil r_1 \rceil,\bullet}$ admits integral L-space filling slopes, contradicting Theorem 1.3.4.

The proof is complete. □

As a corollary we deduce a complete description of all the L-space surgeries on the Whitehead link WL:

Corollary 1.3.6. *Let r_1, r_2 be two rational numbers. The 3-manifold $S^3_{r_1,r_2}(\mathrm{WL})$ is an L-space if and only if $r_1 \geq 1$ and $r_2 \geq 1$*

Proof. Since the Whitehead link is the link L_1 of the family $\{L_n\}_{n\geq 1}$ depicted in Figure 3, we know by virtue of Proposition 1.2.7 that $[1, \infty]^2 \cap \overline{\mathbb{Q}}^2 \subset L(\mathrm{WL})$. The Whitehead link has unknotted components and linking number zero and we can therefore apply Theorem 1.3.5, that immediately implies the thesis. □

So we see that for the Whitehead link the set $L(\mathrm{WL}) \cap \mathbb{Q}^2$ is exactly the set determined in Proposition 1.2.7. The same holds for the other links $\{L_n\}_{n>1}$ but to prove this we have to wait for next chapter, where we construct taut foliations on all the remaining surgeries.

Chapter 2

Taut Foliations

In this chapter we study the existence of taut foliations on the surgeries on fibered hyperbolic two-bridge links, proving Theorem A and Theorem B. Branched surfaces will be our main tool. In Section 2.1 we introduce them and recall some of their basic properties, together with the main result of [71]. In Section 2.2 we recall a general method to construct branched surfaces in fibered manifolds with boundary and in Section 2.3 we focus our attention on surgeries on fibered hyperbolic two-bridge links: we start by proving a few lemmas that allow us to construct taut foliations on all finite surgeries on many fibered two-bridge links; this will reduce our study to the cases of some remaining subfamilies of two-bridge links (containing the links $\{L_n\}_{n\geq 1}$ of Chapter 1) that we study separately. We conclude the chapter by showing how these results can be applied to construct taut foliations on surgeries on some satellite knots and links. In particular these results apply to all Whitehead doubles of non-trivial knots. This is the content of Theorem D and it will be proved in Section 2.4

2.1 Background on foliations and branched surfaces

First of all we specify that in this thesis the term *foliation* will refer to codimension-1 foliations of class $C^{\infty,0}$, as defined for example in [15] and [54]. We recall the definition here. We denote with H^k the k-dimensional Euclidean closed half space

$$\mathrm{H}^k = \{(x_1, \dots, x_k) \in \mathbb{R}^k \,|\, x_k \geq 0\}.$$

Definition 2.1.1. A $C^{\infty,0}$ *codimension-1 foliation* $\mathcal{F}$ of a smooth 3-manifold M with (possibly empty) boundary is a decomposition of M into the union of disjoint smoothly injectively immersed connected surfaces, called the *leaves* of $\mathcal{F}$, together with a collection of charts $(U_i, \phi_i)_{i\in\mathcal{I}}$ covering M such that:

- $\phi_i : U_i \to \mathcal{X}$ is a homeomorphism, where $\mathcal{X}$ is either $\mathbb{R}^2 \times \mathbb{R}$ or $\mathbb{R}^2 \times \mathrm{H}^1$ or $\mathrm{H}^2 \times \mathbb{R}$,

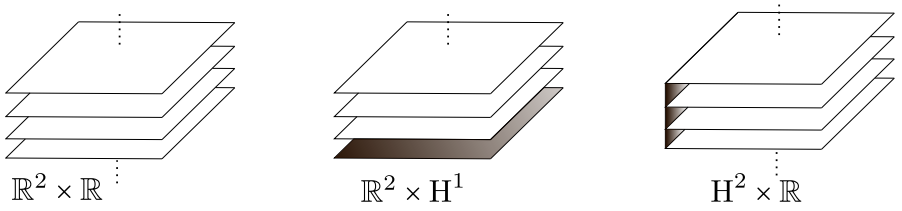

Figure 2.1: Local models for a foliation.

with the property that the image of each component of a leaf intersected with U_i is a slice $\mathbb{R}^2 \times \{\text{point}\}$ or $\mathrm{H}^2 \times \{\text{point}\}$;

- all partial derivatives of any order in the variables x and y on the domain of each transition function $\phi_j \phi_i^{-1}$ are continuous; here we have fixed coordinates (x, y, z) on $\mathcal{X}$.

The three local models for a foliation are depicted in Figure 2.1, where $\partial\mathcal{X}$ is shaded.

Remark 2.1.2. The tangent planes to the leaves of a foliation $\mathcal{F}$ of a 3-manifold M define a continuous plane subbundle of TM, that we denote with $T\mathcal{F}$.

Definition 2.1.3. A foliation $\mathcal{F}$ of a 3-manifold M is *orientable* if the plane bundle $T\mathcal{F}$ is orientable and is *coorientable* if the line bundle $TM/T\mathcal{F}$ is orientable.

Observe that since we work with orientable 3-manifolds, a foliation $\mathcal{F}$ is orientable if and only if is coorientable.

Definition 2.1.4. A foliation $\mathcal{F}$ of a 3-manifold M is *taut* if every leaf of $\mathcal{F}$ intersects a closed transversal, i.e. a smooth simple closed curve in M that is transverse to $\mathcal{F}$.

There are several definitions of tautness and in general they are not equivalent. For details we refer to [23], where also the relations among these different notions are discussed.

In this and in the next sections we assume familiarity with the basic notions of the theory of train tracks; see [110] and [92] for reference. In the cases of our interest train tracks can also have bigons as complementary regions.

Our goal in this chapter is to construct coorientable taut foliations and branched surfaces are the main tool we use. We now introduce these objects and recall some basic facts. We refer to [37] and [84] for more details.

Definition 2.1.5. A *branched surface with boundary* in a 3-manifold M is a closed subset $B \subset M$ that is locally diffeomorphic to one of the models in $\mathbb{R}^3$ of Figure 2.2a) or to one of the models in the closed half space of Figure 2.2b), where $\partial B := B \cap \partial M$ is represented with a bold line.

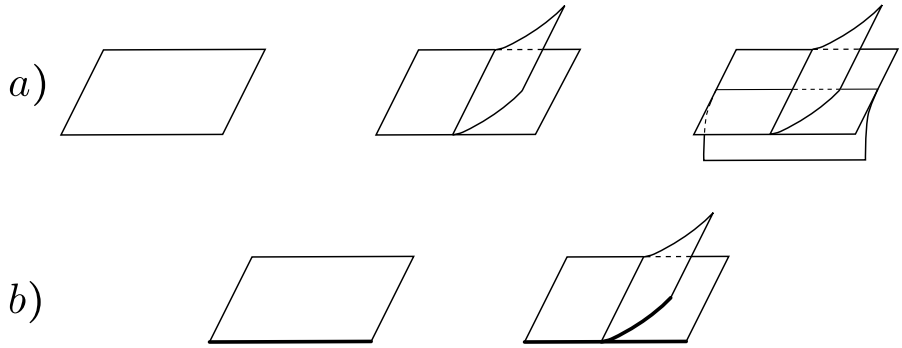

Figure 2.2: Local models for a branched surface.

Figure 2.3: Some examples of cusp directions.

Branched surfaces generalise the concept of train tracks from surfaces to 3-manifolds. When the boundary of B is non-empty it defines a train track ∂B in ∂M.

If B is a branched surface it is possible to identify two subsets of B: the *branch locus* and the set of *triple points*. The branch locus is defined as the set of points where B is not locally homeomorphic to a surface. It is self-transverse and intersects itself in double points only. The set of triple points of B can be defined as the points where the branch locus is not locally homeomorphic to an arc. For example, the rightmost model of Figure 2.2a) contains a triple point.

The complement of the branch locus in B is a union of connected surfaces. The abstract closures of these surfaces under any path metric on M are called the *branch sectors* of B. Analogously, the complement of the set of the triple points inside the branch locus is a union of 1-dimensional connected manifolds. Moreover, to each of these manifolds we can associate an arrow in B pointing in the direction of the smoothing, as in Figure 2.3. We call these arrows *branch directions* or *cusp directions*.

If B is a branched surface in M, we denote by N_B a fibered regular neighbourhood of B constructed as suggested in Figure 2.4.

The boundary of N_B decomposes naturally into the union of three compact subsurfaces $\partial_h N_B$, $\partial_v N_B$ and $N_B \cap \partial M$. We call $\partial_h N_B$ the *horizontal boundary* of N_B and $\partial_v N_B$ the *vertical boundary* of N_B. The horizontal boundary is transverse to the interval fibers of N_B while the vertical boundary intersects, if at all, the fibers of N_B in one or two proper closed subintervals contained in their interior. If we collapse each interval

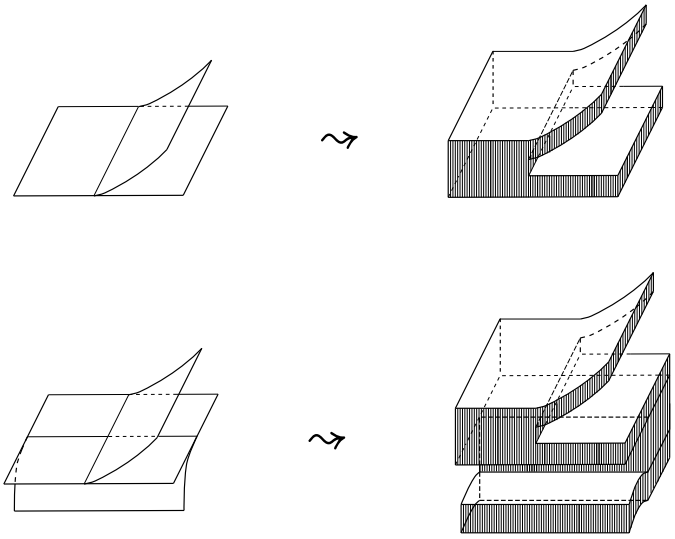

Figure 2.4: Regular neighbourhood of a branched surface.

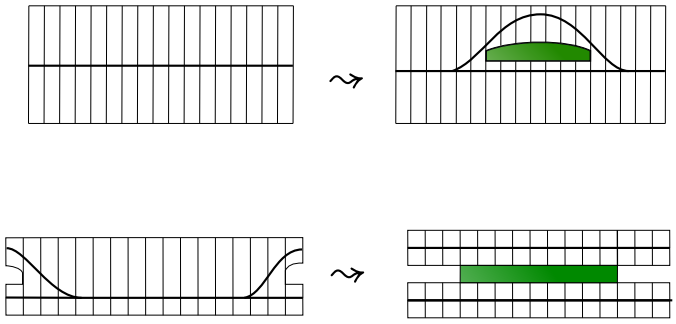

Figure 2.5: Some examples of splittings. The coloured region is the interval bundle J.

fiber of N_B to a point, we obtain a branched surface in M that is isotopic to B, and the image of $\partial_v N_B$ coincides with the branch locus of such a branched surface.

We also recall the definition of *splitting*[1].

Definition 2.1.6. Given two branched surfaces B_1 and B_2 in M we say that B_2 is obtained by *splitting* B_1 if N_{B_1} can be obtained as $N_{B_2} \cup J$, where J is a $[0,1]$-bundle such that $\partial_h J \subset \partial_h N_{B_2}$, $\partial_v J \cap \partial N_{B_2} \subset \partial_v N_{B_2}$ and ∂J meets ∂N_{B_2} so that the fibers agree.

Figure 2.5 shows two examples of splittings, illustrated for the case of 1-dimensional branched manifolds, i.e. train tracks.

Branched surfaces provide a useful tool to construct *laminations* on 3-manifolds.

[1]This operation is referred to as *restriction* in [84].

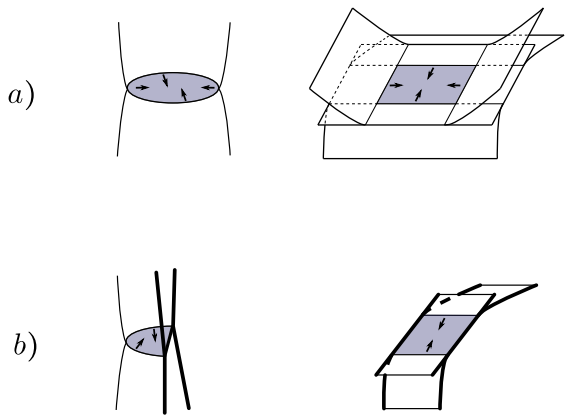

Figure 2.6: Examples of a) sink discs and b) half sink discs.

Definition 2.1.7 (see for example [41])**.** Let B be a branched surface in a 3-manifold M. A *lamination carried by* B is a closed subset Λ of some regular neighbourhood N_B of B such that Λ is a disjoint union of smoothly injectively immersed connected surfaces, called leaves, that intersect the fibers of N_B transversely. We say that Λ is *fully carried* by B if Λ is carried by B and intersects *every* fiber of N_B.

Remark 2.1.8. As in Definition 2.1.7, if S is a closed oriented surface and τ is a train track in S we can define what is a lamination (fully) carried by τ. In this case we say that an oriented simple closed curve γ is *realised* by τ if τ fully carries a union of finitely many disjoint curves that are parallel to γ inside S.

In [70], Li introduces the notion of *sink disc*.

Definition 2.1.9. Let B be a branched surface in M and let S be a branch sector in B. We say that S is a *sink disc* if S is a disc, $S \cap \partial M = \emptyset$ and the branch direction of any smooth curve or arc in its boundary points into S. We say that S is a *half sink disc* if S is a disc, $S \cap \partial M \neq \emptyset$ and the branch direction of any smooth arc in $\partial S \setminus \partial M$ points into S.

In Figure 2.6 some examples of sink discs and half sink discs are depicted. The bold lines represent the intersection of the branched surface with ∂M. Notice that if S is a half sink disc the intersection $\partial S \cap \partial M$ can also be disconnected.

If B contains a sink disc or a half sink disc there is a very simple way to eliminate it, namely it is enough to blow an air bubble in its interior, as in Figure 2.7, so to obtain a new branched surface B'. However there is really no difference between B and B': in fact it is not difficult to see that B carries a lamination if and only if B' carries a lamination.

We do not want to artificially eliminate sink discs with this procedure and so we recall the notion of *trivial bubble*. We say that a connected component of $M \setminus \mathrm{int}(N_B)$ is

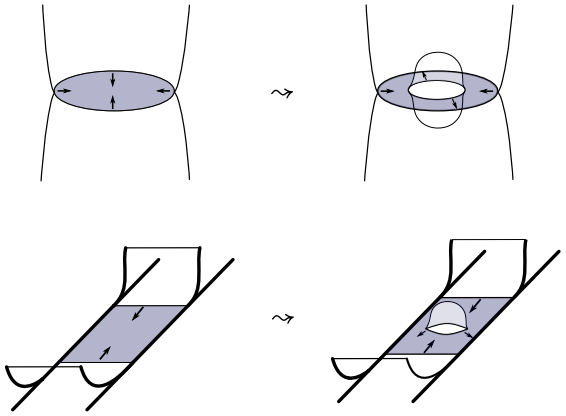

Figure 2.7: How to eliminate a sink disc or a half sink disc by blowing an air bubble.

a $\mathbb{D}^2 \times [0,1]$ *region* if it is homeomorphic to a ball and its boundary can be subdivided into an annular region, corresponding to a component of $\partial_v N_B$, and two $\mathbb{D}^2$ regions corresponding to components of $\partial_h N_B$. We say that a $\mathbb{D}^2 \times [0,1]$ region is *trivial* if the map collapsing the fibers of N_B is injective on $\text{int}(\mathbb{D}^2) \times \{0,1\}$. In this case the image of $\mathbb{D}^2 \times \{0,1\}$ via the collapsing map is called a *trivial bubble* in B. Trivial bubbles and trivial $\mathbb{D}^2 \times [0,1]$ regions are created when we eliminate sink discs as in Figure 2.7.

When M and B have boundary these definitions generalise straightforwardly to the relative case, see [71].

In [70], Li introduces the definition of laminar branched surface and proves that laminar branched surfaces fully carry essential laminations[2]. In [71] he generalises this definition to branched surfaces with boundary as follows:

Definition 2.1.10 ([70])**.** Let B be a branched surface in a 3-manifold M. We say that B is *laminar* if B has no trivial bubbles and the following hold:

1. $\partial_h N_B$ is incompressible and ∂-incompressible in $M \setminus \text{int}(N_B)$, and no component of $\partial_h N_B$ is a sphere or a properly embedded disc in M;

2. there is no monogon in $M \setminus \text{int}(N_B)$, i.e. no disc $D \subset M \setminus \text{int}(N_B)$ such that $\partial D = D \cap N_B = \alpha \cup \beta$, where α is in an interval fiber of $\partial_v N_B$ and β is an arc in $\partial_h N_B$;

3. $M \setminus \text{int}(N_B)$ is irreducible and $\partial M \setminus \text{int}(N_B)$ is incompressible in $M \setminus \text{int}(N_B)$;

4. B contains no Reeb branched surfaces (see [41] for the definition);

5. B has no sink discs or half sink discs.

[2]For the definition of essential lamination see [41], but we will not need their properties for our purposes.

Since $\partial_h N_B$ is not properly embedded in $M \setminus \mathrm{int}(N_B)$ we explain more precisely the request of ∂-incompressibility in 1. : we require that if D is a disc in $M \setminus \mathrm{int}(N_B)$ with $\mathrm{int}(D) \subset M \setminus N_B$ and $\partial D = \alpha \cup \beta$ where α is an arc in $\partial_h N_B$ and β is an arc in ∂M, then there is a disc $D' \subset \partial_h N_B$ with $\partial D' = \alpha \cup \beta'$ where $\beta' = \partial D' \cap \partial M$.

The following theorem of [71] will be used profusely in this section.

Theorem 2.1.11 ([71])**.** *Let M be an irreducible and orientable 3-manifold whose boundary is union of k incompressible tori $T_1, \dots, T_k$. Suppose that B is a laminar branched surface in M such that $\partial M \setminus \partial B$ is a union of bigons. Then for any multislope $(s_1, \dots, s_k) \in \overline{\mathbb{Q}}^k$ that is realised by the train track ∂B, if B does not carry a torus that bounds a solid torus in $M(s_1, \dots, s_k)$, there exists an essential lamination Λ in M fully carried by B that intersects ∂M in parallel simple curves of multislope $(s_1, \dots, s_k)$. Moreover this lamination extends to an essential lamination of the filled manifold $M(s_1, \dots, s_k)$.*

Remark 2.1.12. The statement of Theorem 2.1.11 is slightly more detailed than the version of [71]. The details we have added come from the proof of Theorem 2.1.11. In fact the idea of the proof is to split the branched surface B in a neighbourhood of ∂M so that it intersects T_i in parallel simple closed curves of slopes s_i, for $i = 1, \dots k$. In this way, when gluing the solid tori, we can glue meridional discs of these tori to B to obtain a branched surface $B(s_1, \dots, s_k)$ in $M(s_1, \dots, s_k)$ that is laminar and that by [70, Theorem 1] fully carries an essential lamination. In particular, this essential lamination is obtained by gluing the meridional discs of the solid tori to an essential lamination in M that intersects T_i in parallel simple closed curves of slopes s_i, for $i = 1, \dots, k$.

Remark 2.1.13. In [71] the statement of the theorem is given for M with connected boundary but, as already observed in [53], if M has multiple boundary components we can split B in a neighbourhood of each boundary tori T_i and the same proof of [71] works.

2.2 Constructing branched surfaces in fibered manifolds

In this section we recall a general method to build branched surfaces in compact 3-manifolds with boundary that fiber over the circle. This will be the starting point to construct taut foliations on surgeries on fibered two-bridge links. First of all, we fix some notations and recall the definition of fibered link.

Given an oriented surface S with (possibly empty) boundary and an orientation-preserving homeomorphism $h : S \to S$ fixing ∂S pointwise we denote by M_h the mapping torus of h

$$M_h = \frac{S \times [0,1]}{(h(x),0) \sim (x,1)}.$$

We orient $S \times [0,1]$ as a product and M_h with the orientation induced by $S \times [0,1]$. We also identify S with its image in M_h via the map

$$S \to S \times \{0\} \subset M_h$$
$$x \mapsto (x, 0).$$

The homeomorphism h is called the *monodromy* of M_h.

Definition 2.2.1. Let L be an oriented link in S^3. We say that L is *fibered* if there exists a Seifert surface S for L, an orientation preserving homeomorphism h of S fixing ∂S pointwise and an orientation preserving homeomorphism

$$\chi : S^3 \setminus \mathrm{int}(N_L) \to M_h,$$

where N_L denotes a tubular neighbourhood of L in S^3, so that

- $\chi_{|S}$ is the inclusion $S \subset M_h$;
- $\chi(m_i) = \{x_i\} \times [0,1]$, where m_i is a meridian for the i-th component of L and $x_i \in \partial S$ is a point.

Let S be an oriented surface with boundary and let h be an orientation preserving homeomorphism of S fixing ∂S pointwise. We consider pairwise disjoint properly embedded arcs $\alpha_1, \dots, \alpha_k$ in S and discs $\overline{D}_i = \alpha_i \times [0,1] \subset S \times [0,1]$. Each of these discs has a "bottom" boundary, $\alpha_i \times \{0\}$, and a "top" boundary, $\alpha_i \times \{1\}$. When we consider the images of these discs in M_h under the projection map

$$S \times [0,1] \to M_h$$

we have that the bottom and top boundaries become respectively $\cup_i \alpha_i \subset S$ and $\cup_i h(\alpha_i) \subset S$.

We can isotope simultaneously the discs $\overline{D}_i$'s in a neighbourhood of $S \times \{1\} \subset S \times [0,1]$ so that when projected to M_h their top boundaries define a family of arcs $\{\widetilde{h(\alpha_i)}\}_{i=1,\dots k}$ in S such that for each $i, j \in \{1, \dots, k\}$ the intersection between α_i and $\widetilde{h(\alpha_j)}$ is transverse and minimal. Notice that each arc $\widetilde{h(\alpha_i)}$ is isotopic as a properly embedded arc to $h(\alpha_i)$, via an isotopy that is not the identity on the boundary. We still denote these perturbed arc by $h(\alpha_i)$ and we denote by D_i the projected perturbed disc contained in M_h.

If we assign (co)orientations to these discs, since S is (co)oriented, we can smoothen $S \cup D_1 \cup \dots \cup D_k$ to a branched surface B by imposing that the smoothing preserves the coorientation of S and of the discs. In particular, each disc has two possible coorientations and hence it can be smoothed in two differents ways. This operation is demonstrated in Figure 2.8, where S is a torus with an open disc removed.

The following lemma is probably well-known to experts – for example it is implicitly used in [53] – and states that, under very mild hypotheses, if a branched surface constructed in this way has neither sink discs nor half sink discs then it is laminar.

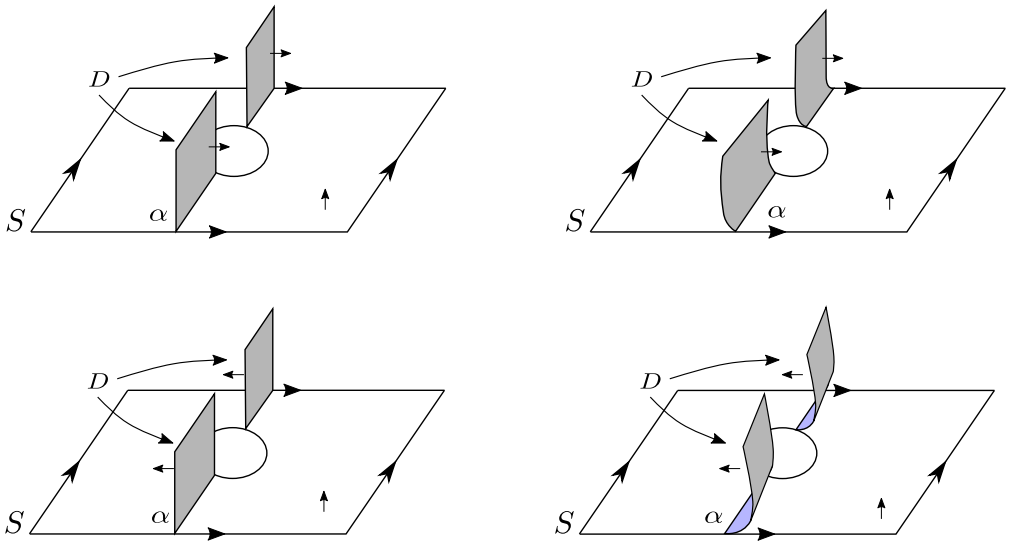

Figure 2.8: How to smoothen $S \cup D$ according to the coorientations.

Lemma 2.2.2. *Let S be a connected and oriented surface with boundary and let h be an orientation preserving homeomorphism of S fixing ∂S pointwise. Let $\{\alpha_i\}_{i=1,\dots,k} \subset S$ be pairwise disjoint properly embedded arcs in S and suppose that $S \setminus \cup_{i=1}^{k} \alpha_i$ has no disc components. Denote by D_i's the discs in M_h associated to the arcs α_i's in the way described above and fix a coorientation for these discs. Let $B = S \cup D_1 \cup \cdots \cup D_k$ denote the branched surface in M_h obtained by smoothing according to these coorientations. Then B has no trivial bubbles and satisfies conditions* 1., 2., 3. *and* 4. *of Definition 2.1.10.*

Proof. We denote by M the mapping torus M_h. We fix for each arc α_i a tubular neighbourhood N_{α_i} in S and we denote with S' the surface $S \setminus \cup_{i=1}^{k} \mathrm{int}(N_{\alpha_i})$. The first observation is that by construction we have

$$M \setminus \mathrm{int}(N_B) \cong S' \times [0,1]$$

with a homeomorphism that identifies

$$\partial_h N_B = S' \times \{0,1\}.$$

and

$$\partial_v N_B = \partial' S' \times [0,1]$$

where $\partial' S'$ denotes the closure of $\partial S' \setminus \partial M$.

Basically, the proof follows from the fact that $M \setminus \mathrm{int}(N_B)$ is homeomorphic to $S' \times [0,1]$ and that S' has no discs components.

First of all, we notice that since by hypothesis $S \setminus \cup_{i=1}^{k} \alpha_i$ has no discs components, there are no $\mathbb{D}^2 \times [0,1]$ regions in $M \setminus \mathrm{int}(N_B)$ and in particular no trivial bubbles. We now verify that conditions $1-4$ of Definition 2.1.10 hold.

1.
   - *The horizontal boundary $\partial_h N_B$ is incompressible in $M \setminus \mathrm{int}(N_B)$:* this follows from the fact that the inclusions of $S' \times \{0\}$ and $S' \times \{1\}$ in $M \setminus \mathrm{int}(N_B)$ are homotopy equivalences. In particular, if a simple closed curve in $\partial_h N_B$ bounds a disc in $M \setminus \mathrm{int}(N_B)$ then it must be nullhomotopic in $\partial_h N_B$ and nullhomotopic simple closed curves in surfaces always bound embedded discs.
   - *The horizontal boundary $\partial_h N_B$ is ∂-incompressible in $M \setminus \mathrm{int}(N_B)$:* suppose that there is a disc $\Delta \subset M \setminus \mathrm{int}(N_B)$ such that $\mathrm{int}(\Delta) \subset M \setminus N_B$ and $\partial\Delta = a \cup b$, where a is an arc in $\partial_h N_B$ and $b = \partial\Delta \cap \partial M$. We have to find a disc $\Delta' \subset \partial_h N_B$ with $\partial\Delta' = a \cup b'$ where $b' = \partial\Delta' \cap \partial M$.
     Without loss of generality we can suppose that $a \subset S' \times \{0\}$. The arc b is an arc in $\partial M \setminus \mathrm{int}(N_B)$ with both endpoints in $S' \times \{0\}$ and since the connected components of $\partial M \setminus \mathrm{int}(N_B)$ are either discs or annuli, there exists a homotopy in $\partial M \setminus \mathrm{int}(N_B)$, relative to the boundary, from the arc b to an arc $b' \subset (S' \times \{0\}) \cap \partial M$. In particular since the simple closed curve $a \cup b$ is nullhomotopic in $M \setminus \mathrm{int}(N_B)$, the curve $a \cup b'$ is nullhomotopic as well.
     To conclude it is enough to observe that since the inclusion of $S' \times \{0\}$ in $M \setminus \mathrm{int}(N_B)$ is a homotopy equivalence, the simple closed curve $a \cup b'$ bounds a disc Δ' in $S' \times \{0\}$.
   - *No component of the horizontal boundary is a sphere or a properly embedded disc:* this follows by our hypotheses.

2. *there is no monogon in $M \setminus \mathrm{int}(N_B)$:* this is a consequence of the fact that the branched surface B admits a coorientation.

3.
   - *$M \setminus \mathrm{int}(N_B)$ is irreducible:* this is a consequence of the fact that each component of $M \setminus \mathrm{int}(N_B)$ is the product of a surface with boundary with $[0, 1]$.
   - *$\partial M \setminus \mathrm{int}(N_B)$ is incompressible in $M \setminus \mathrm{int}(N_B)$:* consider any boundary component T of M. By construction $T \setminus \mathrm{int}(N_B)$ is a union of discs or an annulus (in case there are no endpoints of the arcs α_i on T). In the former case, $T \setminus \mathrm{int}(N_B)$ is obviously incompressible in $M \setminus N_B$, while in the latter it is compressible if and only if it is the boundary of $S' \times [0, 1]$ and $S' \times [0, 1]$ is diffeomorphic to $\mathbb{D}^2 \times [0, 1]$, but this would contradict our hypotheses.

4. *B contains no Reeb branched surfaces:* the presence of a Reeb branched surface would imply that some of the complementary regions of $\mathrm{int}(N_B)$ are $\mathbb{D}^2 \times [0, 1]$ regions (see [41]) and we have already observed that there are no such regions.

The proof is complete. □

Lemma 2.2.3. *Suppose that B is a branched surface constructed as described above and satisfying the hypotheses of Lemma 2.2.2. Suppose also that B has neither sink discs*

nor half sink discs. If $(r_1, \dots, r_n)$ is a multislope realised by ∂B then M_h contains a lamination Λ intersecting the boundary component T_i in parallel curves of slopes r_i, for $i = 1, \dots, n$. Moreover, every leaf of Λ intersects ∂M_h.

Proof. First of all we observe that the boundary of M_h is union of incompressible tori, since M_h is a fiber bundle over the circle whose fiber is not a disc. We use Theorem 2.1.11 to prove that M_h contains the desired lamination. By hypotheses and by construction of B we know that B is laminar and that $\partial M_h \setminus \partial B$ is union of bigons. Moreover any surface carried by B must intersect ∂M_h. In fact, let Σ be a connected surface carried by B. Recall that B is obtained by smoothing $S \cup D_1 \cup \dots \cup D_k$, where S is the fiber surface and $D_1, \dots, D_k$ are the discs spanned by arcs $\alpha_1, \dots, \alpha_k$. If Σ is somewhere parallel to one of these discs, then clearly Σ intersects ∂M_h. If this is not the case, then Σ must be parallel to the fiber surface S and therefore intersect ∂M_h. In particular B does not carry any torus and we can apply Theorem 2.1.11 to deduce that for every multislope $(r_1, \dots, r_n)$ realised by ∂B M_h contains a lamination Λ intersecting the boundary component T_i in parallel curves of slopes r_i, for $i = 1, \dots, n$. Every leaf of Λ must intersect ∂M_h, being it carried by B. This concludes the proof. □

Proposition 2.2.4. *Suppose that B is a branched surface constructed as described above and satisfying the hypotheses of Lemma 2.2.2. Suppose also that B has neither sink discs nor half sink discs. If $(r_1, \dots, r_n)$ is a multislope realised by ∂B then $M_h(r_1 \dots, r_n)$ contains a coorientable taut foliation. More precisely there exists a coorientable taut foliation in M_h intersecting the boundary component T_i in a foliation by curves of slopes r_i, for $i = 1, \dots, n$.*

Proof. Let Λ be the lamination constructed in Lemma 2.2.3 and consider the abstract closures (in a path metric on M_h) of the complementary regions of Λ. These closures are $[0,1]$-bundles; in fact they are unions, along $\partial_v N_B$, of:

- components of $M_h \setminus \mathrm{int}(N_B)$, that are products of the type $F \times [0,1]$, where F is a surface, with
$$\partial_h N_B \cap (F \times [0,1]) = F \times \{0,1\}$$
and
$$\partial_v N_B \cap (F \times [0,1]) = \partial' F \times [0,1]$$
where $\partial' F$ is the closure of $\partial F \setminus \partial M_h$;
- abstract closures of the components of $N_B \setminus \Lambda$. Since Λ intersects transversely the fibers of N_B also these closures are products with the same properties of the components of $M_h \setminus \mathrm{int}(N_B)$.

Each component of the vertical boundary of N_B is an annulus $S^1 \times [0,1]$ or a disc $[0,1] \times [0,1]$, where each interval $\{*\} \times [0,1]$ is contained in a fiber of N_B. Both the product structures of the components of $M_h \setminus \mathrm{int}(N_B)$ and of the abstract closures of the components of $N_B \setminus \Lambda$ define a foliation of the vertical boundary transverse to the interval fibers. Any of two such foliations are isotopic and therefore also the abstract closures of the complementary regions of Λ are products.

In particular, since the horizontal boundary of the closures of these complementary regions are leaves of Λ we can foliate these bundles with parallel leaves to obtain a coorientable foliation $\mathcal{F}$ of M_h that intersects the boundary component T_i in a foliation by curves of slopes r_i, for $i = 1, \dots, n$. Therefore the leaves of this foliation can be capped with the meridional discs of the solid tori to obtain a foliation $\hat{\mathcal{F}}$ of the filled manifold $M_h(r_1, \dots, r_n)$. Since by construction every leaf of this foliation is parallel to some leaf of Λ, and all the leaves of Λ intersect ∂M_h, we deduce that the cores of the glued solid tori define a set of closed transversals that intersect all the leaves of $\hat{\mathcal{F}}$. □

2.3 Fibered hyperbolic two-bridge links

We now focus our attention on fibered hyperbolic two-bridge links: we start by proving a few lemmas that allow us to construct taut foliations on all finite surgeries (i.e. those whose surgery coefficients are in $\mathbb{Q}^2$) on many fibered two-bridge links; this will reduce our study to the cases of some remaining subfamilies of two-bridge links (containing the links $\{L_n\}_{n\geq 1}$ of Chapter 1) that we study separately. Recall from Section 1.1 that fibered hyperbolic two-bridge links are those that can be described as $L(2b_1, \dots, 2b_n)$ where $|b_i| = 1$ for all i's and at least two consecutives b_i's are equal. In this case it is possible to draw an explicit fiber surface S for L. This surface is obtained by starting with the boundary connected sum of a certain number of Hopf bands, and then plumbing other Hopf bands to this surface. This is determined in a straightforward way from the coefficients $(b_1, \dots, b_n)$. One example is described in Figure 2.9. We also fix an orientation of S, so that in the figure the positive side is coloured in pink, and this induces an orientation of the link.

From this very easy description of the fiber surface of L we are able to determine the monodromy of L. More precisely, S can be described in a more abstract way as in Figure 2.10 and the monodromy is given by the diffeomorphism

$$h = \tau_2^{\varepsilon_2} \tau_4^{\varepsilon_4} \dots \tau_{2k}^{\varepsilon_{2k}} \tau_1^{\varepsilon_1} \tau_3^{\varepsilon_3} \dots \tau_{2k+1}^{\varepsilon_{2k+1}} \qquad (*)$$

where $n = 2k+1$, τ_i denotes the positive (i.e. the right) Dehn twist along the curve γ_i shown in Figure 2.10 and

$$\varepsilon_i = \begin{cases} -\mathrm{sgn}(b_i) & \text{when } i \text{ is even} \\ \mathrm{sgn}(b_i) & \text{when } i \text{ is odd} \end{cases}.$$

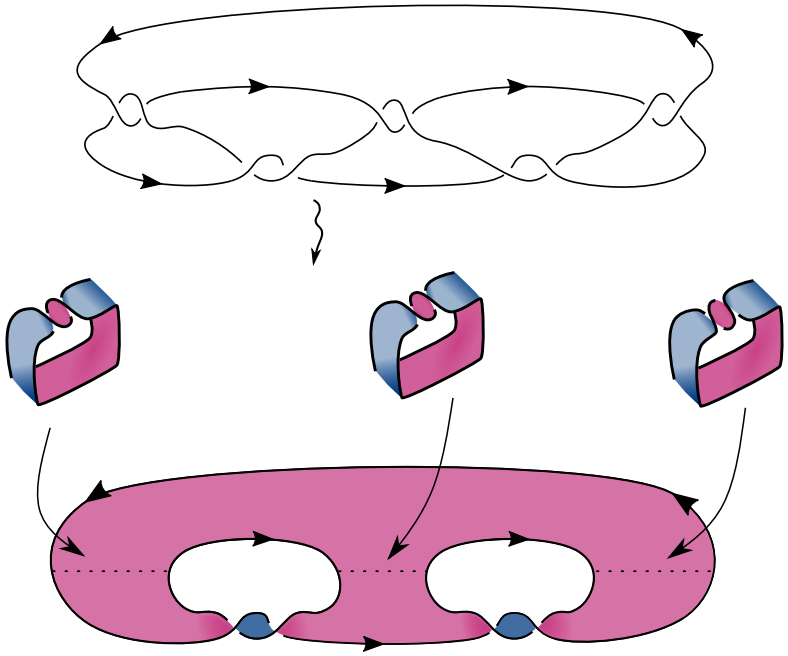

Figure 2.9: The fiber surface of the link $L(-2,-2,-2,2,2)$. The positive side is coloured in pink.

This basically follows from the fact that the monodromy of the boundary of a positive (resp. negative) Hopf band is a positive (resp. negative) Dehn twist along its core and from the way the monodromy of a plumbing or a boundary connected sum (or more generally a Murasugi sum), behaves with respect to the monodromies of the summands, see [39, Corollary 1.4].

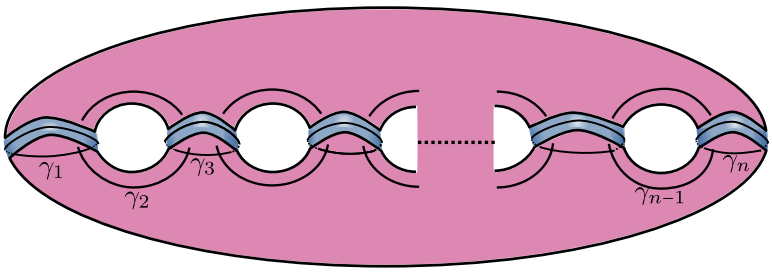

Figure 2.10: An abstract drawing of the fiber surface S together with the curves γ_i's.

2.3.1 The generic case

We are now ready to construct foliations on surgeries on the hyperbolic fibered two-bridge links. The general strategy is simple: we have an explicit description of the monodromies of these links and we want to construct branched surfaces in the way

described in Section 2.2. If we are able to construct these branched surfaces so that they have neither sink discs nor half sink discs, then by Theorem 2.1.11 and Proposition 2.2.4 we can deduce that all the surgeries corresponding to the multislopes realised by these branched surfaces contain coorientable taut foliations. For this reason, we will have to study which multislopes are realised by the boundary train tracks.

In this section we prove a few lemmas that allow us to construct taut foliations on the surgeries of many fibered two-bridge links. This will reduce our study to the cases of some remaining subfamilies of two-bridge links, that we discuss in the next section.

First of all we fix some conventions. As we already did in the previous section, we fix a fiber surface S for the two-bridge link $L = L(2b_1, \dots, 2b_n)$ and we fix its orientation as in Figure 2.9. With the induced orientation, L has linking number

$$\mathrm{lk}(L) = \sum_{i=0}^{k} b_{2i+1}$$

where $n = 2k + 1$. When a link is fibered there is a natural choice of meridians and longitudes for its components that is in general different from the one induced by the ambient manifold S^3. It is obtained as follows. We fix an oriented fiber surface S for the link L, so that $S^3 \setminus \mathrm{int}(N_L) \cong \frac{S\times[0,1]}{\sim_h}$, where N_L is a tubular neighbourhood of L. We fix a point x_i in each boundary component of S and we consider the curves $\mu_i = \frac{\{x_i\}\times[0,1]}{\sim_h}$ oriented in the direction of ascending $t \in [0,1]$ as meridians and the boundary components λ_i of S as longitudes. By definition of fibered link, the meridians defined in this way coincide with the usual meridians of the link. On the other hand these longitudes do not coincide in general with the canonical longitudes of the link. In fact, if for each component K_i of L we denote by l_i the canonical longitude of K_i we have

$$\lambda_i + \sum_{j\neq i} \mathrm{lk}(K_i, K_j)\mu_i = l_i \qquad (\star)$$

as elements in $H_1(\partial N_{K_i}, \mathbb{Z})$, where N_{K_i} is the connected component of N_L containing K_i.

From now on we will refer to the bases (μ_i, λ_i) as the *Seifert framing*, and to the bases (μ_i, l_i) as the *canonical framing*. Unless otherwise stated we use Seifert framings. Moreover, we will always suppose $n > 1$, because when $n = 1$ the only links obtained in this way are the Hopf links and we are interested in hyperbolic links.

Remark 2.3.1. In the following lemma, and also later in the section, we construct branched surfaces by considering *oriented* arcs in the fiber surface S and then by attaching discs as in Section 2.2. We will always coorient the discs with the following convention: we orient them so that the orientations on their boundaries induce the given orientation on the arcs and then we use the orientation of the ambient manifold

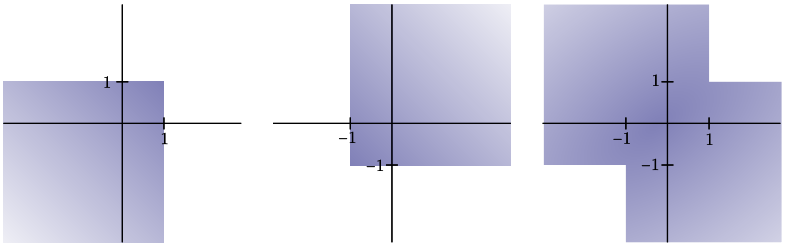

Figure 2.11: From left to right, the slopes (r_1, r_2) in the coloured region yield manifolds with coorientable taut foliations in the case where there is respectively: at least one positive river twist, at least one negative river twist, two river twists with different exponents in the factorisation of the monodromy h.

to coorient them. Analogously, the coorientation of the fiber S is obtained by using the orientation of S and of the ambient manifold.

A good way to keep in mind the cusps directions of branched surfaces constructed in the way is the following: looking at the positive side of S, the cusps directions point to the right along the arcs α_i's with respect to their orientations and point to the left along the oriented arcs $h(\alpha_i)$'s with respect to their orientations. See Figure 2.12.

To ease the exposition of the following lemmas we fix some notation. With reference to Figure 2.10 we say that a Dehn twist along one of the curves $\gamma_1, \gamma_3, \dots, \gamma_n$ is a **bridge twist**, and a Dehn twist along one of the curves $\gamma_2, \gamma_4, \dots, \gamma_{n-1}$ is a **river twist**.

Lemma 2.3.2. *Let $L = L(2b_1, \dots, 2b_n)$ with $|b_i| = 1$ for all i's and let h denote its monodromy as in Equation $(*)$. Let M denote the exterior of L. Then*

1. *if there is at least one positive (resp. negative) river twist in the factorisation of h, the manifold $M(r_1, r_2)$ contains a coorientable taut foliation for every multislope $(r_1, r_2) \in (\infty, 1)^2$ (resp. for all $(r_1, r_2) \in (-1, \infty)^2$); see Figure 2.11a)-b);*

2. *if there are two river twists with different exponents in the factorisation of h, the manifold $M(r_1, r_2)$ contains a coorientable taut foliation for every multislope $(r_1, r_2) \in \big((-1, \infty) \times (\infty, 1)\big) \cup \big((\infty, 1) \times (-1, \infty)\big)$; see Figure 2.11c).*

Proof. 1. Suppose that there is a positive river twist along the curve γ_i. We consider the arcs α and β as in Figure 2.12. The oriented arcs α and β determine a cooriented branched surface B obtained by attaching two discs to the fiber surface S as described in Section 2.2. Since $n > 1$, S is not an annulus and therefore the complement of $\alpha \cup \beta$ has no disc components. Due to the fact that we have chosen α and β so that they are disjoint from γ_j for $j \neq i$ it follows that $h(\alpha) = \tau_i(\alpha)$ and $h(\beta) = \tau_i(\beta)$, as depicted

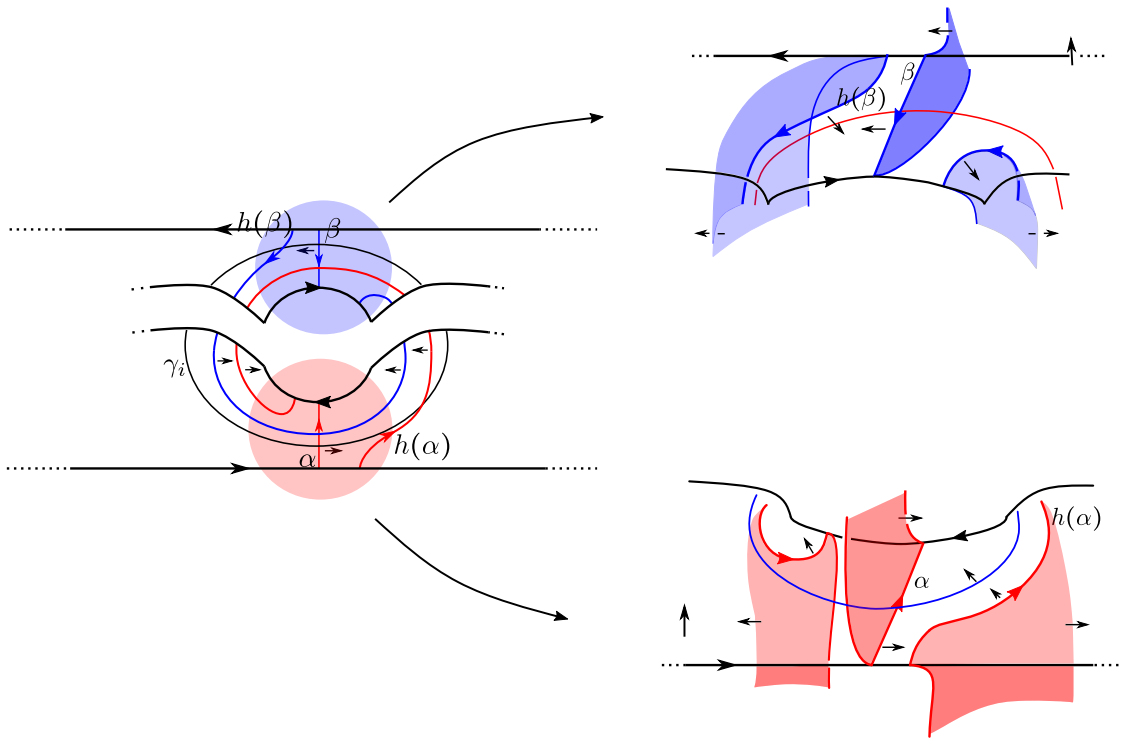

Figure 2.12: The arcs α and β and the cooriented discs spanned by them.

in Figure 2.12. In Figure 2.12 we have also labelled the branch locus of B with the cusps directions and it can be checked from the picture that there are neither sink discs nor half sink discs. For this reason we can apply Proposition 2.2.4 and deduce that $M(r_1, r_2)$ supports a coorientable taut foliation for all the multislopes (r_1, r_2) realised by ∂B. We now want to understand which multislopes are realised by the boundary train tracks of B.

To do this we assign rational weight systems to our boundary train tracks. Given that the train tracks are oriented, we can associate to such a weight system the rational number $\frac{w_\mu}{w_\lambda}$, where w_μ and w_λ are the *weighted* intersections of the train tracks with our fixed meridians μ and longitudes λ, as we would do with oriented simple closed curves. This quotient can be interpreted as a *slope* in the boundary component of M we are interested in. In fact it can be proved that each slope $\frac{p}{q}$ obtained in this way is realised by the train track. We want to study slopes *fully* carried by these train tracks, hence we have to require that each weight is strictly positive: if the weight of an arc is zero, the associated slope will not intersect the fibers over that arc. For details, see [92]. The two boundary train tracks of B are equal to the one illustrated in Figure 2.13 where we have also endowed it with weight systems, depending on two

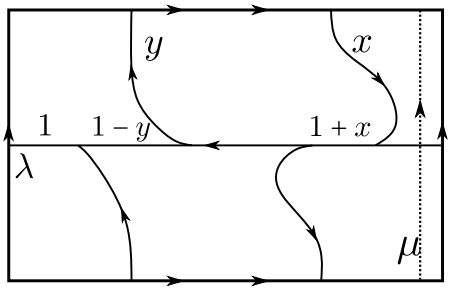

Figure 2.13: On each of the two boundary components of M the branched surface defines this boundary train track. The variables x and y take rational values and define weight systems.

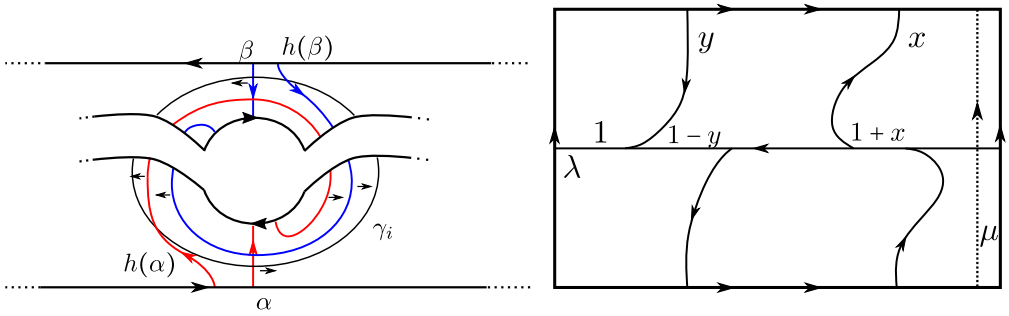

Figure 2.14: The arcs α and β and the boundary train tracks when the river twist is negative.

variables x, y. The slopes of these weight systems are $y - x$. Since we have to impose that each sector has positive weight x must take values in $(0, \infty)$ and y must take values in $(0, 1)$, hence we obtain all the slopes in $(\infty, 1)$. Therefore the boundary train tracks of B realise all the multislopes in $(\infty, 1)^2$. By applying Proposition 2.2.4 we obtain taut foliations on $M(r_1, r_2)$ for all $(r_1, r_2) \in (\infty, 1)^2$.

If there is a negative river twist, we consider the same oriented arcs α and β, and on each of the two boundary components of M we obtain the train track depicted on the right-hand side of Figure 2.14. This train track realises all the slopes in $(-1, \infty)$ and so we obtain taut foliations on $M(r_1, r_2)$ for all $(r_1, r_2) \in (-1, \infty)^2$.

2. Suppose now that there are two river twists with different exponents in the factorisation of h and suppose that the positive one is along the curve γ_i and the negative one is along γ_j. We suppose $i < j$ but the proof does not change if $j < i$. We choose now α and β as in Figure 2.15 and as before we have $h(\alpha) = \tau_i(\alpha)$ and $h(\beta) = \tau_j(\beta)$. Also in this case the complement of $\alpha \cup \beta$ contains no disc components. Moreover the complement of $\alpha \cup \beta \cup h(\alpha) \cup h(\beta)$ is connected and this implies that there are neither sink discs nor half disk discs in the branched surface associated to α and

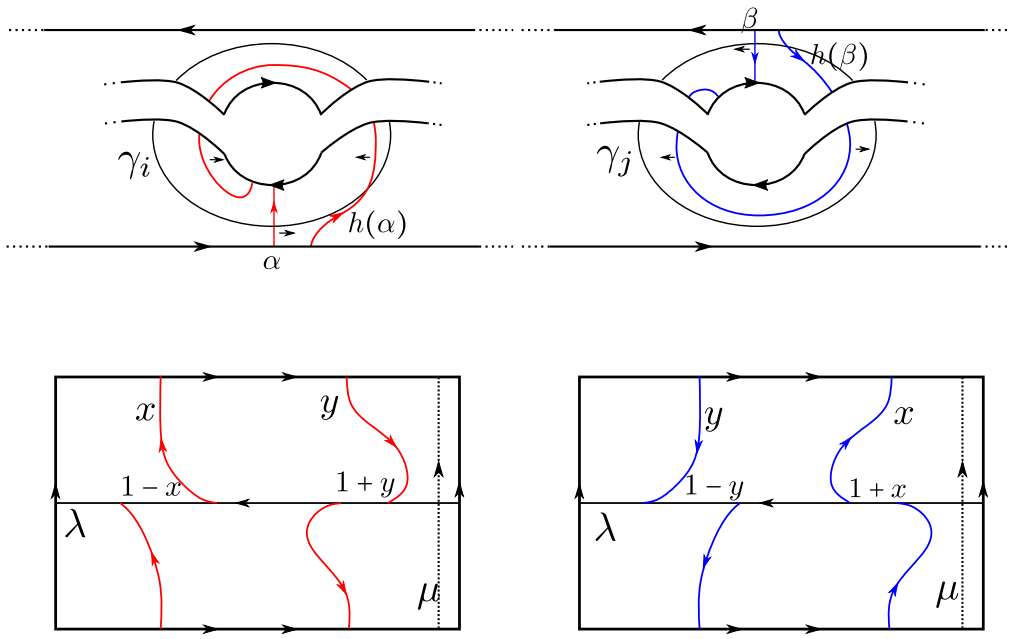

Figure 2.15: This picture describes the choice of the arcs α and β when the twist along the curve γ_i is positive and the one along γ_j is negative. The boundary train tracks of the associated branched surface are also shown.

β. The boundary train tracks (with weight systems) of B are shown in Figure 2.15. The slopes realised by the one on the left side of the figure are the ones contained in $(\infty, 1)$ and the ones realised by the train track on the right are those contained in $(-1, \infty)$. As a consequence of Proposition 2.2.4 we have taut foliations in $M(r_1, r_2)$ for all $(r_1, r_2) \in (\infty, 1) \times (-1, \infty)$. As two-bridge links are symmetric (i.e. there exists an isotopy that exchanges the components), we deduce that there are taut foliations also on the surgeries associated to coefficients $(r_1, r_2) \in (-1, \infty) \times (\infty, 1)$.
This concludes the proof. □

Remark 2.3.3. Recall that we are working with Seifert framings. However we have already noticed that the meridians of the Seifert framing coincide with the canonical meridians of L. This implies that the finite surgeries on L with respect to the Seifert framing coincide with the finite surgeries on L with respect to the canonical framing.

Corollary 2.3.4. *If the factorisation of the monodromy h has two river twists with different exponents, then all the finite surgeries on the link L contain coorientable taut foliations.*

Proof. It follows from the first part of Lemma 2.3.2 that there are coorientable taut foliations on $M(r_1, r_2)$ for $(r_1, r_2) \in (\infty, 1)^2 \cup (-1, \infty)^2$ and it follows from the second part of Lemma 2.3.2 that there are coorientable taut foliations on $M(r_1, r_2)$ for $(r_1, r_2) \in$

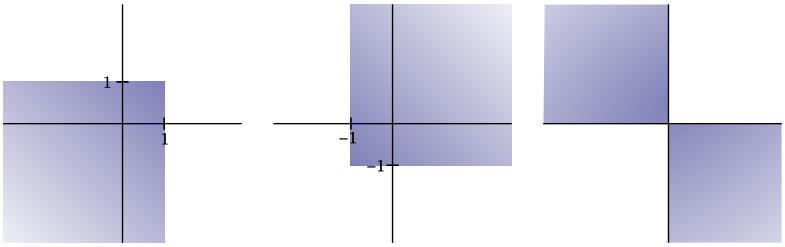

Figure 2.16: From left to right, the slopes (r_1, r_2) in the coloured region yield manifolds with coorientable taut foliations in the case where there are respectively: at least two positive bridge twists, at least twp negative bridge twists, two bridge twists with different exponents in the factorisation of the monodromy h.

$\big((-1,\infty)\times(\infty,1)\big)\cup\big((\infty,1)\times(-1,\infty)\big)$. The union of these sets is exactly the set of all finite multislopes. □

As a consequence of Corollary 2.3.4, by taking mirrors if necessary, we can reduce our study to the case where the river twists are all positives, i.e. to links of the form $L = L(2b_1, -2, 2b_3, \dots, -2, 2b_n)$. We now focus our attention on bridge twists.

Lemma 2.3.5. *Let $L = L(2b_1, \dots, 2b_n)$ with $|b_i| = 1$ for all i's and let h denote its monodromy as in Equation $(*)$. Let M denote the exterior of L. Then*

1. *if there are at least two positive (resp. negative) bridge twists in the factorisation of h, the manifold $M(r_1, r_2)$ contains a coorientable taut foliation for every multislope $(r_1, r_2) \in (\infty, 1)^2$ (resp. for all $(r_1, r_2) \in (-1, \infty)^2$); see Figure 2.16a)-b);*

2. *if there are two bridge twists with different exponents in the factorisation of h, the manifold $M(r_1, r_2)$ contains a coorientable taut foliation for every multislope $(r_1, r_2) \in \big((0,\infty)\times(\infty,0)\big)\cup\big((\infty,0)\times(0,\infty)\big)$, see Figure 2.16c).*

Proof. 1. Suppose that the positive bridge twists are along the curves γ_i and γ_j. We consider the oriented arc α and β as in Figure 2.17. We have $h(\alpha) = \tau_i(\alpha)$: in fact

$$h = \underbrace{\tau_2^{\varepsilon_2}\tau_4^{\varepsilon_4}\dots\tau_{2k}^{\varepsilon_{2k}}}_{\text{river twists}}\underbrace{\tau_1^{\varepsilon_1}\tau_3^{\varepsilon_3}\dots\tau_{2k+1}^{\varepsilon_{2k+1}}}_{\text{bridge twists}}$$

and the only bridge twist that has effect on α is τ_i and the river twists have no effect on $\tau_i(\alpha)$. The same reasoning proves that $h(\beta) = \tau_j(\beta)$. Also in this case we obtain a branched surface that satisfies the hypotheses of Proposition 2.2.4. Therefore we just need to study the multislopes realised by the boundary train tracks of B. These are illustrated in Figure 2.17 and they realise all the multislopes in $(\infty, 1)^2$.

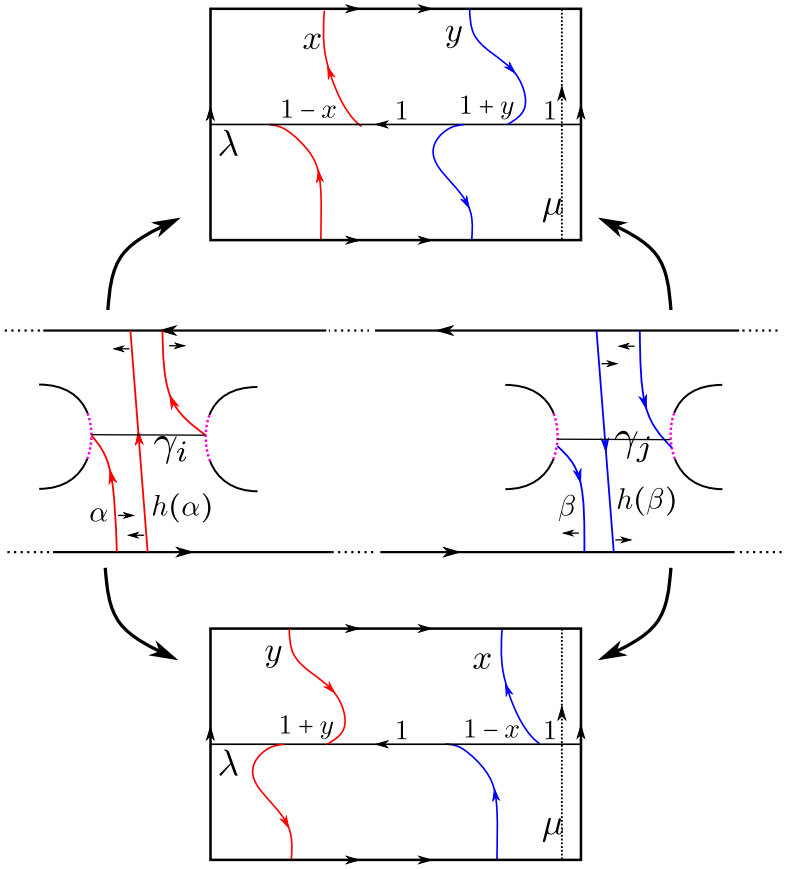

Figure 2.17: The arcs α and β, together with their image via the monodromy h and the cusps directions, are depicted. We also describe the train tracks obtained on the boundaries of M. To simplify the picture we do not draw the 1-handles; we understand that the dashed lines are pairwise identified in the obvious way.

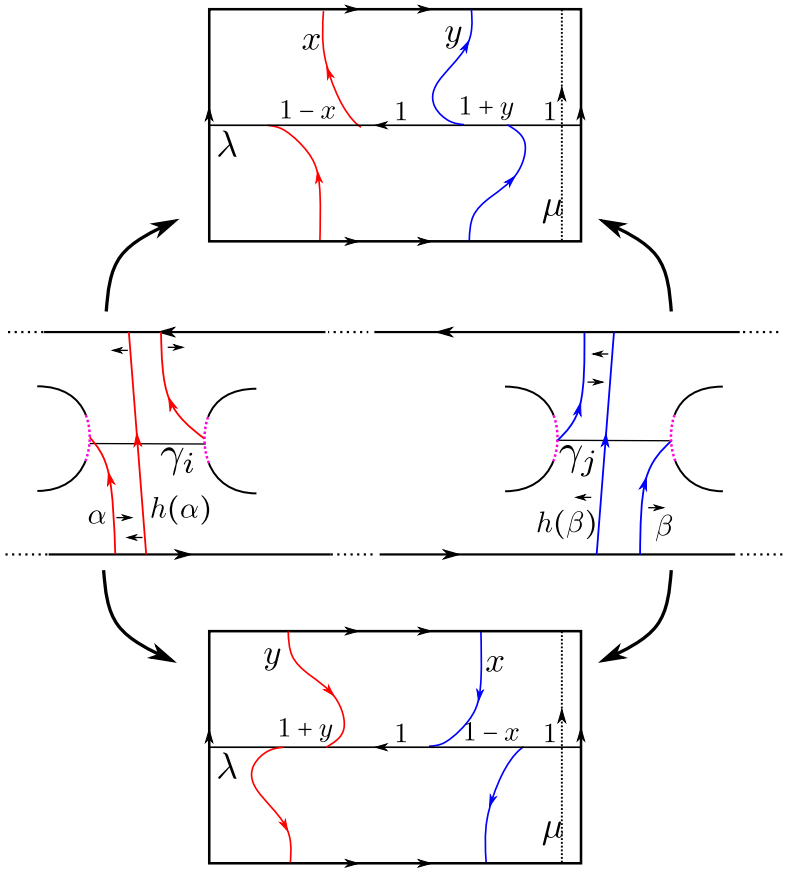

Figure 2.18: The arcs α and β in the case where bridge twist with different exponents and the boundary train tracks realised on the two boundary components of M.

The case where we have two negative bridge twists is analogous: we choose α and β in the same way but now so that they turn right when they meet the curves γ_i and γ_j. Everything works in the same way but now we have train tracks as the one in Figure 2.14 and therefore the multislopes realised are the ones in $(-1, \infty)^2$.

2. Suppose that there are two bridge twists with different exponents in the factorisation of h and suppose that the positive one is along the curve γ_i and the negative one is along γ_j. We choose α and β as in Figure 2.18. Also in this case there are no sink discs and half sink discs. Moreover, the boundary train tracks of the branched surface associated to α and β realise all the slopes in $(0, \infty)$ (see top of Figure 2.18) and $(\infty, 0)$ (see bottom of Figure 2.18).
Using the fact that two-bridge links are symmetric, we obtain the statement. □

Corollary 2.3.6. *Let $L = L(2b_1, -2, 2b_3, \ldots, -2, 2b_n)$ with $|b_i| = 1$ and let h denote its monodromy as in Equation $(*)$. If there are at least two negative bridge twists and one*

positive bridge twist in the factorisation of h then all the finite surgeries on the link L contain coorientable taut foliations.

Proof. As a consequence of the fact that the factorisation of h contains positive river twists, by Lemma 2.3.2 we know that $M(r_1, r_2)$ contains a taut foliation for all the multislopes $(r_1, r_2) \in (\infty, 1)^2$. Moreover, since there are two negative bridge twists it follows from the first part of Lemma 2.3.5 that $M(r_1, r_2)$ contains a taut foliation for all the multislopes $(r_1, r_2) \in (-1, \infty)^2$. As there is also at least one positive bridge twist we can apply the second part of Lemma 2.3.5 and deduce that $M(r_1, r_2)$ contains a taut foliation for all the multislopes $(r_1, r_2) \in \big((0, \infty) \times (\infty, 0)\big) \cup \big((\infty, 0) \times (0, \infty)\big)$. The union of these sets is exactly the set of all finite multislopes. □

2.3.2 Study of the remaining cases

By Corollary 2.3.4 and Corollary 2.3.6 we have reduced our study to the following three families of fibered two-bridge links:

- *Family 0:* links of the form $L = L(2, -2, 2, \dots, -2, 2)$. These are exactly the two-bridge torus links and we do not study them;
- *Family 1:* links of the form $L = L(-2, -2, -2, \dots, -2, -2)$;
- *Family 2:* links of the form $L = L(2b_1, -2, 2b_3, \dots, -2, 2b_m)$ where exactly one b_i is -1 and all the others are equal to 1.

We now focus our attention on the links composing *Family 1.*

Proposition 2.3.7. *Let L be a two-bridge link of the form $L = L(-2, -2, -2, \dots, -2, -2)$. Then all the finite Dehn surgeries on L support a coorientable taut foliation.*

Proof. It follows by Lemmas 2.3.2 and 2.3.5 that, as the monodromy of L has (at least) two negative bridge twists and (at least) one positive river twist, then all the surgery coefficients contained in $(\infty, 1)^2 \cup (-1, \infty)^2$ yield manifolds with coorientable taut foliations. We recall that these coefficients are associated to the Seifert framing. We now consider two cases:

- *L is not the link $L(-2, -2, -2)$:* we construct a branched surface whose boundary train tracks realise all the multislopes in $(\infty, 1) \times (0, \infty)$. Two-bridge links are symmetric, hence this will imply the statement. This branched surface is constructed by considering the arcs α and β in Figure 2.19 and satisfies the hypotheses of Proposition 2.2.4. Therefore it can be used to construct foliations on all the surgeries associated to the multislopes realised by its boundary train tracks illustrated in Figure 2.19: the one on the top realises all the slopes in $(0, \infty)$ and the one on the bottom all the slopes in $(\infty, 1)$.

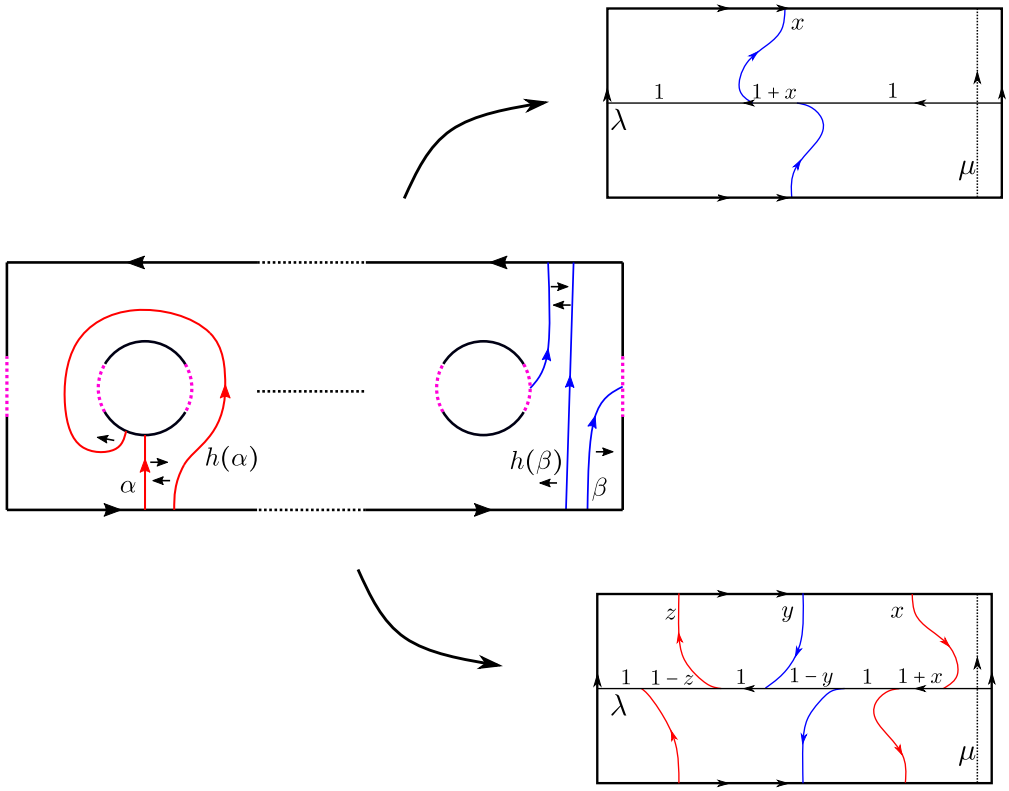

Figure 2.19: When L is not the link $L(-2,-2,-2)$ we consider the arcs α and β. The boundary train tracks of the branched surface associated to these arcs are also shown.

- $L = L(-2,-2,-2)$*:* to study this case we use an idea that will be useful also later on. We construct taut foliations on all the $(r,s)-$surgeries on L, where $r < 0$ or $s < 0$. This is enough because we already know that the surgeries associated to $(r,s) \in (-1,\infty)^2$ contain taut foliations. Observe that L can be described as surgery on a 3-components link $\mathcal{L}$, as in Figure 2.20. The link $\mathcal{L}$ is also fibered, because it is boundary of a surface obtained via a sequence of Hopf plumbings, as described in Figure 2.20.

  Moreover the monodromy of the link $\mathcal{L}$ is given by $h = \tau_4\tau_3^{-1}\tau_2\tau_1^{-1}$, where τ_i denotes the positive Dehn twist along the curve c_i shown in Figure 2.21.

  This description of L will help us to construct the desired taut foliations. The idea is to find a branched surface in the exterior of $\mathcal{L}$ so that the boundary train tracks realise slope -1 on the boundary component associated to K_3'. To do this is important to pay attention to how the surgery coefficients change when passing from $\mathcal{L}$ to L. Recall that the coefficients of the slopes are written by using the identification given by the Seifert framing. The $(a,b,-1)$-surgery on $\mathcal{L}$ coincides with the $(a-1,b+1)$-surgery on L, as the following diagram suggests:

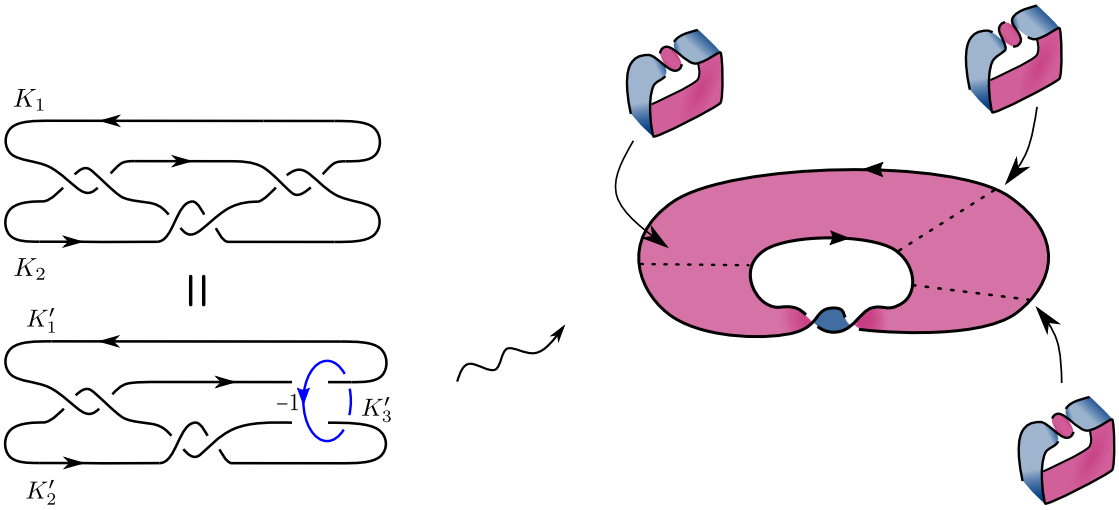

Figure 2.20: How to obtain the link $L(-2,-2,-2)$ as surgery on a 3-component link $\mathcal{L}$. We also describe a fiber surface for $\mathcal{L}$, obtained via a sequence of Hopf plumbings.

$$\begin{array}{ccc} \overbrace{(a,b,-1)}^{\text{Seifert framing for } \mathcal{L}} & \dashrightarrow & \overbrace{(a-1,b+1)}^{\text{Seifert framing for } L} \\ \downarrow & & \uparrow \\ \underbrace{(a,b+2,-1)}_{\text{Canonical framing for } \mathcal{L}} & \longrightarrow & \underbrace{(a+1,b+3)}_{\text{Canonical framing for } L} \end{array} .$$

The changes of coefficients indicated by the vertical arrows are a consequence of formula $(\star)$ and the fact that

$$\mathrm{lk}(K_1,K_2) = -2, \quad \mathrm{lk}(K_1',K_2') = \mathrm{lk}(K_2',K_3') = -1, \quad \mathrm{lk}(K_1',K_3') = 1.$$

We construct two branched surfaces in the exterior of $\mathcal{L}$, associated to the arcs α_i, β_i and γ_i, for $i = 1, 2$, as described in Figure 2.22. It can be checked by direct inspection that for $i = 1, 2$ the complement of $\alpha_i \cup \beta_i \cup \gamma_i$ contains no disc components, and that there are no sink discs and no half sink discs. Hence we can apply Proposition 2.2.4 and deduce that these branched surfaces carry laminations that extend to taut foliations on the manifolds obtained by Dehn filling the boundary tori along the multislopes realised by the boundary train tracks. The boundary train tracks are also depicted in Figure 2.22 and they realise, respectively, all the multislopes in $(\infty,1)\times(0,\infty)\times(\infty,0)$ and in $(\infty,1)^3$. In particular, we have taut foliations on $S^3_{r,s,-1}(\mathcal{L}) = S^3_{r-1,s+1}(L)$ for all $(r,s) \in (\infty,1)\times\mathbb{R}$.

Since L is symmetric, the statement follows. □

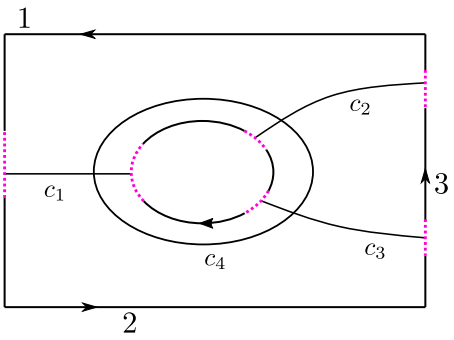

Figure 2.21: An abstract drawing of the fiber surface for the link $\mathcal{L}$, together with the curves c_i's. The boundary component with label i corresponds to the components K_i' of the link, for $i = 1, 2, 3$.

We now focus our attention on the links of *Family 2*, i.e. on the links of the form $L = L(2b_1, -2, 2b_3, \dots, -2, 2b_m)$ where exactly one b_i is -1 and all the others are equal to 1. We first study the case when $b_i = 1$ for some $i \neq 1, m$. We write $m = 2n + 1$ for some positive integer n.

Lemma 2.3.8. *Let $L = L(2b_1, -2, 2b_3, \dots, -2, 2b_m)$ where $b_{2k+1} = -1$ and all the others b_i's are equal to 1 and suppose that $2k+1 \neq 1, m$. Then L is isotopic as unoriented link to to $L(-2k, -2, 2, -2, -2h)$, where $h = n - k$.*

Proof. We will prove this algebraically. We start by computing the fraction associated to the link $L(-2k, -2, 2, -2, -2h)$. We have

$$-2k + \cfrac{1}{-2 + \cfrac{1}{2 + \cfrac{1}{-2 - \cfrac{1}{2h}}}} = -2k + \cfrac{1}{-2 + \cfrac{1}{2 - \cfrac{2h}{4h+1}}} = -2k + \cfrac{1}{-2 + \cfrac{4h+1}{6h+2}} =$$

$$= -2k + \frac{6h+2}{-(8h+3)} = \frac{16kh + 6k + 6h + 2}{-(8h+3)}$$

and this implies $L(-2k, -2, 2, -2, -2h) = b(16kh+6k+6h+2, -(8h+3))$, where $b(p, q)$ denotes the two-bridge link associated to the rational $\frac{p}{q}$.

We now study the fraction corresponding to L. Let

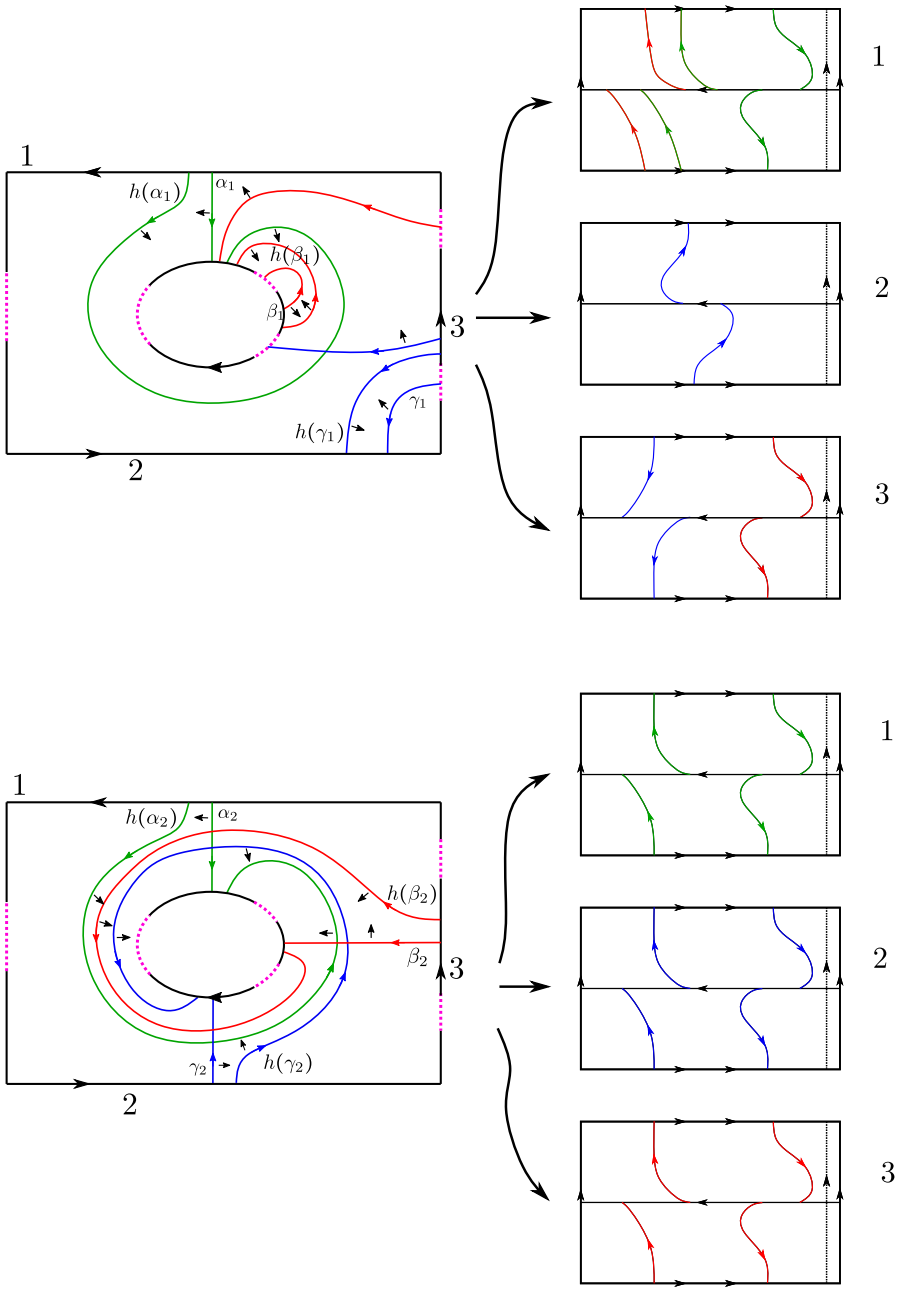

Figure 2.22: The arcs $\alpha_i, \beta_i, \gamma_i$ and their images via the monodromy h, together with the cusp directions of the associated branched surface. The train tracks obtained on the boundary components are also illustrated.

$$\frac{\alpha_{k,h}}{\beta_{k,h}} = 2 + \cfrac{1}{-2 + \cfrac{1}{2 + \cfrac{1}{\ddots + \cfrac{1}{-2 + \cfrac{1}{-2 + \cfrac{q_h}{p_h}}}}}}$$

where we have coloured the -2 corresponding to $2b_{2k+1}$, and where $\frac{p_h}{q_h}$ is defined in the following way

$$\frac{p_h}{q_h} = \overbrace{-2 + \cfrac{1}{2 + \cfrac{1}{-2 + \cfrac{1}{\ddots + \cfrac{1}{2}}}}}^{\text{length } 2h}.$$

It is easy to see that $\frac{p_h}{q_h} = \frac{2h+1}{-2h}$, and hence $p_h = 2h+1$ and $q_h = -2h$.

We now prove by induction on k that

$$\alpha_{k,h} = 16kh + 6k + 6h + 2$$
$$\beta_{k,h} = 16kh - 2h + 6k - 1$$

for every h.

- *Case $k = 1$:* we have that

$$\frac{\alpha_{1,h}}{\beta_{1,h}} = 2 + \cfrac{1}{-2 + \cfrac{1}{-2 + \cfrac{q_h}{p_h}}} = 2 + \cfrac{1}{-2 - \cfrac{1+2h}{6h+2}} = 2 - \frac{6h+2}{14h+5} = \frac{22h+8}{14h+5}$$

  and we use the fact that $\frac{22h+8}{14h+5}$ is a reduced fraction to deduce that $\alpha_{1,h} = 22h+8$ and $\beta_{1,h} = 14h+5$.

- *Case $k > 1$:* we can use the following equality

$$\frac{\alpha_{k,h}}{\beta_{k,h}} = 2 + \cfrac{1}{-2 + \cfrac{\beta_{k-1,h}}{\alpha_{k-1,h}}} = 2 + \frac{\alpha_{k-1,h}}{-2\alpha_{k-1,h} + \beta_{k-1,h}} = \frac{3\alpha_{k-1,h} - 2\beta_{k-1,h}}{2\alpha_{k-1,h} - \beta_{k-1,h}}$$

and the fact that both fractions at the extrema of the this chain of equalities are reduced to deduce that $\alpha_{k,h} = 3\alpha_{k-1,h} - 2\beta_{k-1,h}$ and that $\beta_{k,h} = 2\alpha_{k-1,h} - \beta_{k-1,h}$. Therefore we have

$$\alpha_{k,h} - \beta_{k,h} = \alpha_{k-1,h} - \beta_{k-1,h} = 8h + 3$$
$$\alpha_{k,h} - \alpha_{k-1,h} = 2(\alpha_{k-1,h} - \beta_{k-1,h}) = 16h + 6.$$

These equalities imply

$$\alpha_{k,h} = \alpha_{k-1,h} + 16h + 6 = 16kh + 6k + 6h + 2$$
$$\beta_{k,h} = \alpha_{k,h} - 8h - 3 = 16kh - 2h + 6k - 1$$

and this proves the claim.

To conclude the proof of the lemma we just have to recall from Theorem 1.1.1 that if $\beta' \equiv \alpha + \beta \mod 2\alpha$ then the links $b(\alpha, \beta)$ and $b(\alpha, \beta')$ are isotopic after reversing the orientation of one of the components. In the case of our interest we have

$$\alpha_{k,h} + \beta_{k,h} \equiv -\alpha_{k,h} + \beta_{k,h} \equiv -(8h + 3) \mod 2\alpha_{k,h}$$

and this is exactly what we wanted. □

The description given by the previous lemma allows us to prove:

Proposition 2.3.9. *Let $L = L(2b_1, -2, 2b_3, \ldots, -2, 2b_m)$ where $b_{2k+1} = -1$ and all the others b_i's are equal to 1 and suppose that $2k + 1 \neq 1, m$. Then all the finite Dehn surgeries on L support coorientable taut foliations.*

Proof. By virtue of Lemma 2.3.8 it is equivalent to study surgeries on links of the form $L_{k,h} = L(-2k, -2, 2, -2, -2h)$ where $h > 0$ and $k > 0$. These links can be obtained as surgeries on a 4-components fibered link $\mathcal{L}$, as described in Figure 2.23. Our aim now is to construct foliations on enough surgeries on $\mathcal{L}$.

The monodromy of the link $\mathcal{L}$ is given by $h = \tau_5\tau_3\tau_7\tau_6^{-1}\tau_4\tau_2\tau_1^{-1}$, where τ_i denotes the positive Dehn twist along the curve c_i shown in Figure 2.24 and if we label the components of L and $\mathcal{L}$ as described in Figure 2.23, the surgery coefficients change in the following way

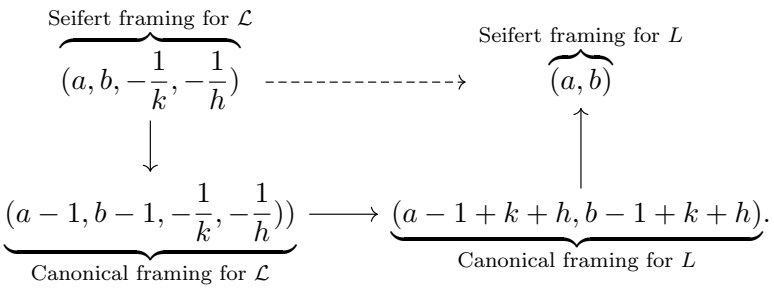

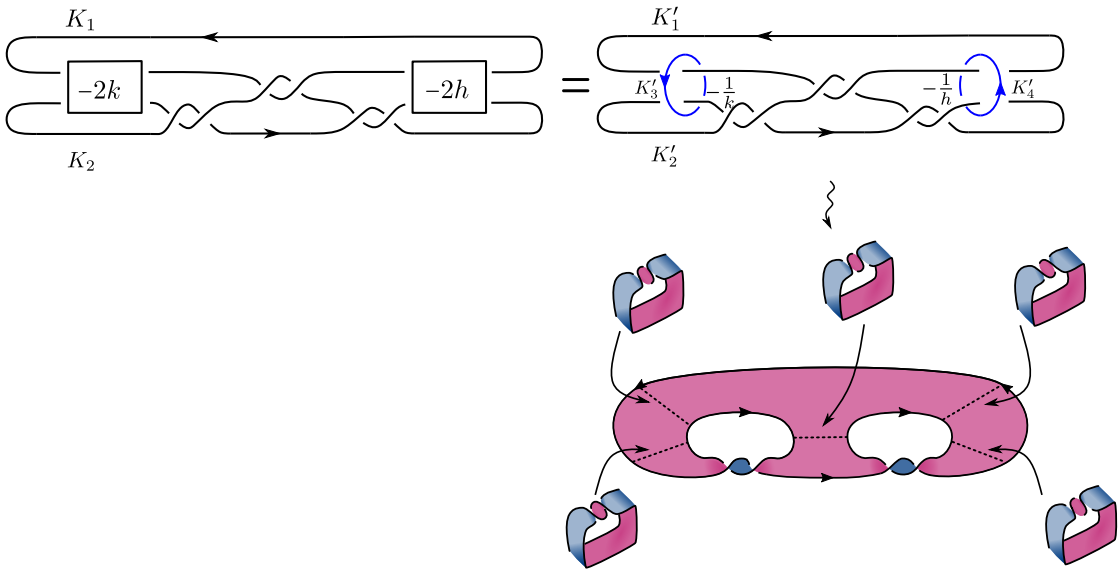

Figure 2.23: How to obtain the link $L(-2k, -2, 2, -2, -2h)$ as surgery on a 4-component link $\mathcal{L}$. We also describe a fiber surface for $\mathcal{L}$, obtained as a sequence of Hopf plumbings.

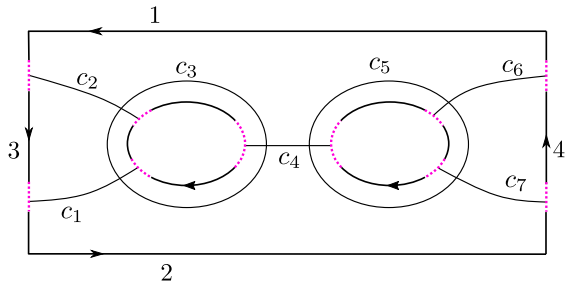

Figure 2.24: An abstract drawing of the fiber surface for the link $\mathcal{L}$, together with the curves c_i's. The boundary component with label i corresponds to the components K_i' of the link, for $i = 1, 2, 3, 4$.

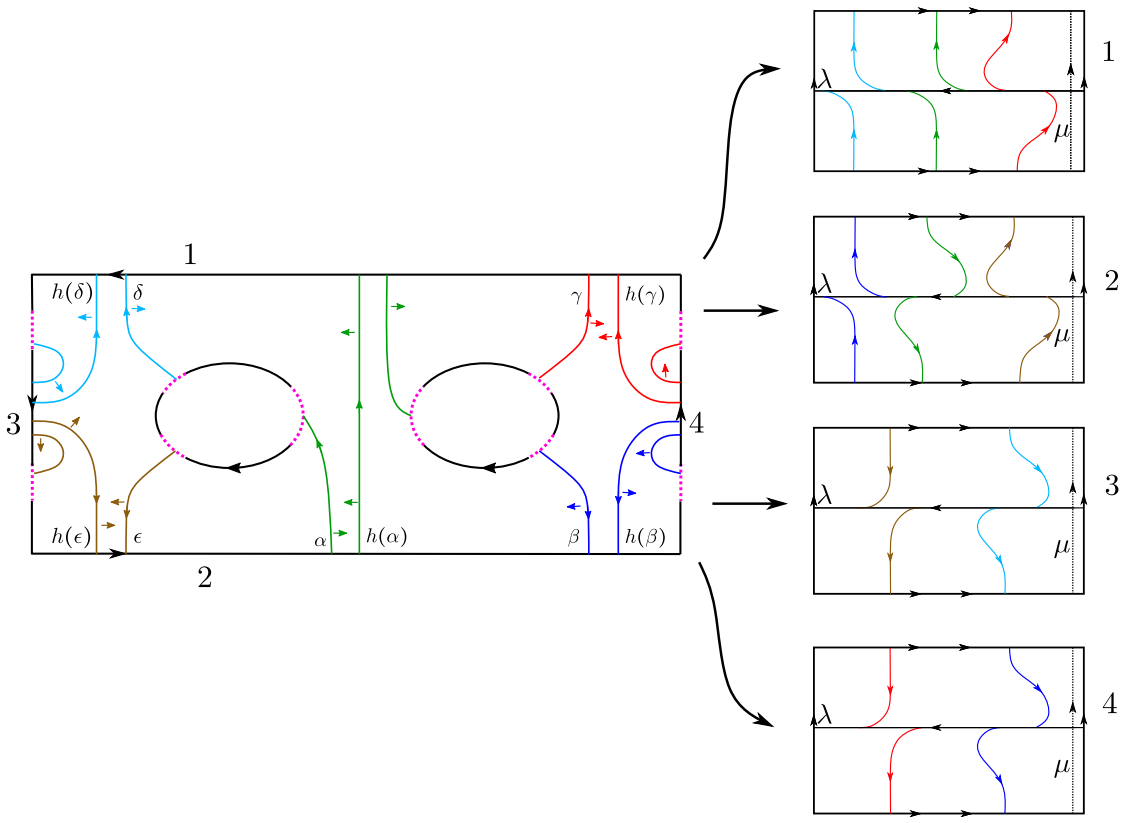

Figure 2.25: The arcs $\alpha, \beta, \gamma, \delta, \epsilon$ and the boundary train tracks of the associated branched surface.

As usual, when constructing foliations it is more natural to work with the framings given by the Seifert surfaces.

We construct two branched surfaces in the exterior of $\mathcal{L}$. The first one is associated to the arcs $\alpha, \beta, \gamma, \delta, \epsilon$ depicted in Figure 2.25. The complement of these arcs in the fiber surface is not a disc (it is easier to see this by considering the complement of the images of these arcs via the diffeomorphism h) and the branched surface does not contain sink discs nor half sink discs. Therefore we can apply Proposition 2.2.4 and deduce that there exist taut foliations on all the surgeries on $\mathcal{L}$ corresponding to multislopes in $(0, \infty) \times \mathbb{R} \times (\infty, 0) \times (\infty, 0)$.

The second branched surface is the one associated to the arcs described in Figure 2.26. In this case we are able to construct foliations on the surgeries corresponding to multislopes in $(\infty, 1)^4$.

This implies that for every $k > 0$ and $h > 0$ all the surgeries on the link $L_{k,h}$ corresponding to multislopes in $(0, \infty) \times \mathbb{R}$ and in $(\infty, 1)^2$ support a coorientable taut foliation. The conclusion follows using the fact that all these links are symmetric.

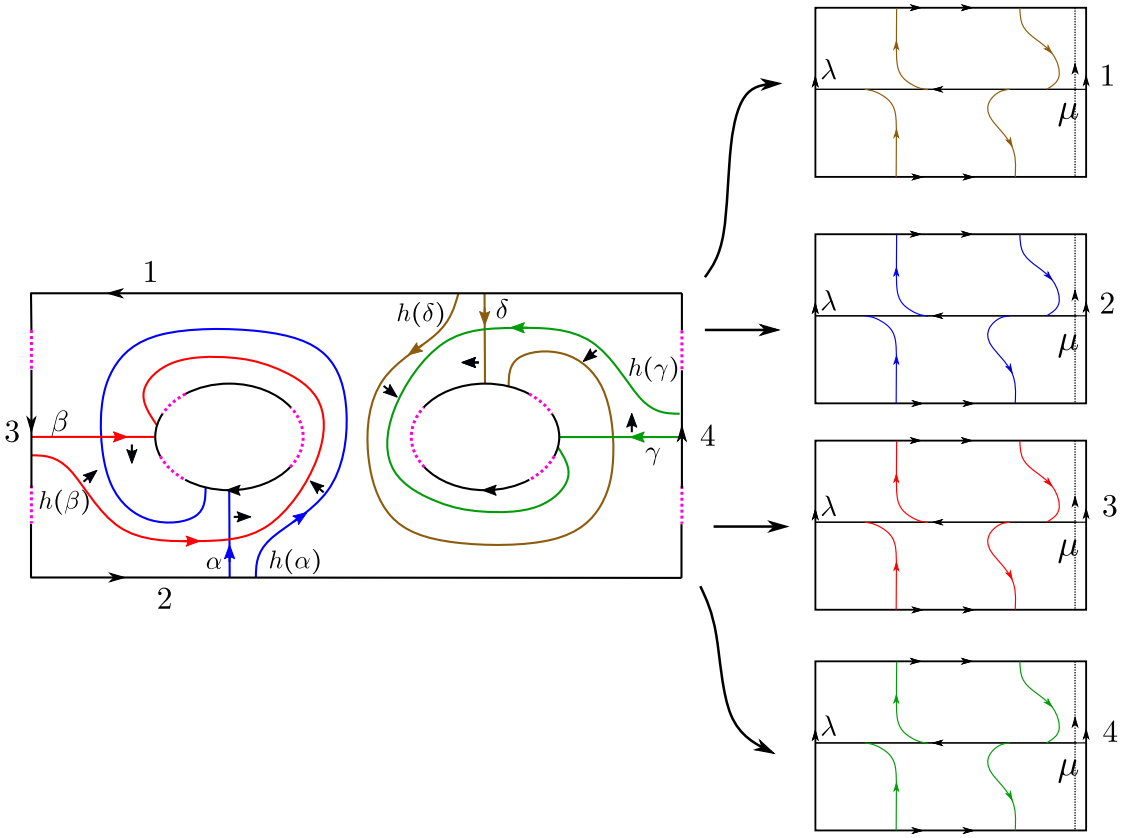

Figure 2.26: The arcs $\alpha, \beta, \gamma, \delta$ used to construct the second branched surface and the train tracks obtained on the boundary.

□

Now we only have to study the links $L = L(2b_1, -2, 2b_3, \dots, -2, 2b_{2n+1})$ where $b_1 = -1$ and all the other b_i's are 1, or where $b_{2n+1} = -1$ and all the other b_i's are 1. The link $L(a_1, a_2, \dots, a_{2n+1})$ is isotopic to $L(a_{2n+1}, \dots, a_2, a_1)$, so we can reduce our study to the case when $b_{2n+1} = -1$ and we denote the corresponding link by L_n. Recall that in Chapter 1 we had already denoted some links by L_n; this is not a coincidence,

Lemma 2.3.10. *The link L_n is isotopic as unoriented link to the link $L(2, -2, -2n)$, illustrated in Figure 3 and studied in Chapter 1.*

Proof. We compute the fractions associated to these links. The one associated to $L(2, -2, -2n)$ is $\dfrac{6n+2}{4n+1}$. Therefore by Theorem 1.1.1 the link $L(2, -2, -2n)$ is isotopic, after reversing the orientation of one of the components, to the link defined by the fraction $\dfrac{6n+2}{-(2n+1)}$.

The fractions $\dfrac{p_n}{q_n}$ associated to L_n satisfy the following recursive equation

$$\frac{p_n}{q_n} = 2 + \frac{1}{-2 + \dfrac{q_{n-1}}{p_{n-1}}} = 2 + \frac{p_{n-1}}{-2p_{n-1} + q_{n-1}} = \frac{3p_{n-1} - 2q_{n-1}}{2p_{n-1} - q_{n-1}}. \tag{2.1}$$

Let us find an explicit formula for p_n and q_n. It follows from Equation (2.1) that

$$p_n - q_n = p_{n-1} - q_{n-1}$$

and as a consequence the quantity $p_i - q_i$ does not depend on the index i. Moreover, Equation (2.1) also implies

$$p_n - p_{n-1} = q_n - q_{n-1} = 2(p_{n-1} - q_{n-1})$$

and therefore also the quantity $p_i - p_{i-1} = q_i - q_{i-1}$ is constant in i. As when $n = 1$ we have $\dfrac{p_1}{q_1} = \dfrac{8}{5}$, we deduce $p_n = 8 + (n-1)6 = 6n + 2$ and $q_n = 5 + (n-1)6$. To conclude the proof is enough to observe that $-(2n+1) \equiv q_n^{-1} \mod 2p_n$ and use again Theorem 1.1.1. □

Recall that by Proposition 1.2.7 we have $\big([n, \infty] \times [n, \infty]\big) \cap \overline{\mathbb{Q}}^2 \subset L(L_n)$, where the surgery coefficients are to be considered in the canonical framing. Given that L-spaces do not support coorientable taut foliations, if we prove that all the other (finite) surgeries on L_n support coorientable taut foliations, then the proofs of Theorem A and Theorem B will follow.

First of all we focus our attention to the Whitehead link, i.e. the link L_1.

Theorem 2.3.11. *Let M be a surgery on the Whitehead link. Then M is not an L-space if and only if M supports a coorientable taut foliation.*

Proof. Since two-bridge links have unknotted components, when one of the surgery coefficients is ∞ the possible surgeries are S^3, lens spaces and $S^2 \times S^1$. Therefore we can limit ourselves to study the case when both the coefficients are finite. We virtue of Lemma 2.3.5 and Lemma 2.3.2 we deduce that all surgeries associated to coefficients in

$$(\infty, 1)^2 \quad \cup \quad (0, \infty) \times (\infty, 0) \quad \cup \quad (\infty, 0) \times (0, \infty)$$

contain coorientable taut foliations, see Figure 2.27. To construct foliations on the remaining non L-space surgeries, we use the fiber surface constructed as in Figure 2.9.

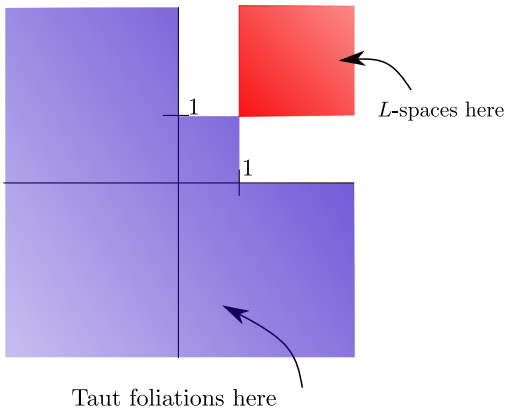

Figure 2.27: The figure describes what we have been able to prove up to now. The blue points are the slopes whose corrisponding surgery supports a coorientable taut foliation; the red points are those whose corresponding surgery is an L-space.

The monodromy is given by $h = \tau_3 \tau_2^{-1} \tau_1$, where τ_i is the positive Dehn twist along the curve c_i of Figure 2.28.

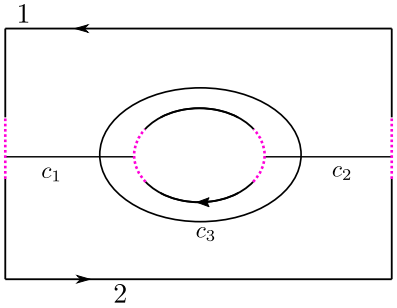

Figure 2.28: An abstract drawing of the fiber surface for the Whitehead link, together with the curves c_i's.

We consider the arcs α and β shown in Figure 2.29. One can check that the branched surface B associated to these arcs has no sink discs nor half sink discs. We can therefore use Proposition 2.2.4 and deduce that all surgeries associated to the multislopes realised by ∂B contain a coorientable taut foliation.

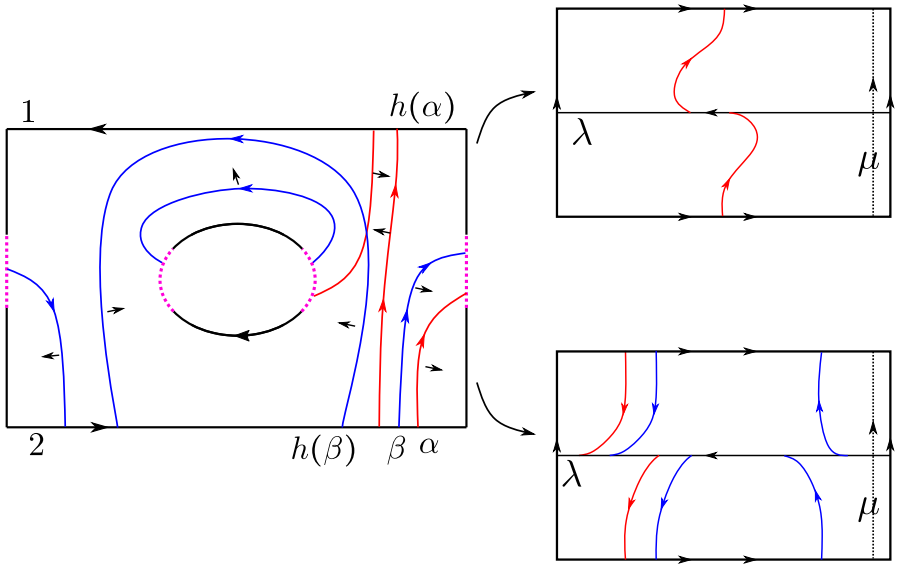

Figure 2.29: The figure describes the arcs α, β, their images via the monodromy h and the boundary train tracks of the associated branched surface.

The train tracks ∂B are shown in Figure 2.29 and they realise all slopes in $(0, \infty) \times (-1, 1)$. This, together with the fact that the Whitehead link is symmetric and that has linking number zero (and therefore Seifert framings and canonical framings coincide) concludes the proof. □

We now conclude the proofs of Theorems A and B by studying the link L_n for $n > 1$.

Proposition 2.3.12. *Let $n > 1$ and let $L_n = L(2b_1, -2, 2b_3, \dots, -2, 2b_{2n+1})$, where $b_{2n+1} = -1$ and all the other b_i's are 1 and let M be a surgery on L_n. Then M is not an L-space if and only if M supports a coorientable taut foliation.*

Proof. We know that, in the canonical framing of L_n, surgeries corresponding to rationals r_1, r_2 such that $r_1 \geq n$ and $r_2 \geq n$ are L-spaces, hence we have to construct taut foliations on the remaining ones. Moreover by Lemma 2.3.10 we have $L_n = L(2, -2, -2n)$ as unoriented links. By using this representation it is evident that $L_n = S^3_{\bullet,\bullet,-\frac{1}{n}}(\mathcal{L})$, where $\mathcal{L}$ is drawn in Figure 2.30. This figure also shows a fiber surface S for $\mathcal{L}$ obtained via a sequence of four Hopf plumbings.

We choose four triples α, β, γ of oriented arcs in S and consider the four branched surfaces in the exterior of $\mathcal{L}$ associated to these arcs, as depicted in Figure 2.31 and

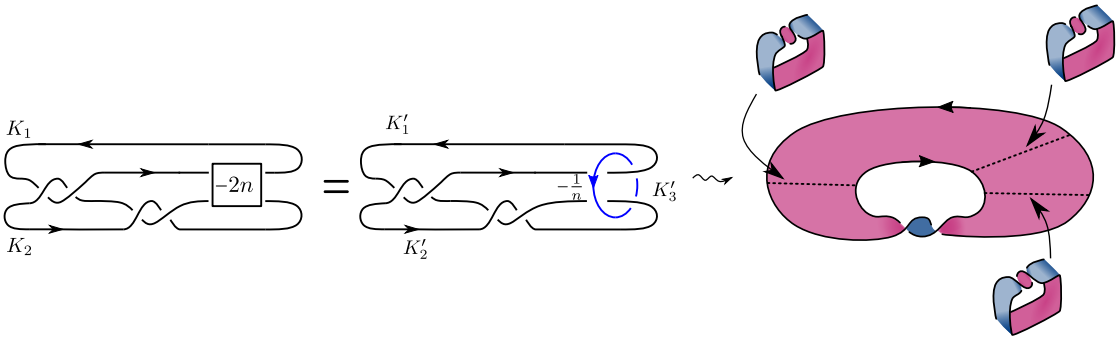

Figure 2.30: How to obtain the links $\{L_n\}_{n\geq 1}$ as surgery on a 3-components link $\mathcal{L}$ and a fiber surface S for $\mathcal{L}$.

Figure 2.32. Each of these triples has the property that its complement in S contains no disc components.

Moreover, it can be checked that these branched surfaces have neither sink discs nor half sink discs. Thus, thanks to Proposition 2.2.4 we only need to study the boundary train tracks of these branched surfaces in order to construct the desired taut foliations. The multislopes realised by these branched surfaces in the Seifert framing of $\mathcal{L}$ are, respectively:

- all the multislopes in $(\infty, 1) \times \mathbb{R} \times (-1, 0)$;
- all the multislopes in $(0, 2) \times (0, \infty) \times (\infty, 0)$;
- all the multislopes in $(0, 2) \times (\infty, 0) \times (-1, 0)$;
- all the multislopes in $(\infty, 2) \times (-1, 1) \times (-1, 0)$.

We now prove that by considering L_n as $-\frac{1}{n}$ surgery on the third component of $\mathcal{L}$, we have constructed the desired foliations on the surgeries on L_n. First of all we observe that

$$\mathrm{lk}(K_1', K_2') = \mathrm{lk}(K_1', K_3') = 1, \quad \mathrm{lk}(K_2', K_3') = -1$$

and by using formula $(\star)$ we deduce the following change of surgery coefficients:

$$\overbrace{(a, b, -\frac{1}{n})}^{\text{Seifert framing for } \mathcal{L}} \quad \to \quad \overbrace{(a-2, b, -\frac{1}{n})}^{\text{Canonical framing for } \mathcal{L}} \quad \to \quad \overbrace{(a+n-2, b+n)}^{\text{Canonical framing for } L_n} .$$

Therefore, for every $n \geq 2$, we obtain taut foliations on all the surgeries on L_n corresponding to multislopes in

- $\mathcal{A} = (\infty, n-1) \times \mathbb{R}$;

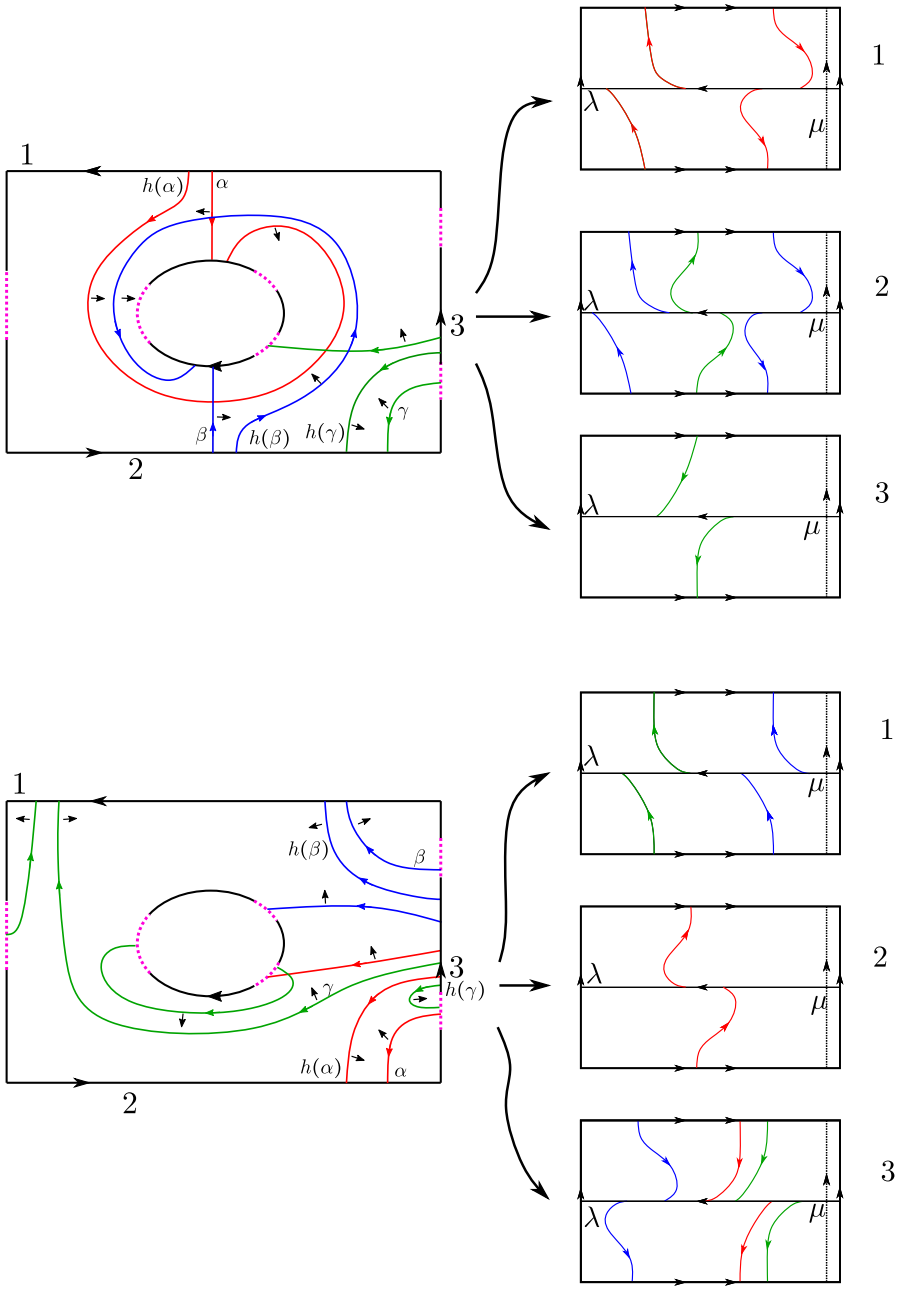

Figure 2.31: How to choose two of the four triples of arcs α, β, γ. The picture also represents their images via the monodromy of $\mathcal{L}$ and the cusp directions and the boundary train tracks of the associated branched surfaces.

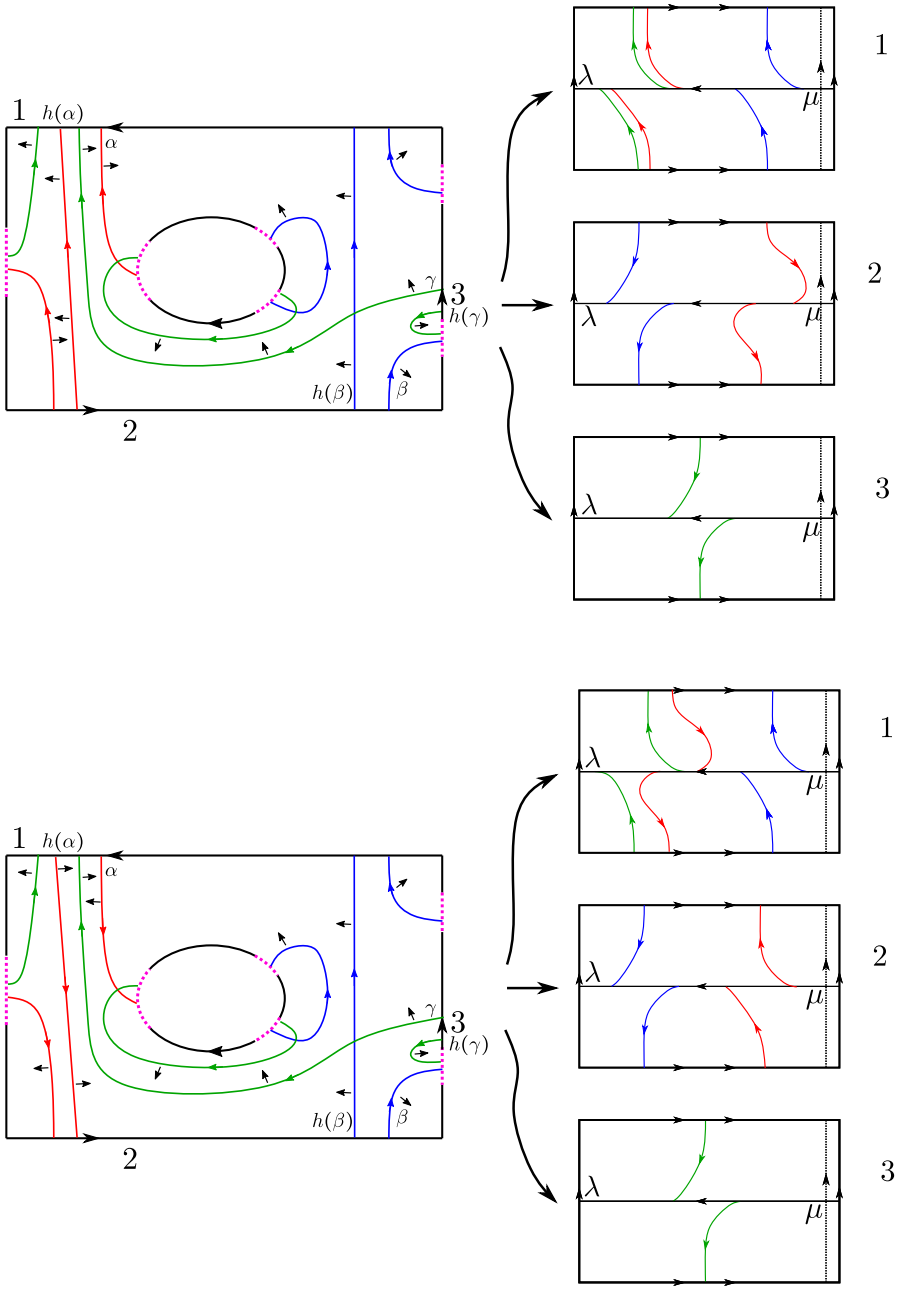

Figure 2.32: How to choose the two other triples of arcs α, β, γ. The picture also represents their images via the monodromy of $\mathcal{L}$ and the cusp directions and the boundary train tracks of the associated branched surfaces.

- $\mathcal{B} = (n-2, n) \times (n, \infty)$;
- $\mathcal{C} = (n-2, n) \times (\infty, n)$;
- $\mathcal{D} = (\infty, n) \times (n-1, n+1)$.

We now show that these four sets are enough to deduce that, for all $n \geq 2$, all the surgeries on L_n corresponding to multislopes (r_1, r_2) where $r_1 < n$ or $r_2 < n$ support a coorientable taut foliation. In fact suppose that we have such a pair (r_1, r_2). Since L_n is symmetric we can suppose that $r_1 < n$ and we have the following cases:

- $r_1 < n-1$*:* in this case the pair is contained in the set $\mathcal{A}$;
- $n-1 \leq r_1 < n$*:* if $r_2 > n$ the pair is contained in $\mathcal{B}$, if $r_2 < n$ we conclude by using the set $\mathcal{C}$ and if $r_2 = n$ we use the set $\mathcal{D}$.

This concludes the proof. □

2.4 Applications to satellite knots and links

In the proof of Theorem A we were able to provide fairly explicit constructions of the foliations. In this section (and also in Chapter 3) we will see how to use this information. In this section we will apply the results obtained so far to study some satellite knots and links.

We start by recalling the satellite operation. Suppose that P is a knot inside a standard solid torus $V = \mathbb{D}^2 \times S^1$ and assume that P is not contained in a 3-ball of V nor isotopic to the longitude of V. Let K be a knot in S^3 and let ϕ be an orientation preserving diffeomorphism between V and a tubular neighbourhood of K. The image of P under ϕ is a knot S, called a *satellite* of K. The knot K is called the *companion* of S and the knot P is called the *pattern* of S. As the mapping class group of the solid torus is non-trivial, the knot S is not uniquely determined by K and P. However, if we fix meridian-longitude bases (μ_K, λ_K) and (μ_V, λ_V) for the tubular neighbourhood of K and for V and impose that ϕ maps μ_V to μ_K and λ_V to λ_K as oriented curves, then S is uniquely determined by K and P.

Let L be a fibered hyperbolic two-bridge link, let denote by K_0 one of its component and orient it arbitrarily. Since two-bridge links have unknotted components, the exterior of K_0 is a solid torus V and we can use the other component as pattern P for producing satellite knots. For convenience, we call *two-bridge replacement* this specific satellite operation. We also fix a meridian-longitude basis for V given by $(\mu_V, \lambda_V) = (\lambda_{K_0}, \mu_{K_0})$, where μ_{K_0} and λ_{K_0} are the canonical meridian and longitude of K_0.

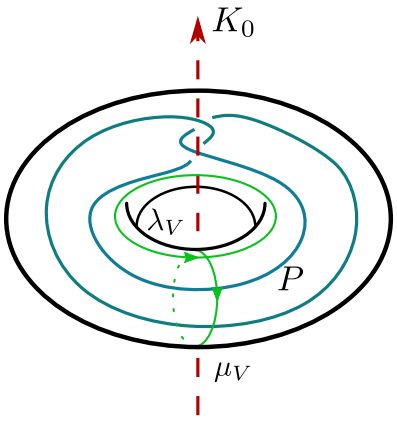

Figure 2.33: The (positive clasped) Whitehead pattern. The meridian μ_V is given by the longitude of the knot K_0 and the longitude λ_V by its meridian. By considering the mirror of the Whitehead link one obtains the negative clasped Whitehead pattern.

Remark 2.4.1. If L is the Whitehead link we obtain the Whitehead pattern. This is the pattern used to define Whitehead doubles of knots, see Figure 2.33. Thus, two-bridge replacement generalises Whitehead doubling.

We remark that in the definition of two-bridge replacement we ask L to be fibered and hyperbolic.

Of course if $\mathcal{L}$ is a link with d components we can carry out this construction for each component, by choosing $L_1, \dots, L_d$ possibly distinct fibered hyperbolic two-bridge links.

The proof of Theorem A , together with results from [53] and [73] imply the following:

Theorem 2.4.2. *Let $\mathcal{L}$ be a fibered link with positive genus or any non-trivial knot and let $\mathcal{L}'$ denote the link obtained by performing two-bridge replacement on each component of $\mathcal{L}$. Then all the manifolds obtained by doing surgery on each component of $\mathcal{L}'$ along a non-meridional slope support a coorientable taut foliation.*

Proof. • We first analyse the case where $\mathcal{L}$ is a non-trivial knot, and we denote it by K. We use the notation introduced above, and so we denote by $L = K_0 \sqcup P$ the fibered hyperbolic two-bridge link used in the definition of two-bridge replacement. Moreover we denote by E_K the exterior of K and by E_L the exterior of L. We fix the canonical meridian-longitude basis (μ_K, λ_K) for the knot K and we use it to identify slopes on K with $\mathbb{Q} \cup \{\infty\}$. The map ϕ, used to define the satellite operation, between the exterior of K_0, that we denote by V, and a tubular neighbourhood of K satisfies:

$$\phi(\lambda_{K_0}) = \phi(\mu_V) = \mu_K$$
$$\phi(\mu_{K_0}) = \phi(\lambda_V) = l\mu_K + \lambda_K$$

for some integer $l \in \mathbb{Z}$. By [73, Theorem 1.1] if K is a non-trivial knot then there exists an interval $(-a, b)$, where $a, b > 0$, such that for every slope $s \in (-a, b)$ there exists a coorientable taut foliation on E_K intersecting the boundary torus in a collection of circles of slope s. Given two coprime integers p, q the map ϕ satisfies

$$p\mu_K + q\lambda_K = \phi((p - ql)\lambda_{K_0} + q\mu_{K_0})$$

and therefore the slope $\frac{p}{q}$ on K corresponds to the slope $(\frac{p}{q} - l)^{-1}$ on K_0. Hence the interval $(-a, b)$ is identified with a neighbourhood U_1 of $-\frac{1}{l} \subset \overline{\mathbb{Q}}$. It follows by the proof of Theorem A that if L is a fibered hyperbolic two-bridge link then for every integer $l \in \mathbb{Z}$ and every neighbourhood U of $-\frac{1}{l} \subset \overline{\mathbb{Q}}$ there exists a slope $r \in U$ such that for every non-meridional slope r' on P there is a coorientable taut foliation on E_L intersecting the boundary tori in circles of slopes r and r' respectively. If we denote by K' the result of two-bridge replacement on K, then $E_{K'} = E_K \cup_\varphi E_L$, where φ is the restriction of ϕ to the boundary of the solid torus V. By choosing a slope $r \in U_1$ guaranteed by the previous observation we are able to find for each non-meridional slope r' in $E_{K'}$ taut foliations $\mathcal{F}$ on E_K and $\mathcal{F}'$ on E_L that can be glued along φ to define a coorientable taut foliation in $E_{K'}$ intersecting the boundary in parallel curves of slope r'. By capping off with meridional discs, these foliations extend to the surgeries on K'.

- When $\mathcal{L} = K_1 \sqcup \cdots \sqcup K_d$ is a fibered link with multiple components and positive genus we can proceed in analogous way. Let S denote the fiber surface for $\mathcal{L}$. By intersecting S with the boundaries of tubular neighbourhoods of the knots $K_1, \ldots, K_d$ we obtain longitudes $\lambda_1^S, \ldots \lambda_d^S$. We use them to define meridian-longitude bases for the components of $\mathcal{L}$ and to identify slopes on the exterior of $\mathcal{L}$ with $\overline{\mathbb{Q}}^d$. It follows by [53, Theorem 1.1] that for every multislope $(r_1, \ldots, r_d)$ in a neighbourhood of $0 \in \overline{\mathbb{Q}}^d$ there exists a coorientable taut foliation in the exterior of $\mathcal{L}$ intersecting the boundary tori in parallel curves of slopes $r_1, \ldots, r_d$ respectively. The statement now follows by applying to each component of $\mathcal{L}$ the same reasoning as in the previous case, where we never made use of the fact that λ_K was the canonical longitude of K.

  This concludes the proof □

Two-bridge replacement generalises Whitehead doubling and we emphasise the following corollary.

Corollary 2.4.3. *Let K be a non-trivial knot and let K' be any Whitehead double of K. Then all non-trivial surgeries on K' support a coorientable taut foliation.*

Appendix

2.A Constructing foliations on fillings of some punctured torus bundles over the circle

In this appendix we show how to construct foliations on fillings of some punctured torus bundles over the circle. We start by fixing some notation. We suppose that S is a torus with k open discs removed. We consider the curves $\gamma_0, \gamma_1, \dots, \gamma_k$ and we label the boundary components of S with numbers in $\{1, \dots, k\}$ as in Figure 2.A.1. We also orient S so that the orientation induced on the boundary components is the one of the figure.

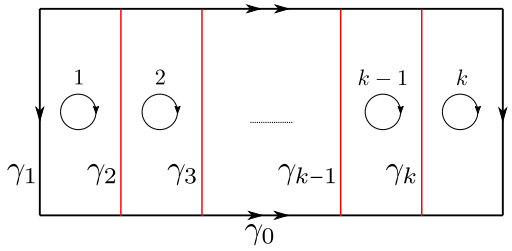

Figure 2.A.1: The oriented torus S with the labelled boundary components.

We denote with τ_i the positive Dehn twist along the curve γ_i. Notice that since $\gamma_i \cap \gamma_j = \emptyset$ for $i \neq j$ and $i, j \in \{1, \dots, k\}$ we have that $\tau_i \tau_j = \tau_j \tau_i$ for $i, j = 1, \dots, k$.

We focus on homeomorphisms of S of the following type:

$$h = \tau_0^{a_0} \tau_1^{a_1} \cdots \tau_k^{a_k} \quad a_0 \in \mathbb{Z},\ a_i \in \mathbb{Z} \setminus \{0\} \text{ for } i \neq 0$$

where the factorisation of h should be read from right to left.

We fix the following convention:

Convention: *the indices* $1, \dots, k$ *have to be considered ordered cyclically; so we set* $a_{k+1} = a_1$ *and think of* a_1 *as consecutive to* a_k*.*

Let $\partial_i S$ denote the boundary component of S labelled with i. Given such a homeomorphism h we assign to $\partial_i S$ a label with the following rule:

- we assign to $\partial_i S$ the label p_+ if a_i and a_{i+1} are both positive;
- we assign to $\partial_i S$ the label p_- if a_i and a_{i+1} are both negative;
- we assign to $\partial_i S$ the label n if a_i and a_{i+1} have different signs.

Figure 2.A.2 shows an example. Notice that in this example, following our convention, to assign a label to $\partial_3 S$ we have to check the signs of a_3 and a_1, since a_1 is consecutive to a_3. Also notice that when $k = 1$, *i.e.* S has only one boundary component we have that $\partial_1 S$ has label p_+ when a_1 is positive and label p_- when a_1 is negative.

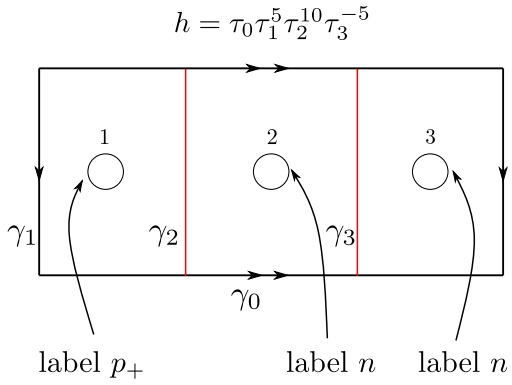

Figure 2.A.2: Example with $h = \tau_0\tau_1^5\tau_2^{10}\tau_3^{-5}$.

Finally we assign to each boundary component $\partial_i S$ two intervals I_i and J_i in $\overline{\mathbb{Q}}$ in the following way:

- if $\partial_i S$ has label p_+ we set $I_i = J_i = (\infty, 1)$;
- if $\partial_i S$ has label p_- we set $I_i = J_i = (-1, \infty)$;
- let $i_1 < \cdots < i_{2c}$ the indices of the boundary components labelled with n. We set $I_{i_a} = (\infty, 0)$ when $a \in \{1, \dots, 2c\}$ is odd and we set $I_{i_a} = (0, \infty)$ when $a \in \{1, \dots, 2c\}$ is even.

  Therefore we have $I_{i_1} = (\infty, 0)$, $I_{i_2} = (0, \infty)$, $I_{i_3} = (\infty, 0)$ and so on.

  On the contrary, we set $J_{i_a} = (0, \infty)$ when $a \in \{1, \dots, 2c\}$ is odd and $J_{i_a} = (\infty, 0)$ when $a \in \{1, \dots, 2c\}$ is even.

Example 2.A.1. In the example of Figure 2.A.2 we have

$$I_1 = J_1 = (\infty, 1)$$

$$I_2 = (\infty, 0) \quad J_2 = (0, \infty)$$

$$I_3 = (0, \infty) \quad J_3 = (\infty, 0).$$

We are now ready to state the theorem. In the statement of the theorem, for each boundary torus T_i of the manifold M_h we have fixed as longitude the oriented curve $\partial_i S$ and as meridian the image in M_h of the curve $\{x_i\} \times [0,1]$, oriented as $[0,1]$, where $x_i \in \partial_i S$.

Theorem 2.A.2. *Let S be a k-holed torus as in Figure 2.A.1 and let h be a homeomorphism of S of the following form:*

$$h = \tau_0^{a_0} \tau_1^{a_1} \cdots \tau_k^{a_k}$$

where $a_0 \in \mathbb{Z}$ and $a_i \in \mathbb{Z} \setminus \{0\}$ for $i = 1, \ldots, k$. Then:

1. *if $a_0 > 0$ (resp. $a_0 < 0$) then $M_h(s_1, \ldots, s_k)$ supports a coorientable taut foliation for each multislope $(s_1, \ldots, s_k) \in (\infty, 1)^k$ (resp. $(-1, \infty)^k$);*
2. *for any multislope $(s_1, \ldots, s_k) \in (I_1 \times \cdots \times I_k) \cup (J_1 \times \cdots \times J_k)$, the filled manifold $M_h(s_1, \ldots, s_k)$ supports a coorientable taut foliation, where the intervals I_i's and J_i's are the ones described above.*

Remark 2.A.3. Notice that if h' is conjugated in $\mathrm{MCG}(S, \partial S)$ to a homeomorphism h that satisfies the hypotheses of Theorem 2.A.2, then the conclusion of the theorem holds also for $M_{h'}$.

2.A.1 Proof of the first part of Theorem 2.A.2

To prove Theorem 2.A.2 we will build branched surfaces in M_h satisfying the hypotheses of Theorem 2.1.11 by following the construction presented before Lemma 2.2.2.

We start by proving the first part of the theorem. We define a branched surface as follows. We consider the parallel arcs $\alpha_1, \ldots, \alpha_k$ depicted in Figure 2.A.3.

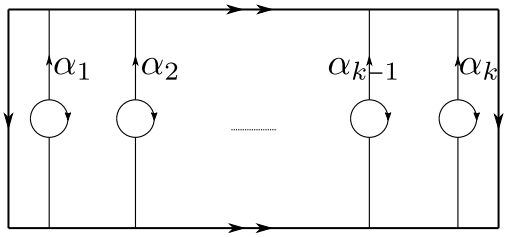

Figure 2.A.3: The parallel arcs $\alpha_1 \ldots, \alpha_k$

We consider the discs $\alpha_i \times [0,1]$, perturb them in a neighbourhood of $S \times \{1\}$ as explained in the discussion before Lemma 2.2.2, and project them to the mapping torus M_h. We consider the (co)oriented branched surface B in M_h obtained by adding these discs D_i to the surface S. The discs D_i's are oriented so that the orientation on their

boundary induces the given orientation on the arcs α_i's. For an example, see Figure 2.A.4, where also some cusp directions are showed. Recall that a good way to deduce the cusp directions along the arcs α_i's and $h(\alpha_i)$'s is the following: they point to the right along the arcs α_i's and they point to the left along the arcs $h(\alpha_i)$'s, where the latter are oriented as the image of the arcs α_i's.

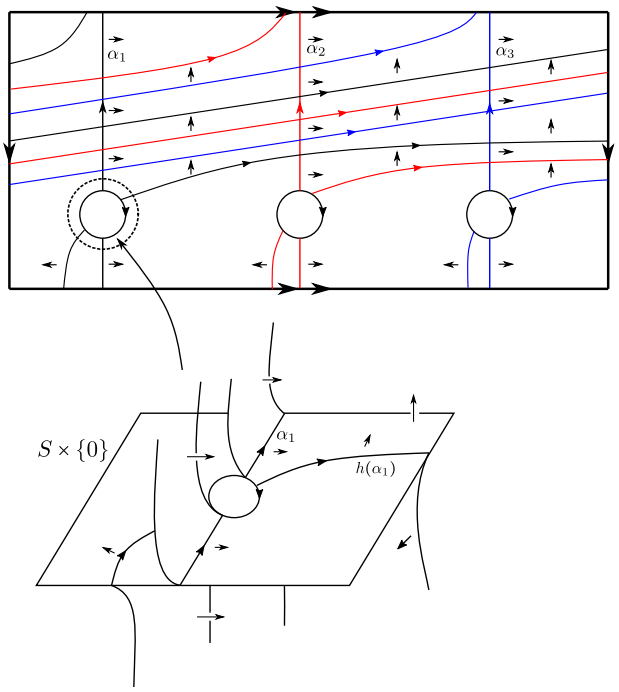

Figure 2.A.4: In this example, $a_0 = 2$ and $k = 3$. We also show the details of our branched surface in a neighbourhood of $\partial_1 S$.

Lemma 2.A.4. *The branched surface B has no sink discs or half sink discs.*

Proof. There are k sectors of B that are half discs and that coincide with the discs D_i's; these sectors are never sink by construction (see Figure 2.8). The other sectors coincide with the abstract closures of the connected components of $S \setminus (\bigcup_i \alpha_i \cup h(\alpha_i))$. Being a_0 non-zero, these sectors are discs and half discs[3]. We can organise these sectors in the following way. We refer to Figure 2.A.4 to visualise the situation. If we cut S along the arcs α_i's we obtain k oriented annuli $A_1, \dots, A_k$, so that $\partial A_i \supset -\alpha_i \cup \alpha_{i+1}$ for $i \in \{1, \dots, k\}$, where $-\alpha_i$ denotes the arc α_i with the opposite orientation. Also notice that the cusp directions along α_i point inside A_i and the cusp directions along α_{i+1} point outside A_i.

It follows by the definition of the arcs α_i that $h(\alpha_i) = \tau_0^{a_0}(\alpha_i)$. Each of these annuli intersects $h(\alpha_j)$ in $|a_0|$ subarcs, for each $j = 1, \dots, k$. Therefore, when we cut along the

[3]When the product $k|a_0|$ satisfies $k|a_0| \leq 3$ there are only half disc sectors.

$h(\alpha_i)$'s we subdivide each of this annuli in $k|a_0|$ discs and these discs coincide with the sectors of B in S. By construction each of these discs is contained in an annulus, say A_i, and intersects both α_i and α_{i+1} and therefore there is a cusp direction pointing outside it. □

Since the branched surface B has no sink discs or half sink discs we can apply Proposition 2.2.4 and to conclude the proof of the first part of Theorem 2.A.2 we need to study the boundary train tracks of B.

Proposition 2.A.5. *If $a_0 > 0$, $M_h(s_1, \dots, s_k)$ contains a coorientable taut foliation for each multislope $(s_1, \dots, s_k) \in (\infty, 1)^k$. If $a_0 < 0$ the same happens for each multislope $(s_1, \dots, s_k) \in (-1, \infty)^k$.*

Proof. We study the multislopes realised by ∂B. The boundary train tracks of B are all the same for each boundary tori, and only depend on the sign of a_0. The two possible types of boundary train tracks are depicted in Figure 2.A.5.

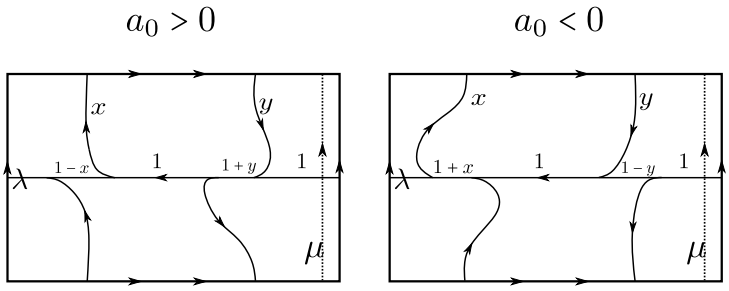

Figure 2.A.5: The two possible boundary train tracks with weight systems.

We also endowed the two train tracks with weight systems. The slopes of these weight systems are always $x - y$, but since we have to impose that each sector of the train tracks has positive weight we have that:

- if $a_0 > 0$, x can vary in $(0, 1)$ and y can vary in $(0, +\infty)$;
- if $a_0 < 0$, x can vary in $(0, +\infty)$ and y can vary in $(0, 1)$.

By letting x, y vary we have that when $a_0 > 0$ the boundary train tracks realise all multislopes in $(\infty, 1)^k$ and when $a_0 < 0$ the boundary train tracks realise all slopes in $(-1, \infty)^k$. By applying Proposition 2.2.4 we conclude the proof. □

Remark 2.A.6. In the terminology of [53], if $|a_0| = 1$ then the pair of parallel k-uples

$$(\widetilde{h(\alpha)}, \alpha)$$

is good and oriented, where $\alpha = (\alpha_1, \dots, \alpha_k)$ and $\widetilde{h(\alpha)} = (\widetilde{h(\alpha_1)}, \dots, \widetilde{h(\alpha_k)})$. In this case the branched surface constructed in the previous discussion coincides with the branched surface associated to the sequence $(h(\alpha), \alpha)$ by Kalelkar and Roberts in [53].

2.A.2 Proof of the second part of Theorem 2.A.2

We now focus our attention on the second part of Theorem 2.A.2 and we define a new branched surface. We fix a new set of arcs $\alpha_1, \dots, \alpha_k$ in the following way. We consider arcs $\beta_1, \dots, \beta_k$ as in Figure 2.A.6 and choose α_i so that $h(\alpha_i) = \beta_i$. One example is depicted in Figure 2.A.7.

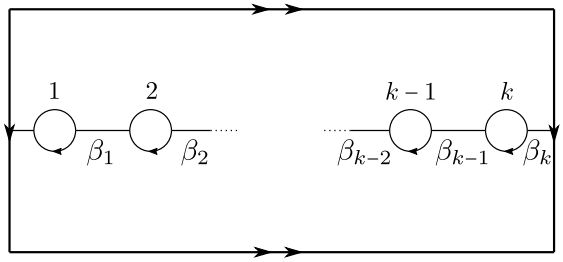

Figure 2.A.6: The arcs β_i's.

We now give orientations to the arcs α_i's in order to build our branched surfaces. It will be simpler to state how to assign orientations to the β_i's and we will orient each α_i as isotopic to $h^{-1}(\beta_i)$, for $i = 1, \dots, k$.

Definition 2.A.7. We say that an orientation of the arcs β_i's is *coherent* if the following hold:

- if a boundary component $\partial_i S$ has label p_+ or p_- the arcs β_{i-1} and β_i intersecting $\partial_i S$ are oriented so that the first starts at $\partial_i S$ and the second ends at $\partial_i S$, or viceversa. In this case we say that β_{i-1} and β_i *have the same direction*;

- if a boundary component $\partial_i S$ has label n the arcs β_{i-1} and β_i intersecting $\partial_i S$ are oriented so that both start or both end at $\partial_i S$. In this case we say that β_{i-1} and β_i *have opposite directions*. In case the arcs both start at $\partial_i S$ we say that the component is of type $n_{\mathbf{o}}$ (the subscript **o** stands for "out") and if both end at $\partial_i S$ we say that is of type $n_{\mathbf{i}}$ (**i** standing for "in").

See Figure 2.A.7 for an example[4]. Notice that there is always an even number of boundary components of S with label n. Moreover the boundary components with label n are alternately of type $n_{\mathbf{o}}$ and $n_{\mathbf{i}}$. We will soon use coherent orientations to build branched surfaces. First of all we prove the following lemma.

Lemma 2.A.8. *There always exist exactly two different coherent orientations of the arcs β_i's.*

[4]recall that the factorisation of the monodromy h is to be read from right to left; this should help to figure out why $h(\alpha_i) = \beta_i$.

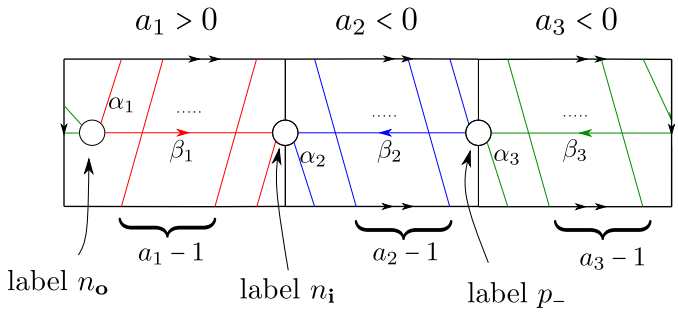

Figure 2.A.7: An example of a coherent orientation. In this case the arcs β_2 and β_3 have the same direction, while the arcs β_1 and β_2 and the arcs β_3 and β_1 have opposite directions.

Proof. We fix an orientation of the arc β_1. We prove that there exists a unique coherent orientation of the arcs β_i's agreeing with the fixed orientation on β_1 and this implies the thesis. We orient the arcs β_i's inductively. Suppose that we have oriented $\beta_1, \dots, \beta_j$. Then:

- if $\partial_{j+1}S$ has label p_+ or p_- we orient β_{j+1} so that it has the same direction of β_j;
- if $\partial_{j+1}S$ has label n we orient β_{j+1} so that its direction is opposite to the one of β_j.

In other words, once we have fixed an orientation on β_1 the coherence condition completely determines the orientations of $\beta_2, \dots, \beta_k$. The only thing to be checked in order to prove that this orientation is actually coherent is the behaviour of β_k and β_1 at $\partial_1 S$. Since there is always an even number of boundary components of S with label n it follows that:

- if $\partial_1 S$ has label p_+ or p_- then the direction changes an even number of times between β_1 and β_k and therefore β_1 and β_k have the same direction;
- if $\partial_1 S$ has label n then the direction changes an odd number of times between β_1 and β_k and therefore β_1 and β_k have opposite directions.

Therefore the orientation defined in this way is coherent and this concludes the proof. □

We fix a coherent orientation and as usual we consider the branched surface B that is the union of S and the images in M_h of the discs $\alpha_i \times [0,1] \subset S \times [0,1]$. We denote the image of $\alpha_i \times [0,1]$ with D_i and orient the discs D_i's so that the orientation on their boundary induces the given orientation on the α_i's. Exactly as before we have:

Lemma 2.A.9. *The branched surface B has no sink discs or half sink discs.*

Proof. There are k sectors of B that coincide with the discs D_i's and they always have cusp directions pointing outside. We focus our attention on the sectors contained in S. We consider the k annuli A_i obtained by cutting S along the arcs of Figure 2.A.3. Each of these annuli contains in its interior some disc and half disc sectors and intersects two other half disc sectors. The former are never sink because each of these sectors has in its boundary two parallel subarcs of some arc of the α_i's, as for example Figure 2.A.8 shows.

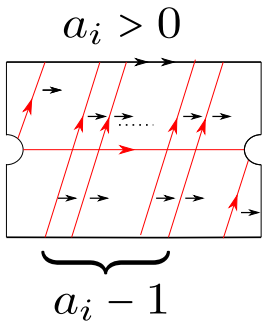

Figure 2.A.8: The annulus A_i.

We now claim the following:

Claim: since we have fixed a coherent orientation of the arcs β_i's, the cusp directions along the arcs α_i's all point in the same direction.

The claim implies that the sectors belonging to two consecutives annuli are never sink because each of these sectors has in its boundary two subarcs of two consecutive arcs of the α_i's. For an example, see Figure 2.A.9.

Proof of the claim: We first notice that when $a_i > 0$ (resp. $a_i < 0$) the cusp direction along the arc α_i has the same (resp. opposite) direction of β_i (recall that the cusp direction always points to the right along the oriented arcs α_i's). Therefore to prove the claim it is sufficient to prove that β_i and β_j have the same direction if and only if $a_i a_j > 0$, and to prove this it is enough to prove that $a_1 a_i > 0$ if and only if β_1 and β_i have the same direction. We prove this by induction on i. If $i = 2$ this follows from the definition of coherent orientation. We suppose now that the thesis is true for i and we prove it for $i + 1$. Suppose that $a_1 a_{i+1} > 0$; then if $a_1 a_i > 0$ we know by inductive hypothesis that β_1 and β_i have the same direction. Moreover we deduce that $a_i a_{i+1} > 0$ and by the definition of coherent orientation that β_i and β_{i+1} have the same direction and therefore also β_1 and β_{i+1} have the same direction. The other cases can be analysed similarly. This concludes the proof of the claim.

□

Proposition 2.A.10. *Let $I_1, \dots, I_k$ and $J_1, \dots, J_k$ be the intervals defined in the discussion before the statement of Theorem 2.A.2 and let B denote the branched surface*

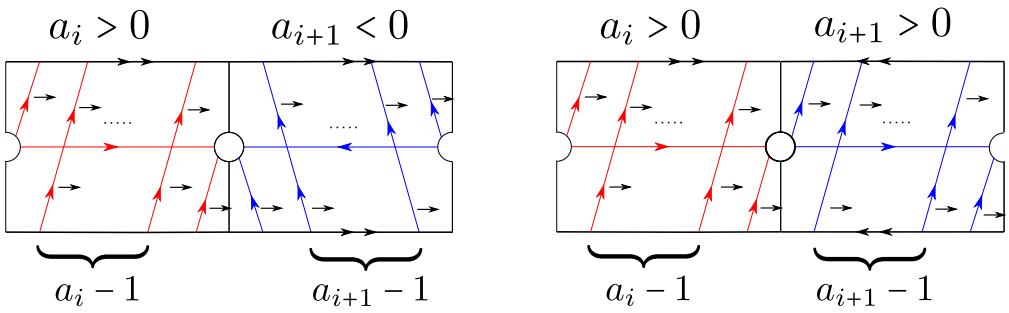

Figure 2.A.9: The figure shows how the choice of a coherent orientation implies that the cusp directions along the arcs α_i's all have the same direction.

associated to a coherent orientation of the arcs β_i's. Then for one choice of coherent orientation of the arcs β_i's, the train track ∂B realises all multislope $(s_1, \dots, s_k)$, for $(s_1, \dots, s_k) \in I_1 \times \cdots \times I_k$. In particular all the fillings associated to these multislopes contain a coorientable taut foliation. Choosing the other coherent orientation yields B whose boundary train track realise all multislope $(s_1, \dots, s_k)$, for $(s_1, \dots, s_k) \in J_1 \times \cdots \times J_k$, and all the filling associated to these multislopes contain coorientable taut foliations.

Proof. We focus our attention on the boundary train tracks of B. For a fixed boundary component of S we have the four possible configurations showed in Figure 2.A.10 and for each of this configurations we have two possible way to fix a coherent orientation.

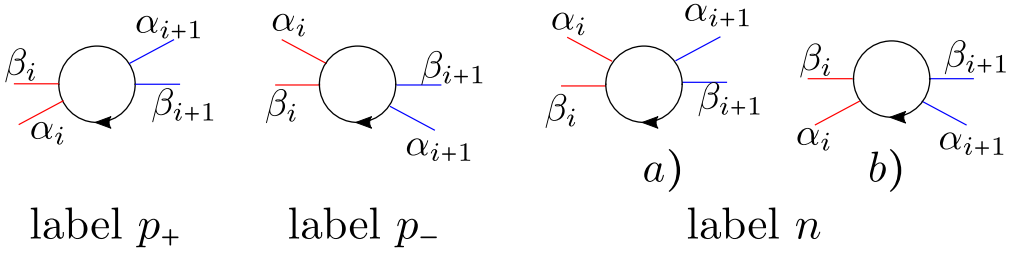

Figure 2.A.10: The four possible configuration of arcs in a neighbourhood of $\partial_{i+1} S$.

If the boundary component has label p_+ or p_- the type of the boundary train track does not depend on the choice of the coherent orientation, and is described in Figure 2.A.11, where for concreteness we have assigned an orientation to the arcs, and where in the middle picture we have also described the branched surface in a neighbourhood of the boundary component. If we consider the other coherent orientation, we obtain the same train tracks. By assigning weights to these train tracks as usual we deduce that if the label is p_+ the train track realises all the slopes in the interval $(\infty, 1)$, while if the label is p_- the slopes realised are those in the interval $(-1, \infty)$.

On the other hand if the boundary component has label n the choice of the orientation yields two different train tracks. We represent the possible train tracks in Figure 2.A.12.

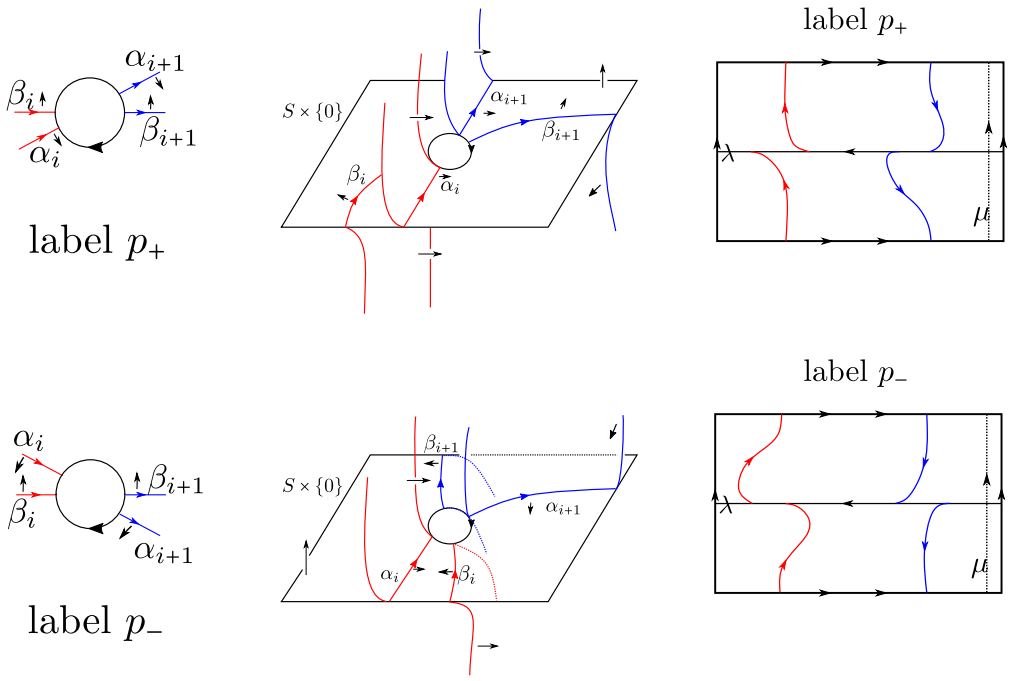

Figure 2.A.11: In this figure we describe the branched surface in a neighbourhood of the $(i+1)$-th boundary component of M_h and its boundary train track in the case of label p_+ and p_-.

Notice that the train tracks depend only on the orientation of the arcs, and not on the label a) or b) of the configuration.

The train tracks on the left realise all the slopes in the interval $(0, \infty)$, while those on the right realise the slopes in the interval $(\infty, 0)$.

By fixing one or the other of the two possible coherent orientations, we have that the boundary train tracks of B realise all the multislopes in $I_1 \times \cdots \times I_k$ and $J_1 \times \cdots \times J_k$. By virtue of Lemma 2.A.9, we know that B is laminar and we can apply Proposition 2.2.4 to obtain the desired foliations. □

Example 2.A.11. For each natural number n we consider the n-component oriented link $\mathcal{L}_n$ in Figure 2.A.13.

We can represent the link $\mathcal{L}_n$ in a different way, as in Figure 2.A.14. With this representation, it is evident that $\mathcal{L}_n$ can be realised as a plumbing of Hopf bands. Therefore $\mathcal{L}_n$ is a fibered link, with fiber surface a torus with n open discs removed, and the monodromy associated to this fiber is

$$h = \tau_0^{-1} \tau_1 \dots \tau_n$$

where τ_i is the positive Dehn twist along the curve γ_i.

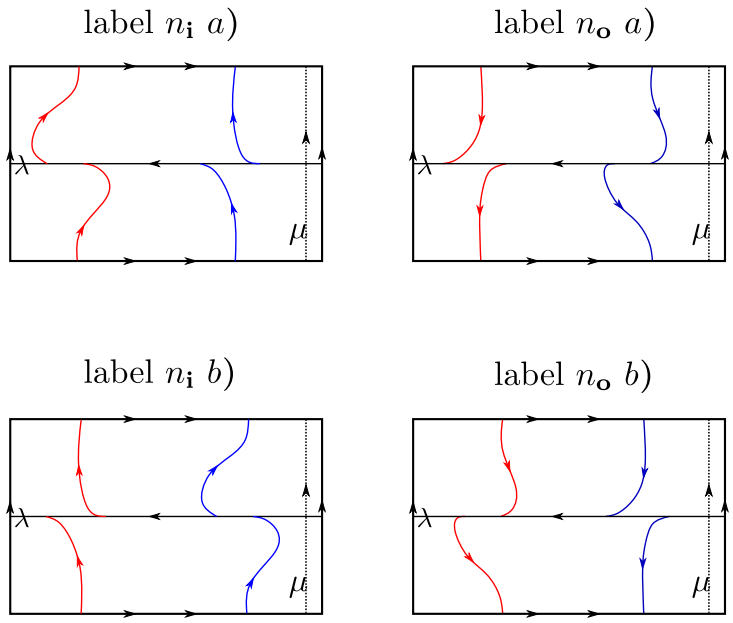

Figure 2.A.12: The possible boundary train tracks associated to a boundary component with label n. Notice that the train tracks depend only on the orientation of the arcs, and not on the label a) or b) of the configuration.

We now prove that $\mathcal{L}_n$ is a hyperbolic link. We recall the following theorem of Penner [91]:

Theorem 2.A.12. ([91]) *Suppose that $\mathcal{C}$ and $\mathcal{D}$ are each disjointly embedded collections of essential simple closed curves (with no parallel components) in an oriented surface F so that $\mathcal{C}$ hits $\mathcal{D}$ efficiently and $\mathcal{C} \cup \mathcal{D}$ fills F. Let $R(\mathcal{C}^+, \mathcal{D}^-)$ be the free semigroup generated by the Dehn twists $\{\tau_c^{+1} : c \in \mathcal{C}\} \cup \{\tau_d^{-1} : d \in \mathcal{D}\}$. Each component map of the isotopy class of $w \in R(\mathcal{C}^+, \mathcal{R}^-)$ is either the identity or pseudo-Anosov, and the isotopy class of w is itself pseudo-Anosov if each τ_c^{+1} and τ_d^{-1} occur at least once in w.*

In the statement of the previous theorem, "$\mathcal{C} \cup \mathcal{D}$ *fills* F" means that each component of the complement of $\mathcal{C} \cup \mathcal{D}$ is a disc, a boundary-parallel annulus, or a puncture-parallel punctured disc. Moreover "$\mathcal{C}$ *hits* $\mathcal{D}$ *efficiently*" if there is no bigon in F with boundary made of one arc of a curve $c \in \mathcal{C}$ and one arc of a curve $d \in \mathcal{D}$.

In our case we set $\mathcal{C} = \{\gamma_1, \dots, \gamma_n\}$ and $\mathcal{D} = \{\gamma_0\}$ and we can apply this theorem to deduce that the monodromy associated to $\mathcal{L}_n$ is a pseudo-Anosov map; applying Thurston [112] we deduce these links are hyperbolic.

Moreover Theorem 2.A.2 applies to these links and we can deduce that for any multislope $(s_1, \dots, s_n) \in (\infty, 1)^n \cup (-1, \infty)^n$, the filling of the exterior of $\mathcal{L}_n$ with multislope $(s_1, \dots, s_n)$ supports a coorientable taut foliation. Recall that these slopes are referred to the meridian-longitude bases given by the mapping torus; since the components of

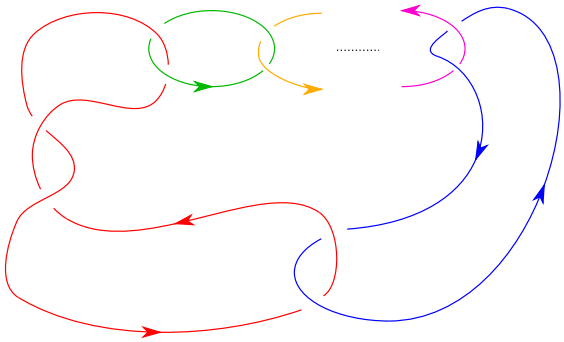

Figure 2.A.13: The link $\mathcal{L}_n$.

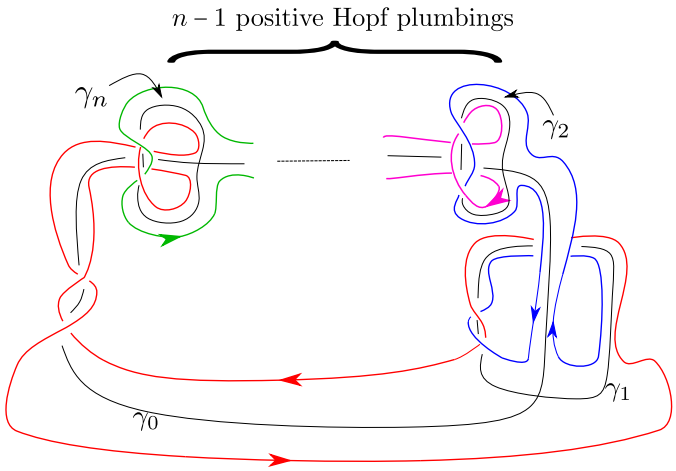

Figure 2.A.14: A description of $\mathcal{L}_n$ as a plumbing of Hopf bands.

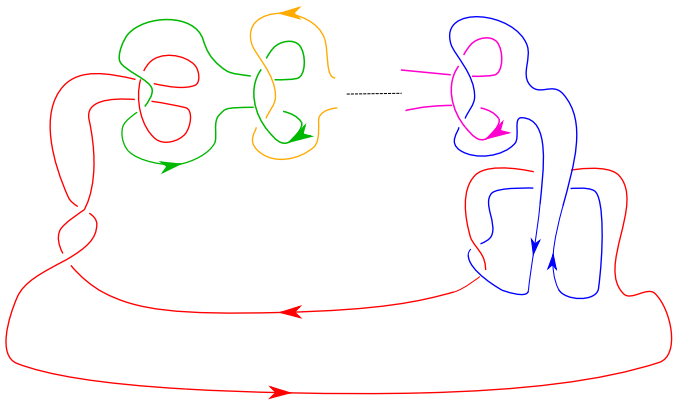

Figure 2.A.15: Another picture of the link $\mathcal{L}_n$. Without the cores of the Hopf bands it may be easier to see the isotopy to the link depicted in Figure 2.A.13.

the link $\mathcal{L}_n$ do not have pairwise linking number zero, the longitudes of these bases do not coincide with the canonical longitudes of the link.

Chapter 3

Left-orderability

This chapter is devoted to the study of the left-orderability of some surgeries on the Whitehead link. The main result is Theorem C. We will also record some other results from the literature regarding the orderability (and non-orderability) of surgeries on the Whitehead link.

3.1 Central extensions and cohomology of groups

In this section we recall how the problem of finding lifts of certain homomorphisms can be rephrased in terms of group coholomogy. More precisely we show how equivalences classes of central extension of a group G by $\mathbb{Z}$ can be identified with the cohomology group $H^2(G, \mathbb{Z})$. We start with some definitions.

Definition 3.1.1. A *central extension of G (by $\mathbb{Z}$)* is a short exact sequence of groups

$$0 \to \mathbb{Z} \to E \to G \to 1$$

with the property that the image of $\mathbb{Z}$ in G is in the center of G.

Definition 3.1.2. Two central extension of G

$$0 \to \mathbb{Z} \to E \to G \to 1$$
$$0 \to \mathbb{Z} \to E' \to G \to 1$$

are *equivalent* if there exists a homomorphism $E \to E'$ such that the following diagram commutes

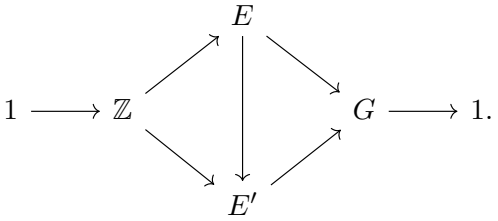

The condition in the previous definition forces the homomorphism $E \to E'$ to be an isomorphism. We denote the set of equivalence classes of central extensions of G by $\mathcal{E}(G, \mathbb{Z})$.

Also recall that the second cohomology group of G with coefficients in $\mathbb{Z}$ (and trivial action on $\mathbb{Z}$) can be defined as

$$H^2(G;\mathbb{Z}) = Z^2(G;\mathbb{Z})/B^2(G;\mathbb{Z})$$

where

$$Z^2(G;\mathbb{Z}) = \left\{ f : G^2 \to \mathbb{Z} \text{ s.t.} \quad \begin{array}{c} f(g_2,g_3) - f(g_1g_2,g_3) + f(g_1,g_2g_3) - f(g_1,g_2) = 0 \\ \text{and } f(id_G, g) = f(g, id_G) = 0 \end{array} \right\}$$

and

$$B^2(G;Z) = \left\{ f : G^2 \to \mathbb{Z} \text{ s.t.} \quad \begin{array}{c} \exists h : G \to \mathbb{Z} \text{ with } f(g_1,g_2) = h(g_1) + h(g_2) - h(g_1g_2) \\ \text{and } h(id_G) = 0 \end{array} \right\}.$$

There is a bijection between $\mathcal{E}(G, \mathbb{Z})$ and $H^2(G;\mathbb{Z})$, defined in the following way:

- given a central extension $0 \to \mathbb{Z} \xrightarrow{i} E \xrightarrow{\pi} G \to 1$, consider a set-theoretical section $s : G \to E$, i.e. a map satisfying $s \circ \pi = \mathrm{Id_G}$, such that $s(id_G) = id_E$. Then we can associate to s an element $f \in Z^2(G;\mathbb{Z})$ defined as $f(g_1, g_2) = s(g_1)s(g_2)s(g_1g_2)^{-1}$;
- given $f \in Z^2(G;\mathbb{Z})$, we define the group G_f as the set $G \times \mathbb{Z}$ endowed with the multiplication $(g_1, a)(g_2, b) = (g_1g_2, a + b + f(g_1, g_2))$. We can identify a copy of $\mathbb{Z}$ in G_f by considering the subgroup generated by $(id_G, 1)$ and there is an obvious projection $G_f \xrightarrow{\pi} G$ obtained by projecting on the first factor. We have defined in this way a central extension of G.

The previous maps induce well-defined maps between $\mathcal{E}(G, \mathbb{Z})$ and $H^2(G;\mathbb{Z})$ and one can check that these are inverses one of the other, and that the class of the trivial central extension $G \times \mathbb{Z}$ is identified with the class in $H^2(G;\mathbb{Z})$ represented by the constant zero cocycle.

We will soon be interested in studying the following problem. Suppose that we have a central extension $0 \to \mathbb{Z} \xrightarrow{i} E \xrightarrow{\pi} G \to 1$ and let $\varphi : H \to G$ a homomorphism: when is it possible to lift φ to a homomorphism $\widetilde{\varphi} : H \to E$?

Observe that φ induces by pullback a map $\varphi^* : H^2(G;\mathbb{Z}) \to H^2(H;\mathbb{Z})$ and let denote by $[f_E] \in H^2(G;\mathbb{Z})$ the cohomology class associated to the above central extension of G. By abuse of notation, we denote by e_φ the cohomology class $\varphi^*([f_E])$ and omit the dependence on the central extension.

Proposition 3.1.3. *There exists a lift $\widetilde{\varphi} : H \to E$ of φ if and only if the class e_φ is trivial in $H^2(H;\mathbb{Z})$.*

Proof. (Sketch) We consider the central extension of H defined by using φ in the following way: consider the following subgrop of $E \times H$

$$E_\varphi = \{(e,h) \in E \times H | \pi(e) = \varphi(h)\}$$

with projection π' on H, given by projecting on the second factor. Since $\pi : E \to G$ is surjective, also π' is and one can check that the kernel of π' can be identified with $i(\mathbb{Z}) \times \{id_H\} \subset E_\varphi$, that is a copy of $\mathbb{Z}$. This central extension of H is uniquely associated to a cohomology class $[f_{E_\varphi}] \in H^2(H;\mathbb{Z})$ and one can check that this class is exactly e_φ. By the very definition of E_φ it follows that a lift $\widetilde{\varphi} : H \to E$ of φ exists if and only if there exists a section of $\pi' : E_\varphi \to H$. This happens exactly when the class of this central extension in $\mathcal{E}(H,\mathbb{Z})$ is the trivial, i.e. if and only if $[f_{E_\varphi}] = e_\varphi$ is trivial. □

3.2 Euler classes of foliations on surgeries on the Whitehead link

In this section we study the Euler classes of the foliations we have constructed in Chapter 2. We prove the following theorem. Recall that we were able to construct foliations on the (r_1, r_2)-surgery on the Whitehead link, where at least one of the two rational coefficient is smaller than 1.

Theorem C. *Let $S^3_{\frac{p_1}{q_1},\frac{p_2}{q_2}}(\mathrm{WL})$ be the $\left(\frac{p_1}{q_1},\frac{p_2}{q_2}\right)$-surgery on the Whitehead link, with $q_1, q_2 \neq 0$ and $p_1, p_2 > 0$.*

Then the taut foliations constructed in the proof of the Theorem A have vanishing Euler class if and only if $|q_i| \equiv 1 \pmod{p_i}$ for $i = 1, 2$.

In particular, for all these manifolds the L-space conjecture holds.

We start by recalling the definition of left-orderable group and briefly explain how taut foliations can be used to prove that some 3-manifold groups are left-orderable.

Definition 3.2.1. Let G be a group. G is *left-orderable* if there exists a total order $<$ on G that is invariant for the left multiplication by elements in G, i.e. such that for any $g, g' \in G$ we have that $g < g'$ if and only if $hg < hg'$ $\forall h \in G$.

If G is the fundamental group of a closed, orientable, irreducible 3-manifold, left-orderability translates in the following dynamical property.

Theorem 3.2.2 ([9])**.** *Let N be a closed, irreducible, orientable 3-manifold. Then $\pi_1(N)$ is left-orderable if and only if there exists a non-trivial homomorphism $\varphi : \pi_1(N) \to \mathrm{Homeo}^+(\mathbb{R})$.*

This result yields us a theoretical way to connect taut foliations to left-orderability in the following way. Suppose that $\mathcal{F}$ is a cooriented taut foliation on a rational homology 3-sphere N. We can associate to $\mathcal{F}$ its tangent bundle $T\mathcal{F}$, that is a plane bundle over N. Being it an orientable plane bundle, we can associate to $T\mathcal{F}$ its Euler class $e(T\mathcal{F}) \in H^2(N;\mathbb{Z})$. Moreover, by a construction of Thurston (see [14]), it is possible to associate to $\mathcal{F}$ a non-trivial homomorphism

$$\varphi : \pi_1(N) \to \mathrm{Homeo}^+(S^1).$$

The universal cover $\widetilde{\mathrm{Homeo}^+}(S^1)$ of $\mathrm{Homeo}^+(S^1)$ can be identified with the subgroup $\mathrm{Homeo}^+_{\mathbb{Z}}(\mathbb{R}) \subset \mathrm{Homeo}^+(\mathbb{R})$ of orientation preserving homeomorphisms of $\mathbb{R}$ that commute with integer translations and it defines a central extension of $\mathrm{Homeo}^+(S^1)$. Therefore, in order to apply Theorem 3.2.2, it is natural to look for lifts $\widetilde{\varphi}$ of φ to $\widetilde{\mathrm{Homeo}^+}(S^1)$. By virtue of Proposition 3.1.3 we have that such a lift exists if and only if e_φ is trivial in $H^2(\pi_1(N);\mathbb{Z})$. Recall that since N contains a coorientable taut foliation, its universal cover is $\mathbb{R}^3$. Therefore N is a $K(\pi_1(N),1)$-space and the cohomology groups of M coincide with the cohomology groups of $\pi_1(N)$. There is hope to give an interpretation of e_φ as element in $H^2(N;\mathbb{Z})$. In fact, the following theorem holds:

Theorem 3.2.3 ([8])**.** *Let N be a rational homology sphere. Then the class e_φ coincides, up to sign, with $e(T\mathcal{F})$. In particular, if a rational homology sphere contains a coorientable taut foliation with vanishing Euler class, then it is left-orderable.*

We now consider the taut foliations obtained in Chapter 2 and determine which of them have vanishing Euler class. To do this we will adapt part of the content of [51] to our context.

We fix some notation. We denote with M the exterior of the Whitehead link WL and we denote with S the 2-holed torus (constructed for example with the same procedure of Figure 2.9) that is the fiber surface for WL. We fix a multislope $\left(\frac{p_1}{q_1}, \frac{p_2}{q_2}\right)$, with $\frac{p_1}{q_1} < 1$ or $\frac{p_2}{q_2} < 1$, and we denote with $\mathcal{F}$ the foliation in M intersecting ∂M in parallel curves of multislope $\left(\frac{p_1}{q_1}, \frac{p_2}{q_2}\right)$, as constructed in the proof of Theorem A. This foliation extends to a foliation $\hat{\mathcal{F}}$ of the filled manifold $S^3_{\frac{p_1}{q_1},\frac{p_2}{q_2}}(\mathrm{WL})$ so that in the glued solid tori N_1 and N_2 the foliation $\hat{\mathcal{F}}$ restricts to the standard foliations $\mathcal{D}_1$ and $\mathcal{D}_2$, which are the foliations by meridional discs. We can suppose without loss of generality that $p_1, p_2 > 0$. We orient the meridional disc D_i of N_i so that the gluing map identifies ∂D_i with the oriented curve $p_i\mu_i + q_i\lambda_i$ in ∂M.

The second homology group $H_2(M, \partial M;\mathbb{Z})$ is isomorphic to $\mathbb{Z}^2$ and in particular we can fix as generators two properly embedded surfaces S_1 and S_2 that are duals to the meridians of the two components of the Whitehead link. Since the Whitehead link has

linking number zero, these surfaces can be taken to be Seifert surfaces for the components of the link. In particular, these can be chosen to be tori with one disc removed, so that $\partial S_i = \lambda_i$. One of these tori is showed in Figure 3.2.1 and the other can be obtained by an isotopy of S^3 exchanging the two components of WL.

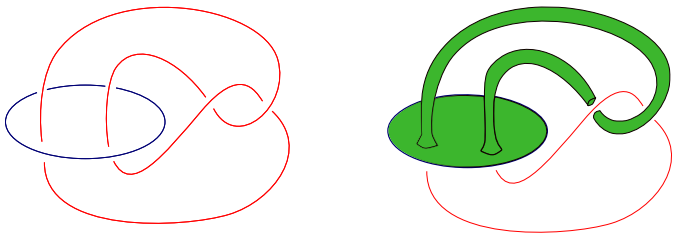

Figure 3.2.1: The 1-holed torus depicted in this figure is one of the two generators of $H_2(M, \partial M; \mathbb{Z})$.

We fix a nowhere vanishing section σ of $(T\mathcal{F})_{|\partial M}$ that is everywhere pointing outside of M. Hence the restrictions of σ to the boundary components of M also define nowhere vanishing sections σ_i of $(T\mathcal{D}_i)_{|\partial N_i}$ everywhere pointing inside N_i, for $i = 1, 2$. These sections yield us relative Euler classes in $H^2(M, \partial M; \mathbb{Z})$, $H^2(N_1, \partial N_1; \mathbb{Z})$ and $H^2(N_2, \partial N_2; \mathbb{Z})$, that we denote respectively with $e_\sigma(T\mathcal{F})$, $e_{\sigma_1}(T\mathcal{D}_1)$ and $e_{\sigma_2}(T\mathcal{D}_2)$. See [51] for details.

Finally, we set $a_i = \langle e_\sigma(T\mathcal{F}), [S_i]\rangle$ and $b_i = \langle e_{\sigma_i}(T\mathcal{D}_i), [D_i]\rangle$, where D_i is a meridional disc in N_i.

Remark 3.2.4. Notice that since $\mathcal{D}_i$ is the standard foliation of the solid torus by meridional discs, we have that b_i coincides with $\pm\langle e_{\sigma_i}(TD_i), [D_i]\rangle = \pm\chi(D_i) = \pm 1$, where TD_i denotes the tangent bundle of D_i and where the sign depends on the orientation of the foliation $\mathcal{D}_i$.

We are interested in knowing when $e(T\hat{\mathcal{F}})$ vanishes. The following proposition tells us exactly when this happens. Recall that without loss of generality we are supposing $p_1, p_2 > 0$, whereas the signs of q_1 and q_2 are arbitrary.

Proposition 3.2.5. *We have that $e(T\hat{\mathcal{F}}) = 0$ if and only if $e(T\mathcal{F}) = 0$ and $a_i q_i \equiv b_i \pmod{p_i}$.*

Proof. The statement of this proposition is the generalisation to our case of the statements of [51, Lemma 3.1] and [51, Theorem 1.4] and the proof that is presented there adapts almost unaltered. We give a brief sketch of the proof and refer to [51] for the details. In what follows the cohomology and homology groups are all implicitly assumed with integer coefficients and we will denote with $\overline{M}$ the $(\frac{p_1}{q_1}, \frac{p_2}{q_2})$-surgery on M. Since $\overline{M}$ is a rational homology sphere as a consequence of the long exact sequence of the pair $(\overline{M}, \partial M)$ we have

$$0 \to H^1(\partial M) \xrightarrow{\delta} H^2(\overline{M}, \partial M) \xrightarrow{\iota} H^2(\overline{M}) \to 0. \tag{3.1}$$

Moreover as a consequence of the Mayer-Vietoris sequence there is an isomorphism

$$H^2(M, \partial M) \oplus H^2(N_1, \partial N_1) \oplus H^2(N_2, \partial N_2) \cong H^2(\overline{M}, \partial M) \tag{3.2}$$

defined by mapping the relative classes (c_M, c_{N_1}, c_{N_2}) to the sum $\overline{c_M} + \overline{c_{N_1}} + \overline{c_{N_2}}$, where each of these cohomology classes is obtained by extending to $\overline{M}$ the corresponding relative class by the zero map.

By using the identification given by the isomorphism in (3.2) we obtain a short exact sequence:

$$0 \to H^1(\partial M) \xrightarrow{\psi} H^2(M, \partial M) \oplus H^2(N_1, \partial N_1) \oplus H^2(N_2, \partial N_2) \xrightarrow{\varphi} H^2(\overline{M}) \to 0 \tag{3.3}$$

where

$$\psi(\beta) = (\delta_M \beta, (\delta_{N_1} \circ f_1^*)(\beta), (\delta_{N_2} \circ f_2^*)(\beta))$$

with $f_1 : \partial N_1 \hookrightarrow \partial M$ and $f_2 : \partial N_2 \hookrightarrow \partial M$ denoting the gluing maps of the solid tori and with

$$\delta_M : H^1(\partial M) \to H^2(M, \partial M)$$
$$\delta_{N_1} : H^1(\partial N_1) \to H^2(N_1, \partial N_1)$$
$$\delta_{N_2} : H^1(\partial N_2) \to H^2(N_2, \partial N_2)$$

denoting the maps appearing in the long exact sequences of the pairs $(M, \partial M)$, $(N_1, \partial N_1)$ and $(N_2, \partial N_2)$.

We suppose now that $e(T\hat{\mathcal{F}}) = 0$. By naturality of the Euler class, $e(T\mathcal{F})$ is the image of $e(T\hat{\mathcal{F}}) = 0$ under the map induced by the inclusion $M \hookrightarrow \overline{M}$ and therefore we have that $e(T\mathcal{F}) = 0$.

Moreover it also holds that

$$\varphi(e_\sigma(T\mathcal{F}), e_{\sigma_1}(T\mathcal{D}_1), e_{\sigma_2}(T\mathcal{D}_2)) = e(T\hat{\mathcal{F}}) = 0$$

and therefore there exists $\beta \in H^1(\partial M)$ such that $\psi(\beta) = (e_\sigma(T\mathcal{F}), e_{\sigma_1}(T\mathcal{D}_1), e_{\sigma_2}(T\mathcal{D}_2))$; in other words β satisfies

$$\begin{cases} \delta_M \beta = e_\sigma(T\mathcal{F}) \\ (\delta_{N_1} \circ f_1^*)(\beta) = e_{\sigma_1}(T\mathcal{D}_1) \\ (\delta_{N_2} \circ f_2^*)(\beta) = e_{\sigma_2}(T\mathcal{D}_2) \end{cases}.$$

The following calculation verifies that $a_i q_i \equiv b_i \pmod{p_i}$:

$$b_i = \langle e_{\sigma_i}(T\mathcal{D}_i), [D_i] \rangle = \langle (\delta_{N_i} \circ f_i^*)(\beta), [D_i] \rangle = \langle \beta, [f_i(\partial D_i)] \rangle =$$

$$= \langle \beta, p_i\mu_i + q_i\lambda_i \rangle = p_i\langle \beta, \mu_i \rangle + q_i\langle \beta, \lambda_i \rangle = p_i\langle \beta, \mu_i \rangle + q_i a_i$$

where in the last equality we have used that

$$\langle \beta, \lambda_i \rangle = \langle \beta, [\partial S_i] \rangle = \langle \delta_M \beta, [S_i] \rangle = \langle e_\sigma(T\mathcal{F}), [S_i] \rangle = a_i.$$

We now prove that if $e(T\mathcal{F}) = 0$ and $a_i q_i \equiv b_i \pmod{p_i}$ for $i = 1, 2$, then $e(T\hat{\mathcal{F}}) = 0$.

We consider again the short exact sequence in (3.1). The nowhere vanishing section σ defines an element $e_\sigma(T\hat{\mathcal{F}}) \in H^2(\overline{M}, \partial M)$ that satisfies $\iota(e_\sigma(T\hat{\mathcal{F}})) = e(T\hat{\mathcal{F}})$ and therefore if we prove that $e_\sigma(T\hat{\mathcal{F}})$ belongs to the image of $\delta : H^1(\partial M) \to H^2(\overline{M}, \partial M)$ we obtain the thesis. Morever under the isomorphism (3.2) the element $(e_\sigma(T\mathcal{F}), e_{\sigma_1}(T\mathcal{D}_1), e_{\sigma_2}(T\mathcal{D}_2))$ corresponds to $e_\sigma(T\hat{\mathcal{F}})$ and therefore it is enough to prove that $(e_\sigma(T\mathcal{F}), e_{\sigma_1}(T\mathcal{D}_1), e_{\sigma_2}(T\mathcal{D}_2))$ belongs to the image of ψ in the short exact sequence (3.3).

If we consider the long exact sequence of the pair $(M, \partial M)$ we have the following

$$H^1(M; \mathbb{Z}) \overset{\iota'_M}{\to} H^1(\partial M) \overset{\delta_M}{\to} H^2(M, \partial M) \overset{\iota''_M}{\to} H^2(M)$$

and since $\iota''_M(e_\sigma(T\mathcal{F})) = e(T\mathcal{F}) = 0$ we deduce that there exists $\beta_0 \in H^1(\partial M)$ such that $\delta_M(\beta_0) = e_\sigma(T\mathcal{F}) \in H^2(M, \partial M)$. We now want to modify β_0 in order to find $\beta \in H^1(\partial M)$ that satisfies

$$\psi(\beta) = (e_\sigma(T\mathcal{F}), e_{\sigma_1}(T\mathcal{D}_1), e_{\sigma_2}(T\mathcal{D}_2))$$

that is to say, such that

$$\begin{cases} \delta_M \beta = e_\sigma(T\mathcal{F}) \\ (\delta_{N_1} \circ f_1^*)(\beta) = e_{\sigma_1}(T\mathcal{D}_1) \\ (\delta_{N_2} \circ f_2^*)(\beta) = e_{\sigma_2}(T\mathcal{D}_2). \end{cases}$$

We denote with $\mu_i^* \in H^1(\partial M)$ the dual of $\mu_i \in H_1(\partial M)$ and we define

$$\beta = \beta_0 + n_1\mu_1^* + n_2\mu_2^* \quad \text{where } n_i = -\langle \beta_0, \mu_i \rangle - \frac{a_i q_i - b_i}{p_i}.$$

Since $a_i q_i \equiv b_i \pmod{p_i}$ for $i = 1, 2$ it follows that n_i is an integer. Moreover, since $\beta - \beta_0 \in \iota'_M(H^1(M))$ we have that $\delta_M(\beta_0) = \delta_M(\beta) = e_\sigma(T\mathcal{F}) \in H^2(M, \partial M)$. We have to prove that $(\delta_{N_i} \circ f_i^*)(\beta) = e_{\sigma_i}(T\mathcal{D}_i)$ for $i = 1, 2$. Since

$$H^2(N_i, \partial N_i) \cong \mathrm{Hom}(H_2(N_i, \partial N_i, \mathbb{Z}))$$

it is enough to prove that $\langle (\delta_{N_i} \circ f_i^*)(\beta), [D_i] \rangle = \langle e_{\sigma_i}(T\mathcal{D}_i), [D_i] \rangle$ and this is a consequence of the following computation (the case $i = 2$ is analogous).

$$\langle (\delta_{N_1} \circ f_1^*)(\beta), [D_1] \rangle = \langle \beta, f_1(\partial D_1) \rangle =$$

$$= \langle \beta_0, p_1\mu_1 + q_1\lambda_1 \rangle + n_1\langle \mu_1^*, p_1\mu_1 + q_1\lambda_1 \rangle + n_2\langle \mu_2^*, p_1\mu_1 + q_1\lambda_1 \rangle =$$

$$= p_1\langle\beta_0,\mu_1\rangle + a_1q_1 + p_1\left(-\langle\beta_0,\mu_1\rangle - \frac{a_1q_1-b_1}{p_1}\right) = b_1 = \langle e_{\sigma_1}(T\mathcal{D}_1),[D_1]\rangle$$

where in the last line we have used again that

$$\langle\beta_0,\lambda_1\rangle = \langle\beta_0,[\partial S_1]\rangle = \langle\delta_M\beta_0,[S_1]\rangle = \langle e_\sigma(T\mathcal{F}),[S_1]\rangle = a_1.$$

and that $\langle\mu_2^*,\mu_1\rangle = \langle\mu_2^*,\lambda_1\rangle = 0$ □

We are now ready to prove the following

Theorem C. *Let $S^3_{\frac{p_1}{q_1},\frac{p_2}{q_2}}(\mathrm{WL})$ be the $\left(\frac{p_1}{q_1},\frac{p_2}{q_2}\right)$-surgery on the Whitehead link, with $q_1,q_2\neq 0$ and $p_1,p_2>0$.*

Then the taut foliations constructed in the proof of the Theorem A have vanishing Euler class if and only if $|q_i|\equiv 1 \pmod{p_i}$ for $i=1,2$.

In particular, for all these manifolds the L-space conjecture holds.

Proof. First of all we prove that $e(T\mathcal{F})=0$. In fact, let T denote one of the boundary components of M; the inclusion of T in M induces an isomorphism $\iota: H^2(M;\mathbb{Z})\to H^2(T;\mathbb{Z})$. Therefore we have

$$e(T\mathcal{F})=0 \Leftrightarrow \iota(e(T\mathcal{F}))=0.$$

By naturality of the Euler class we have that

$$\iota(e(T\mathcal{F})) = e(T(\mathcal{F}_{|T}))$$

and since $\mathcal{F}_{|T}$ admits a nowhere vanishing section we have that the last quantity is zero.

We now want to compute the numbers a_i. As a consequence of the proof of Theorem 1.7 in [51] we have that

- $b_i=1$ if $q_i<0$, for $i=1,2$;
- $b_i=-1$ if $q_i>0$, for $i=1,2$;
- $\langle e_\sigma(T\mathcal{F}),[S]\rangle = \chi(S) = -2$.

Since by construction S intersects positively in one point the meridians of the components of the Whitehead link, we have the equality $[S]=[S_1+S_2]$ in $H_2(M,\partial M;\mathbb{Z})$ and hence

$$a_1+a_2 = \langle e_\sigma(T\mathcal{F}),[S_1]\rangle + \langle e_\sigma(T\mathcal{F}),[S_2]\rangle = \chi(S) = -2.$$

As a consequence of [111, Corollary 1, p. 118] for any $[F]\in H_2(M,\partial M;\mathbb{Z})$ we have the inequality

$$|\langle e_\sigma(T\mathcal{F}),[F]\rangle| \leq |\chi(F)|$$

and since S_1 and S_2 are 1-holed tori, this implies that $a_i=\langle e_\sigma(T\mathcal{F}),[S_i]\rangle = -1$ for $i=1,2$. Therefore, by virtue of Proposition 3.2.5 we have $e(T\hat{\mathcal{F}})=0$ if and only if for each $i=1,2$ it holds one of the following:

- q_i is positive and $q_i \equiv 1 \pmod{p_i}$;
- q_i is negative and $q_i \equiv -1 \pmod{p_i}$.

In other words $e(T\hat{\mathcal{F}}) = 0$ if and only if

$$|q_i| \equiv 1 \pmod{p_i} \quad \text{for } i = 1, 2$$

that is exactly what we wanted. □

We point out the following straightforward consequence of Theorem C.

Corollary 3.2.6. *Let d_1, d_2 be two integers such that $d_1 < 0$ or $d_2 < 0$. Then the manifold $S^3_{d_1,d_2}(\mathrm{WL})$ satisfies the L-space conjecture.* □

We conclude by collecting from the literature some results regarding the orderability (or non-orderability) of some surgeries on the Whitehead link, obtaining a generalisation of Corollary 3.2.6.

Proposition 3.2.7. *Let $m \leq -1$ be an integer. Then the manifolds $S^3_{m,r}(\mathrm{WL})$ and $S^3_{r,m}(\mathrm{WL})$ have left-orderable fundamental group for all rationals r. On the other hand, all L-space surgeries on* WL *are non left-orderable. That is to say $S^3_{r_1,r_2}(\mathrm{WL})$ is non left-orderable for all rationals $r_1 \geq 1$, $r_2 \geq 2$.*

In particular, all the rational homology spheres obtained by integer surgery on WL *satisfy the L-space conjecture.*

Proof. The second part of the proposition follows from the main result of [72]: an irreducible, orientable, left-orderable M with Heegaard genus at most 2 supports a coorientable taut foliation. All surgeries on two-bridge links have at most Heegaard genus 2 and since L-spaces do not support coorientable taut foliations the statement follows. For what concerns the first part of the proposition, the manifold $S^3_{m,\bullet}(\mathrm{WL})$ fibers over the circle if and only if m is an integer (see [49]). Moreover, in this case the fiber is a punctured torus. When $m \leq -1$ the monodromy of $S^3_{m,\bullet}(\mathrm{WL})$ can be extended to an Anosov diffeomorphism ϕ of the torus that preserves the orientations of its stable and unstable foliations, see [49]. The manifold $S^3_{m,r}(\mathrm{WL})$ can be obtained by surgery along a closed orbit of ϕ in the mapping torus M_ϕ and as a consequence of [117, Theorem 1] we have that all the non-trivial fillings of $S^3_{m,\bullet}(\mathrm{WL})$ have left-orderable fundamental group. Since WL is symmetric, the same result holds for $S^3_{\bullet,m}(\mathrm{WL})$. This concludes the proof. □

Remark 3.2.8. Notice that even if the content of Corollary 3.2.6 is generalised by Proposition 3.2.7, the statement of Theorem C is not; in fact there are also non-integer rationals $\frac{p_1}{q_1}$ and $\frac{p_2}{q_2}$ that satisfy the hypotheses of Theorem C.

In [30] Dunfield considers a census of more than 300,000 hyperbolic rational homology spheres, testing the conjecture for this census. These manifolds are obtained by filling 1-cusped hyperbolic 3-manifolds that can be triangulated with at most 9 ideal tetrahedra, see [12]. We checked whether some of these manifolds studied by Dunfield arise as Dehn surgery on the Whitehead link and obtained the following

Proposition 3.2.9. *Among the* $307,301$ *rational homology spheres studied in [30] at least* 625 *are obtained as Dehn surgery on the Whitehead link. In [30] it is proved that:*

- 300 *of these manifolds are left-orderable;*
- 250 *are not left-orderable.*

It follows from Proposition 3.2.7 that 16 *of the remaining* 75 *manifolds are orderable and* 39 *are non-left-orderable.*

The code of the program can be found at [20]. The surgery coefficients yielding these manifolds are plotted in Figure 3.2.2.

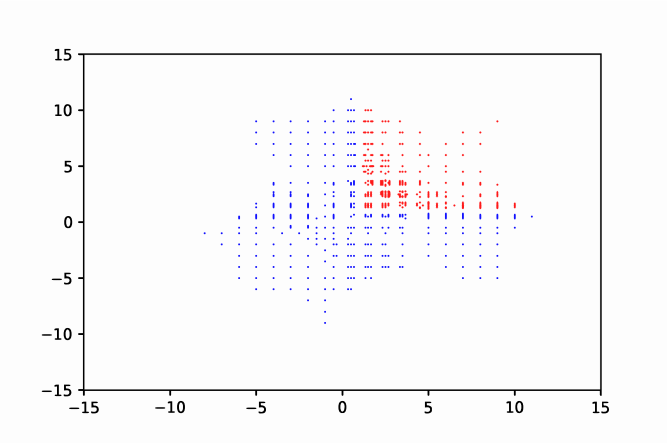

Figure 3.2.2: In this figure the red dots represent the coefficients whose corresponding surgery is non-left-orderable and the blue dots represent the coefficients whose corresponding surgery is left-orderable.

The examples of Proposition 3.2.7 and Proposition 3.2.9 are consistent with the conjecture, and together with Theorem A confirm that the L-space conjecture holds also for all these manifolds.

Chapter 4

Dodecahedral L-spaces and hyperbolic 4-manifolds

The last chapter of the thesis will focus on a slightly different topic, and will be about a joint work with Ludovico Battista and Leonardo Ferrari [3], where we study and classify the L-spaces among some hyperbolic 3-manifolds with particularly nice geometric properties. We then use this information to construct some hyperbolic 4-manifolds with vanishing Seiberg-Witten invariants.

We start the chapter by introducing the problem and recalling some definitions. In Section 4.2, we recall the techniques used by Dunfield to classify the L-spaces in [30]. We then elaborate on these techniques and describe an algorithm that can be used to prove that a hyperbolic rational homology sphere is an L-space and prove Theorem E. Section 4.3 contains the details of the construction necessary for the proof of Theorem F. In Section 4.3.1 we recall the general theory of manifolds with right-angled corners and colourings; then, in Section 4.3.2, we move to the explicit construction.

Appendices 4.A-4.B contain a detailed description of the algorithm used in Section 4.2, with some examples.

4.1 Introduction

Definition 4.1.1. A hyperbolic 3-manifold is *dodecahedral* if it can be tessellated by regular right-angled hyperbolic dodecahedra.

The dodecahedral manifolds tessellated with four or less dodecahedra were classified in [43]. Using this, we fix the following notation:

Notation 4.1.2. We denote by $\mathscr{D}$ the set of the 29 dodecahedral hyperbolic rational homology spheres tessellated with four or less dodecahedra (see Table 4.1.1).

To identify the L-spaces in $\mathscr{D}$, we elaborate on some ideas presented by Dunfield in [30], and we use the algorithm described in Section 4.2. With the help of the code provided by Dunfield in [30], we show that the remaining 3-manifolds are not L-spaces, so we can conclude:

Theorem E. *Among the 29 manifolds in $\mathscr{D}$, 6 are L-spaces and 23 are not; see Tables 4.1.1 - 4.2.1.*

The information given by Theorem E is very little compared with the one from [30], where L-spaces among more than $300,000$ hyperbolic manifolds are classified. Nevertheless, the geometric properties of the manifolds in $\mathscr{D}$ can be used to answer a question asked by Agol and Lin in [1]. Before stating the question, we give a brief introduction to the problem.

Seiberg-Witten invariants are smooth invariants for 4-manifolds with $b_2^+ \geq 2$ and were defined in [101, 102, 116] by Seiberg and Witten. These invariants, coming from gauge theory, soon established surprising connections between the topology and the geometry of smooth 4-manifolds. For example, if a 4-manifold with $b_2^+ \geq 2$ has a metric with positive scalar curvature then these invariants all vanish [116], while on the other hand Taubes [103] proved that any symplectic 4-manifold with $b_2^+ \geq 2$ has a non-zero Seiberg-Witten invariant. Putting together these results, we have that any symplectic 4-manifold with $b_2^+ \geq 2$ does not admit a metric with positive scalar curvature.

In [69] LeBrun conjectured that the Seiberg-Witten invariants of a closed hyperbolic 4-manifold are all zero. In [1] Agol and Lin showed the existence of infinitely many commensurability classes of hyperbolic 4-manifolds containing representatives with vanishing Seiberg-Witten invariants. This is shown by proving that there exist hyperbolic 4-manifolds that contain separating L-spaces. More precisely, they used the following result. For a proof we refer to [61] and also [1, Proposition 2.2].

Proposition 4.1.3. *Let N be a 4-manifold given as $N = N_1 \cup_{M'} N_2$, where M' is an L-space and where $b_2^+(N_i) \geq 1$ for $i = 1, 2$. Then all the Seiberg-Witten invariants of N vanish.*

Remark 4.1.4. To be precise, the right notion of L-space to use in the previous proposition is the one of *monopole Floer* L-space, but the monopole Floer/Heegaard Floer correspondence, proved by the works of Kutluhan-Lee-Taubes [63, 64, 65, 66, 67], implies that a manifold is a monopole Floer L-space if and only if it is an Heegaard-Floer L-space. A different proof of the correspondence monopole Floer/Heegaard Floer can be obtained by combining the works of Taubes [104, 105, 106, 107, 108] and Colin-Ghiggini-Honda [22].

Part of Agol and Lin strategy to find such examples was based on a result regarding the embeddings of arithmetic hyperbolic manifolds proved by Kolpakov-Reid-Slavich

[56]. As a consequence of this the hyperbolic 4-manifolds of [1] are not explicitly constructed. Therefore they ask the following:

Question 2 ([1, Conclusions (1)])**.** Can one find an explicit hyperbolic 4-manifold N such that $N = N_1 \cup_{M'} N_2$, where the separating hypersurface M' is an L-space and such that $b_2^+(N_i) \geq 1$ for $i = 1, 2$?

The separating hypersurfaces that we will use are built from the ones in $\mathscr{D}$ and to build the 4-manifold we will follow the construction presented in [79]. We discuss all the details in Section 4.3. Here we just premise that the methods used in [79] allow to construct the 4-manifold in an explicit way. In fact, if M is a dodecahedral manifold tessellated into n dodecahedra, the result of [79] yields, under certain hypotheses, a 4-manifold N tessellated into at most $2^{44} \cdot n$ hyperbolic right-angled 120-cells [79, Proof of Theorem 3] in which M geodesically embeds. Notice that this gives a bound on the volume of N. This bound on the number of 120-cells is in general not sharp and in practice our examples are tessellated by less 120-cells than predicted by this bound.

Using this construction, the manifold M is non-separating inside N. However, inside N it is easy to find a certain number of copies of M that, all together, separate. At this point if M is an L-space one can use an argument as in [1, Corollary 2.5] to obtain a separating L-space M' that is diffeomorphic to the connected sum of several copies of M. There is also a natural way to ensure that $b_2^+(N_i) \geq 1$. The details are discussed in Section 4.3.

With the help of Theorem E, we prove the following:

Theorem F. *There are two hyperbolic 4-manifolds $\mathcal{N}_{11}$ and $\mathcal{N}_{28}$ tessellated with 2^9 right-angled 120-cells that can be obtained as $N_1 \cup_{M'} N_2$, where the separating hypersurface M' is an L-space and such that $b_2^+(N_i) \geq 1$ for $i = 1, 2$.*

The manifolds in the statement are built by colouring 4-manifolds with right-angled corners tessellated in 120-cells (see Section 4.3) and are explicitly described in Section 4.3.2. It is possible to generalise the notion of colouring lowering the number of 120-cells in the tessellation to 2^8; we present this construction in Section 4.3.2, but we do not go into the details. The Betti numbers with coefficients in $\mathbb{R}$ and $\mathbb{Z}_2$ of the explicit examples that we build can be found in Tables 4.3.1 - 4.3.2 - 4.3.3 - 4.3.4. We also tried to obtain the integral homology, but the computation was too intensive for our computational resources.

We point out that dodecahedral manifolds satisfy the hypotheses of [56, Theorem 1.1] and therefore their theorem can be used to prove that they embed in hyperbolic 4-manifolds, but the use of the construction of [79] allows us to describe the 4-manifolds explicitly.

The proof of Theorem E is achieved by rigorous computer-assisted computations. In particular, we make use of the code written by Nathan Dunfield [30] and SnapPy [26] in

a Sage [109] environment. All the code used is available at [21], and it can be used to check if a given manifold is an L-space.

The proof of Theorem F is also computer-assisted. We make use of Regina [13] in a Sage [109] environment, and in particular of modules written by Tom Boothby, Nathann Cohen, Jeroen Demeyer, Jason Grout, Carlo Hamalainen, and William Stein. All the code used is available at [21].

4.2 Finding L-spaces

In this section we describe an algorithm that can determine whether a hyperbolic rational homology sphere ($\mathbb{Q}HS$ for short) is an L-space. The two main ingredients of this algorithm are the Rasmussen-Rasmussen Theorem 1.2.2 and part of the work of Dunfield in [30].

In [30] Dunfield considered a census $\mathscr{Y}$ of more than $300,000$ hyperbolic rational homology spheres. These are obtained as Dehn fillings of 1-cusped hyperbolic 3-manifolds that can be triangulated with at most 9 ideal tetrahedra; the latter were enumerated by Burton [12]. We denote the census of these rational homology solid tori ($\mathbb{Q}HT$s for short) with $\mathscr{C}$. The hyperbolic structure of a $\mathbb{Q}HT$ is always intended on its interior; notice that such a metric is always finite-volume, see [4, Proposition D.3.18].

Dunfield, while investigating the L-space conjecture for the manifolds in $\mathscr{Y}$, has in particular proved the following:

Theorem 4.2.1 ([30, Theorem 1.6])**.** *Of the* $307,301$ *hyperbolic rational homology* 3*-spheres in* $\mathscr{Y}$ *exactly* $144,298$ (47.0%) *are L-spaces and* $163,003$ (53.0%) *are non-L-spaces.*

The key idea that Dunfield used to prove Theorem 4.2.1 is to use Theorem 1.2.2 to start a bootstrapping procedure. In fact by virtue of the Rasmussen-Rasmussen theorem, it is sufficient to know two L-spaces fillings of a rational homology solid torus in $\mathscr{C}$ to determine exactly its set of L-space filling slopes, and therefore to obtain information about the L-space status of the manifolds in $\mathscr{Y}$. This, together with the fact that many of the manifolds in $\mathscr{Y}$ admit multiple descriptions as fillings of manifolds in $\mathscr{C}$, allows to increase simultaneously the level of knowledge about the manifolds in $\mathscr{Y}$ and in $\mathscr{C}$.

Notice that the manifolds in $\mathscr{Y}$ have bounded volume: since they are fillings of 1-cusped manifolds that are triangulated with at most 9 ideal tetrahedra, their volume is bounded by $9v_3 < 9.14$, where v_3 is the maximal volume of a hyperbolic tetrahedron.

Following the bootstrap idea of Dunfield, we now present an algorithm that can be used to determine in certain cases whether a hyperbolic rational homology sphere is an L-space. Before describing the algorithm, we recall a definition:

Index	N. dod.	Volume	H_1	L-space
0	2	8.612	Z/11 + Z/11	Yes
1	2	8.612	Z/87	No
2	2	8.612	Z/4 + Z/28	Yes
3	2	8.612	Z/2 + Z/2 + Z/2 + Z/2	No
4	2	8.612	Z/3 + Z/15	No
5	4	17.225	Z/2 + Z/4 + Z/180	No
6	4	17.225	Z/714	No
7	4	17.225	Z/2 + Z/2 + Z/44	No
8	4	17.225	Z/7 + Z/182	Yes
9	4	17.225	Z/4 + Z/44	No
10	4	17.225	Z/2 + Z/4 + Z/60	No
11	4	17.225	Z/2 + Z/2 + Z/120	Yes
12	4	17.225	Z/12 + Z/12	No
13	4	17.225	Z/2 + Z/2 + Z/144	No
14	4	17.225	Z/2 + Z/4 + Z/4 + Z/4	No
15	4	17.225	Z/513	Yes
16	4	17.225	Z/4 + Z/4 + Z/8	No
17	4	17.225	Z/2 + Z/2 + Z/2 + Z/2 + Z/4	No
18	4	17.225	Z/4 + Z/4 + Z/8	No
19	4	17.225	Z/4 + Z/4 + Z/8	No
20	4	17.225	Z/2 + Z/4 + Z/8	No
21	4	17.225	Z/2 + Z/4 + Z/8	No
22	4	17.225	Z/4 + Z/4 + Z/8	No
23	4	17.225	Z/2 + Z/2 + Z/56	No
24	4	17.225	Z/4 + Z/4 + Z/8	No
25	4	17.225	Z/2 + Z/2 + Z/2 + Z/4 + Z/4	No
26	4	17.225	Z/2 + Z/2 + Z/8 + Z/8	No
27	4	17.225	Z/4 + Z/4 + Z/8	No
28	4	17.225	Z/2 + Z/2 + Z/8 + Z/8	Yes

Table 4.1.1: The manifolds in $\mathscr{D}$: the hyperbolic 3-manifolds tessellated with four or less right-angled dodecahedra that are rational homology spheres. The indexing is the one provided by SnapPy, where $\mathscr{D}$ can be accessed by typing `CubicalOrientableClosedCensus(betti=0)`. We list the index of the manifold as given in the SnapPy census, the number of right-angled dodecahedra in its tessellation, its approximated volume, its first homology and whether it is an L-space or not. Compare with Table 4.2.1.

Definition 4.2.2. A rational homology solid torus Y is *Turaev simple* when every coefficient of the Turaev torsion of Y is either 0 or 1.

In [93, Proposition 1.4] it is proved that being Turaev simple is a necessary condition for being Floer simple. The converse is not true in general.

We also use the following notation: when M is a $\mathbb{Q}HS$, we say that the *L-space value of* M is `True` if M is an L-space and `False` otherwise.

The algorithm takes in input a rational homology sphere M and returns `True` if a proof that M is an L-space is found and `False` otherwise.

The rough idea of the algorithm is the following:

1. We start with M, a hyperbolic $\mathbb{Q}HS$. If it belongs to the Dunfield census, we return its L-space value; otherwise we go on with Step 2.;

2. we drill the shortest geodesic given by SnapPy out of M so to obtain Y, a hyperbolic $\mathbb{Q}HT$ that is Turaev simple. We fix a meridian-longitude basis of ∂Y so that the filling $1/0$ on Y gives back M, and we identify $Sl(Y)$ with $\mathbb{Q} \cup \{\infty\}$;

3. using a script provided by Dunfield in [30], we compute $\iota^{-1}(D^{\tau}_{>0}(Y))$ and we select an interval $\mathcal{I}$ in $Sl(Y)$ whose endpoints are consecutive elements in $\iota^{-1}(D^{\tau}_{>0}(Y))$ and such that $1/0 \in \mathcal{I}$. In the case $D^{\tau}_{>0}(Y) = \emptyset$ we take $\mathcal{I}$ as $Sl(Y) \setminus [l]$, where $[l]$ is the homological longitude of Y;

4. we search for two slopes in $\mathcal{I}$ so that the associated fillings are hyperbolic and have minimal volumes. We denote these fillings with M_1 and M_2. By Theorem 1.2.2, if we prove that they are L-spaces, then M also is;

5. we start two new instances of the algorithm with M_1 and M_2; if they both return `True`, we return `True`; otherwise, we return `False`.

The details of the algorithm and one example can be found in Appendices 4.A-4.B. For the moment, let us underline the following facts:

- the answer `True` is rigorous, but we stress that the answer `False` does not imply that M is not an L-space. In particular, the rational homology torus Y can be not Floer simple. We simply assure that it is Turaev simple, since this is an easier condition to check. This means that, even if we start with an actual L-space, the algorithm can return `False`: M could be the only filling of Y that is an L-space;

- we need to avoid that the algorithm enters an infinite loop: for example, it can happen that M is the lowest-volume filling of Y inside $\mathcal{I}$. This would cause an infinite loop. In the code there is a check to avoid such problems;

- we do not know whether a rational homology torus Y as in Step 2. always exists, even if we assume that M is an L-space. See Questions 3 - 4;
- in Step 3. there could be two of such intervals; this happens when $1/0$ is an element of $\iota^{-1}(D^{\tau}_{>0}(Y))$. In this case, we look for L-spaces in both such intervals;
- there is no guarantee that the volumes of M_1 and M_2 are smaller than the volume of M. In particular, the algorithm is not guaranteed to end;
- we need the hyperbolicity of M for two reasons: SnapPy can drill curves only when a manifold has a hyperbolic structure, and we use the hyperbolic volume;
- the key idea of the algorithm is to minimize the hyperbolic volume of M_1 and M_2 to approach the Dunfield census. While M having small volume does not guarantee that M is in $\mathscr{Y}$, in practice this condition makes the algorithm terminate quite fast.

Despite these potential problems, the algorithm was powerful enough to prove the following:

Proposition 4.2.3. *The manifolds with index 0, 2, 8, 11, 15 and 28 in the census $\mathscr{D}$ (recall Notation 4.1.2) are L-spaces (see Tables 4.1.1 - 4.2.1).* □

4.2.1 Classification of Dodecahedral manifolds

We are left with proving that the manifolds in Proposition 4.2.3 are the only ones in $\mathscr{D}$ that are L-spaces. Recall that if M supports a coorientable taut foliation then it is not an L-space. In [30, Section 7], Dunfield introduced the notion of *foliar orientation* and used it to construct co-orientable taut foliations on a given $\mathbb{Q}HS$. He also provided an algorithm that searches for foliar orientations. Applying his algorithm, we are able to prove the following:

Lemma 4.2.4. *The manifolds with index different from 0, 2, 8, 11, 15 and 28 in the census $\mathscr{D}$ are not L-spaces (see Tables 4.1.1 - 4.2.1).* □

This lemma, together with Proposition 4.2.3, implies the following:

Theorem E. *Of the 29 manifolds in $\mathscr{D}$, 6 are L-spaces and 23 are not; see Tables 4.1.1 - 4.2.1.*

In [30], Dunfield provides several algorithms to check the left-orderability and the non-left-orderability of the fundamental group of a $\mathbb{Q}HS$. We apply these algorithms, and the details can be found in Table 4.2.1. In particular, all the results are consistent with the L-space conjecture.

Index	N. dod.	L-space	Co-or. taut foliation	Left-orderable π_1
0	2	Yes[1]	No[2]	No[5]
1	2	No[2]	Yes[3]	?
2	2	Yes[1]	No[2]	No[5]
3	2	No[2]	Yes[3]	Yes[4]
4	2	No[2]	Yes[3]	Yes[4]
5	4	No[2]	Yes[3]	?
6	4	No[2]	Yes[3]	?
7	4	No[2]	Yes[3]	Yes[4]
8	4	Yes[1]	No[2]	No[5]
9	4	No[2]	Yes[3]	Yes[4]
10	4	No[2]	Yes[3]	?
11	4	Yes[1]	No[2]	No[5]
12	4	No[2]	Yes[3]	Yes[4]
13	4	No[2]	Yes[3]	?
14	4	No[2]	Yes[3]	Yes[4]
15	4	Yes[1]	No[2]	No[5]
16	4	No[2]	Yes[3]	?
17	4	No[2]	Yes[3]	Yes[4]
18	4	No[2]	Yes[3]	Yes[4]
19	4	No[2]	Yes[3]	Yes[4]
20	4	No[2]	Yes[3]	?
21	4	No[2]	Yes[3]	Yes[4]
22	4	No[2]	Yes[3]	?
23	4	No[2]	Yes[3]	Yes[4]
24	4	No[2]	Yes[3]	Yes[4]
25	4	No[2]	Yes[3]	Yes[4]
26	4	No[2]	Yes[3]	Yes[4]
27	4	No[2]	Yes[3]	Yes[4]
28	4	Yes[1]	No[2]	No[5]

Table 4.2.1: The manifolds in $\mathscr{D}$: the hyperbolic 3-manifolds tessellated with four or less right-angled dodecahedra that are rational homology spheres. The indexing is the one provided by SnapPy, where $\mathscr{D}$ can be accessed by typing `CubicalOrientableClosedCensus(betti=0)`. The apices indicate in which way we obtain the result. In particular: 1) algorithm in Section 4.2; 2) Theorem 0.0.11 by [85, 5, 54]; 3) algorithm in [30], see [30, Section 7]; 4) algorithm in [30], see [30, Section 9]; 5) algorithm in [30], see [30, Section 5]. Compare with Table 4.1.1.

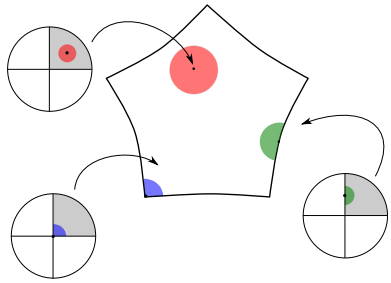

Figure 4.3.1: An example of charts for a 2-manifold with right-angled corners.

4.3 Building up the 4-manifold

We now show how the existence of a dodecahedral manifold that is an L-space can be used to prove Theorem F. To do this, we recall some concepts behind the construction in [79].

4.3.1 Embedding dodecahedral manifolds in 4-manifolds with corners

Let $\mathbb{D}^n$ be the disc model for the hyperbolic space and $\mathcal{O}^n = \{x \in \mathbb{D}^n \mid x_i \geq 0\}$ the positive orthant. A *hyperbolic n-manifold with (right-angled) corners* W is a topological n-manifold equipped with an atlas taking values in open subsets of $\mathcal{O}^n$ and transition maps that are restrictions of isometries. One can visualize this as the natural extension of a manifold with geodesic boundary, where the atlas takes values in open subsets of $\{x \in \mathbb{D}^n \mid x_1 \geq 0\}$.

The boundary ∂W is the set of points in W that do not admit a neighborhood homeomorphic to $\mathbb{R}^n$; it is stratified into vertices, edges, ..., s-faces,..., and facets. Each s-face is an s-manifold with corners, and distinct s-faces meet at right-angles. A facet is called *isolated* if it does not meet any other facet, and as such it must be a geodesic boundary component of W.

Under certain hypotheses, gluing manifolds with corners along (possibly more than one) pair of isometric facets yields another manifold with corners, as the following example shows.

Example 4.3.1. Consider the surface S in Figure 4.3.2-right, obtained by gluing two copies of the right-angled pentagon on the left along the coloured edges. This is a hyperbolic manifold with corners, with edges F_1, F_2 and F_3 and vertices p and q. We have $F_1 \cap F_2 = \{p, q\}$, while the facet $F_3 \cong S^1$ is isolated.

More generally, similarly to right-angled polytopes [55, Section 2], a manifold with corners can be coloured along its facets. More precisely, let $\mathcal{F}_W$ be the set of facets of a manifold with corners W. A *k-colouring* of W is a surjective map $\lambda : \mathcal{F}_W \to \{1, ..., k\}$ that associates distinct numbers (called *colours*) to adjacent facets. Let $e_1, \ldots, e_k$ be

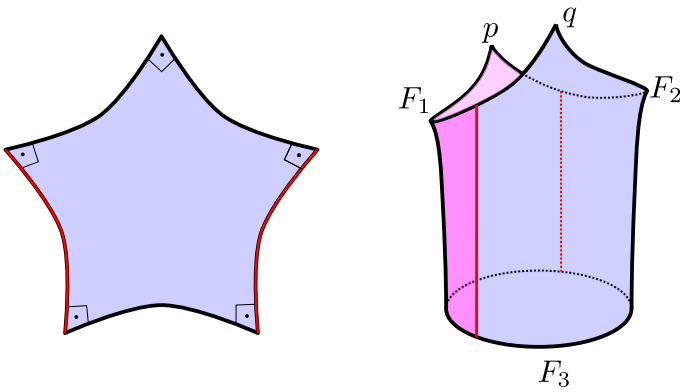

Figure 4.3.2: An example of a right-angled pentagon and the manifold with corners obtained by mirroring it along the red edges.

the canonical basis of $\mathbb{Z}_2^k$. We can define the topological space $\mathcal{M}_\lambda = (W \times \mathbb{Z}_2^k)/_\sim$, where distinct $W \times \{u\}$, $W \times \{v\}$ are glued along the identity on a facet $F \in \mathcal{F}_W$ if $u - v = e_{\lambda(F)}$.

Proposition 4.3.2 ([79], Proposition 6)**.** *The resulting $\mathcal{M}_\lambda$ is a connected, orientable, hyperbolic n-manifold tessellated into 2^k copies of W. If W is compact $\mathcal{M}_\lambda$ is closed.*

Example 4.3.3. Take the manifold with corners from Example 4.3.1 and its colouring λ given by $\lambda(F_i) = i$. These colours are represented by red, blue and purple respectively in Figure 4.3.3.

An useful method to visualize the manifold $\mathcal{M}_\lambda$ is by iteratively mirroring along facets with the same colour. This procedure goes as follows:

- we start with a manifold M with corners and a k-colouring λ;
- we mirror M along the facets F such that $\lambda(F) = k$. We obtain a new manifold M' with corners. The facets of M' are of two types:
  - the facets in M that are adjacent to a facet with colour k are mirrored along their intersection with these facets. Notice that, by using the combinatorics of the intersections of faces of $\mathcal{O}^n$, one can prove that the intersection of two facets is empty or a common sub-facet (see also [35, Definition 2.2] and the discussion thereafter). As an example, see what happens to the blue facet from Figure 4.3.3, (a) to Figure 4.3.3, (b);
  - the facets in M that do not intersect any facet with colour k are doubled: each of them produces two isometric copies of itself. As an example, see what happens to the purple facet from Figure 4.3.3, (a) to Figure 4.3.3, (b);

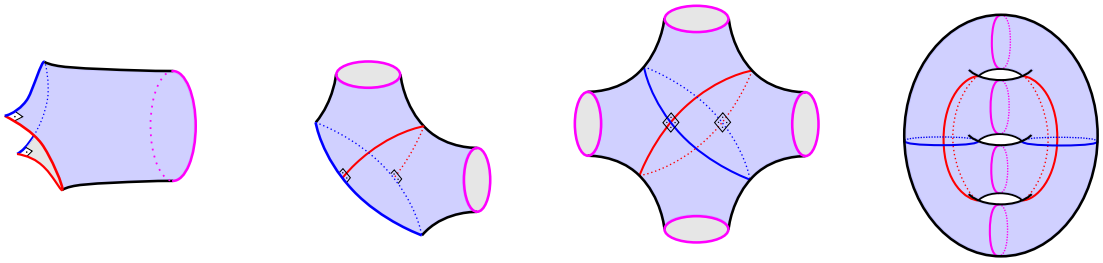

(a) (b) (c) (d)

Figure 4.3.3: From left to right, the four steps described in Example 4.3.3.

- we build a natural colouring λ' on M': each facet of M' comes from a facet of M, by mirroring or doubling. We assign to each facet the colour of the corresponding facet in M. This is a $(k-1)$-colouring;
- if $k-1=0$, we have no facets lefts and we have obtained $\mathcal{M}_\lambda$; otherwise we start again this procedure with M' and λ'.

By performing this on our example, after mirroring along the red and blue facets we get a compact manifold with $2^{3-1}=4$ copies of $F_3 \cong S^1$ as boundary (see Figure 4.3.3, (c)). Then, by mirroring this manifold along its boundary, we get $\mathcal{M}_\lambda$ and the 4 copies of F_3 as a separating submanifold.

Remark 4.3.4. We point out that there can exist manifolds with corners that do not admit any colouring. In fact it can happen that some facet F of a manifold with corners W is not *embedded*. In this case, such a facet is technically adjacent to itself and a colouring of W should assign two different colours to F, which is impossible. This is an important issue we will take care of. See also Example 4.3.7.

Concerning dodecahedral manifolds, [79, Proposition 4 - Remark 5] gives us the following:

Proposition 4.3.5. *Every dodecahedral manifold M embeds geodesically in the interior of a connected, complete, compact, orientable hyperbolic 4-manifold W with corners. If M is connected and tesselated into k dodecahedra, W is tesselated into $2k$ 120-cells.*

Remark 4.3.6. Notice that the 120-cell is a compact hyperbolic 4-dimensional polytope that has 120 3-facets that are right-angled dodecahedra. For more information on this, see [80, Section 1]. The idea of the construction in [80] is to take one 120-cell $\mathcal{H}_i$ for each right-angled dodecahedron $\mathcal{D}_i$ of the decomposition of M, then consider each $\mathcal{D}_i$ as one facet of $\mathcal{H}_i$, and then extend each gluing between two faces $F \in \mathcal{D}_i$ and $G \in \mathcal{D}_j$ to a gluing of the dodecahedral facets $\mathcal{A} \in \mathcal{H}_i$ and $\mathcal{B} \in \mathcal{H}_j$ such that $\mathcal{D}_i \cap \mathcal{A} = F$ and

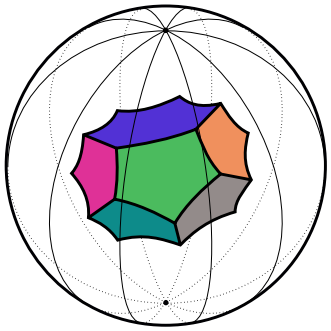

Figure 4.3.4: The Löbell polyhedron $R(6)$ in the disc model of the hyperbolic space. In blue, one hexagonal facet. Opposite to it, there is another hexagonal facet, that is not visible. All the other facets are pentagons.

$\mathcal{D}_j \cap \mathcal{B} = G$. This operation produces a manifold with corners W' in which M is an isolated facet. The manifold W is obtained by considering the mirror of W' along M. This can be visualized by mirroring the manifold with corners in Figure 4.3.2 along F_3. We denote these two copies of W' inside W as W'_+ and W'_-. As a consequence of this construction, we have that

$$\mathcal{F}_W = (\mathcal{F}_{W'_+} \setminus M) \sqcup (\mathcal{F}_{W'_-} \setminus M),$$

and a facet in $\mathcal{F}_{W'_+} \setminus M$ is never adjacent to a facet in $\mathcal{F}_{W'_-} \setminus M$. This decomposition induces a natural involution

$$s \colon \mathcal{F}_W \to \mathcal{F}_W,$$

that sends each facet F of W to the corresponding facet in the other copy of W' in W.

We now describe a situation where a construction analogous to the one contained in the proof of Proposition 4.3.5 yields a manifold with corners with some non embedded facets. For the cases of our interests we tackle this issue in Proposition 4.3.14.

Example 4.3.7. Recall that the regular right-angled hyperbolic hexagon is one facet of the Löbell polyhedron $R(6)$. This is a 3-dimensional right-angled hyperbolic polyhedron with 14 faces: 2 hexagonal faces and 12 pentagonal faces arranged in the same pattern as the lateral surface of a dodecahedron. Löbell polyhedra were defined in [115], see also [114] and see Figure 4.3.4 for a picture of $R(6)$.

Therefore if a closed surface S is tessellated by regular right-angled hyperbolic hexagons, by performing the same construction of Proposition 4.3.5 it is possible to embed geodesically S in the interior of a hyperbolic 3-manifold with corners tessellated by copies of $R(6)$. We now consider a regular right-angled hyperbolic hexagon E and glue two of its edges as depicted in Figure 4.3.5 a). In this way we obtain a 2-dimensional manifold with corners and by colouring its three facets we obtain a closed hyperbolic

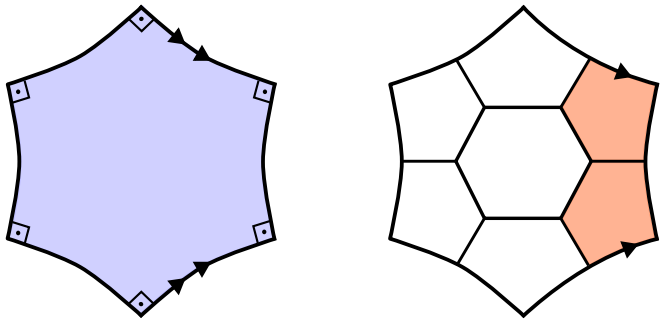

Figure 4.3.5: On the left, the gluing that give raise to the non-embedded facet in Example 4.3.7. On the right, the facets of $R(6)$ not adjacent to the one that is identified with the hexagon; the two pentagons that become the same facet after the gluing are coloured.

surface S tessellated by hexagons. When extending the gluings among the hexagons to the faces of the $R(6)$ polyhedra we have that two adjacent pentagonal faces (the coloured ones in Figure 4.3.5 *b*)) of the polyhedron placed above E are glued along one edge and become a non-embedded facet of the final 3-manifold with corners in which S embeds.

We now introduce a special, yet very natural, type of colourings that will be useful for our constructions. Recall from Remark 4.3.6 that there is an involution s on the set of facets of the manifold W provided by Proposition 4.3.5.

Definition 4.3.8. A colouring λ of W is *symmetric* if $\lambda \circ s = \lambda$ (see Figure 4.3.6).

In other words, a colouring of W is symmetric if and only if corresponding facets in the two copies of W' in W have the same colour. Asking for a symmetric colouring is not a restrictive request; in fact we have the following:

Lemma 4.3.9. *If the manifold with corners W admits a k-colouring then it also admits a symmetric h-colouring with $h \leq k$.*

Proof. Suppose that we have a k-colouring $\lambda\colon \mathcal{F}_W \to \{1, \dots, k\}$. We can define a new colouring $\bar{\lambda}$ such that:

- on a facet $F \in \mathcal{F}_{W'_+} \setminus M$ it takes value $\lambda(F)$;
- on a facet $F \in \mathcal{F}_{W'_-} \setminus M$ it takes value $\lambda \circ s(F)$.

We now show that the map $\bar{\lambda}$ assigns to adjacent facets different colours. Let F, G be two adjacent facets in $\mathcal{F}_W$. From Remark 4.3.6, they both belong to $\mathcal{F}_{W'_+} \setminus M$ or to $\mathcal{F}_{W'_-} \setminus M$. In the first case, $\bar{\lambda}$ takes the same value as λ, hence they have different image. In the second case, F and G are adjacent if and only if $s(F)$ and $s(G)$ are, hence

$$\bar{\lambda}(F) = \lambda \circ s(F) \neq \lambda \circ s(G) = \bar{\lambda}(G).$$

The new colouring $\bar{\lambda}$ could be not surjective onto $\{1,\dots,k\}$. In this case, we fix a bijection b from the image of $\bar{\lambda}$ and $\{1,\dots,h\}$ and consider $b\circ\bar{\lambda}$. □

Remark 4.3.10. Note that the manifold $\mathcal{M}_\lambda$ obtained from a symmetric k-colouring of W is isometric to the manifold $\mathcal{M}_\mu$ obtained by the colouring μ on W' such that $\mu(F)=\lambda(F)$ if $F\neq M$ (where F is seen both as a facet of W' and as $W'_+\cong W'$) and $\mu(M)=k+1$. Indeed, if we mirror W' along M (which was given a different colour than the rest of W') and colour its copy with the same colours on corresponding facets, we get back the symmetric colouring λ on W.

Let M be a dodecahedral manifold, W the manifold with corners provided by Proposition 4.3.5 and N the manifold obtained by a symmetric k-colouring of W. We now describe how the copies of M are located in N.

Lemma 4.3.11. *The disconnected manifold $M\times\mathbb{Z}_2^k$ embeds totally geodesically in N as a separating submanifold. More precisely, the image of $M\times\mathbb{Z}_2^k$ separates N in two isometric connected components N_+ and N_-.*

Proof. We have that $M\times\mathbb{Z}_2^k$ embeds totally geodesically in $W\times\mathbb{Z}_2^k$. We also have the quotient $W\times\mathbb{Z}_2^k\xrightarrow{\pi}(W\times\mathbb{Z}_2^k)/_\sim=N$, which identifies facets of $W\times\mathbb{Z}_2^k$. Since $M\times\mathbb{Z}_2^k$ lies in $\mathrm{int}(W)\times\mathbb{Z}_2^k$, we have that it embeds geodesically in N as well. From now on we will identify $M\times\mathbb{Z}_2^k$ with its image in N.

It follows by the construction of W (see Remark 4.3.6) that M separates W in two isometric copies of $W'\setminus M$ and therefore $M\times\mathbb{Z}_2^k$ separates $W\times\mathbb{Z}_2^k$ in two isometric copies of $(W'\setminus M)\times\mathbb{Z}_2^k$. Of course the image of these two copies via π is exactly the complement of $M\times\mathbb{Z}_2^k$ inside N and since they are saturated sets for the $\mathbb{Z}_2^k$ action their images are disjoint open sets in W. In order to conclude the proof we are then left to prove that their images are connected and isometric. This is a consequence of the colouring being symmetric. In fact each colouring of W induces, by restriction, a colouring of each of the two copies of $W'\setminus M$. If the colouring is symmetric, then the induced colourings on the the two copies of $W'\setminus M$ coincide. By definition, the images of the two copies of $(W'\setminus M)\times\mathbb{Z}_2^k$ in W are exactly the manifolds obtained by colouring $W'\setminus M$ with these induced colourings, and therefore they are connected and isometric. □

Remark 4.3.12. The construction described in the proof above can also be visualized in Figure 4.3.6 and 4.3.7 where the geodesic hypersurface is the purple circle. In this case, we have that $N_+\cong N_-$ and N is the mirror of N_+ along its boundary.

We are now ready to prove that if M is an L-space the manifold N contains a separating L-space:

Proposition 4.3.13. *Suppose that the dodecahedral manifold M is an L-space. Then the manifold N can be written as $N=N_1\cup_{M'}N_2$, where M' is an L-space and $b_2^+(N_i)\geq 1$*

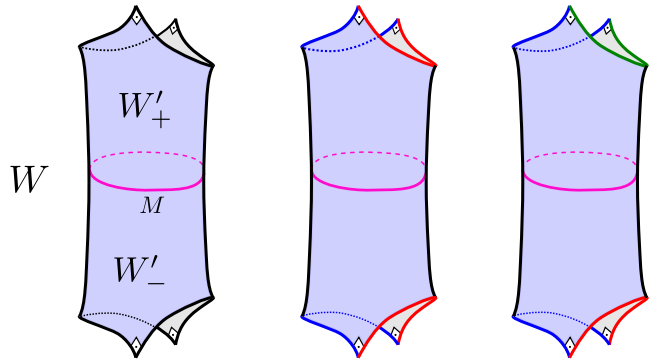

Figure 4.3.6: The manifold W built in Proposition 4.3.5, with a symmetric and a non-symmetric colouring (see Definition 4.3.8). The manifold obtained using the symmetric colouring is isometric to the one in Figure 4.3.3. See also Figure 4.3.7.

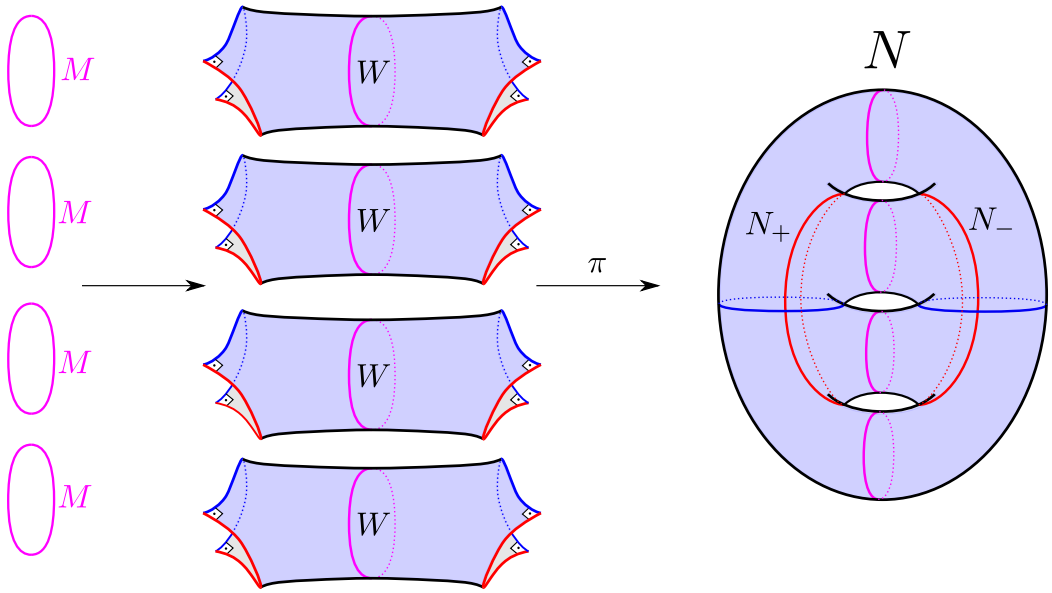

Figure 4.3.7: A schematic picture of the embedding of the separating dodecahedral space, described in the proof of Lemma 4.3.11.

for $i = 1, 2$. In particular, by Proposition 4.1.3, the Seiberg-Witten invariants of N all vanish.

Proof. We use the same notations of Lemma 4.3.11 and we divide the proof in few steps.

- *Step 1: $b_2^+(N) \geq 2$.*

  Recall that the Euler characteristic of a closed, connected, orientable 4-manifold satisfies

  $$\chi = 2 - 2b_1 + b_2$$

  and that $b_2 = b_2^+ + b_2^-$. Moreover, as a consequence of the Hirzebruch signature formula and [17, Theorem 3], hyperbolic 4-manifolds have signature zero and therefore $b_2^+ = b_2^-$; hence, the Euler characteristic of N satisfies

  $$\chi(N) = 2(1 - b_1(N) + b_2^+(N)).$$

  This formula implies that if $\chi(N) > 4$ then $b_2^+(N) \geq 2$. In order to conclude we note that if N is tessellated into n 120-cells, then

  $$\chi(N) = \frac{17}{2} \cdot n.$$

  This can be proved by using the notions of *orbifold covering* and *characteristic simplex*, see *e.g.* [80, Section 1.4]. As a consequence, we have that $\chi(N) > 8$.

- *Step 2: $b_2^+(N_+) = b_2^+(N_-) \geq 1$ and $b_2^+(N_+) + b_2^+(N_-) = b_2^+(N)$.*

  Recall from the construction of N and from the proof of Lemma 4.3.11 that N is obtained by gluing together N_+ and N_- along their boundaries (that are made up by 2^k disjoint copies of the dodecahedral manifold M). Also recall that N_+ is isometric, and therefore diffeomorphic, to N_-. This implies that $b_2^+(N_+) = b_2^+(N_-)$. Since N_+ and N_- are glued along a disjoint union of rational homology spheres, by applying the Mayer-Vietoris sequence we deduce that $H_2(N, \mathbb{Q}) \cong H_2(N_+, \mathbb{Q}) \oplus H_2(N_-, \mathbb{Q})$ and that

  $$b_2^+(N) = b_2^+(N_+) + b_2^+(N_-).$$

  Since $b_2^+(N) \geq 2$ we also deduce that $b_2^+(N_+) \geq 1$ and $b_2^-(N_-) \geq 1$.

- *Step 3: there exists an L-space M' such that $N = N_1 \cup_{M'} N_2$.*

  The L-space M' is diffeomorphic to the connected sum of copies of M and $\overline{M}$, where $\overline{M}$ denotes M with the opposite orientation. This operation of connected sum can be performed inside N in the following way: we label the boundary components of N_+ with numbers $\{1, 2 \ldots, 2^k\}$ and we consider $(2^k - 1)$ pairwise disjoint properly

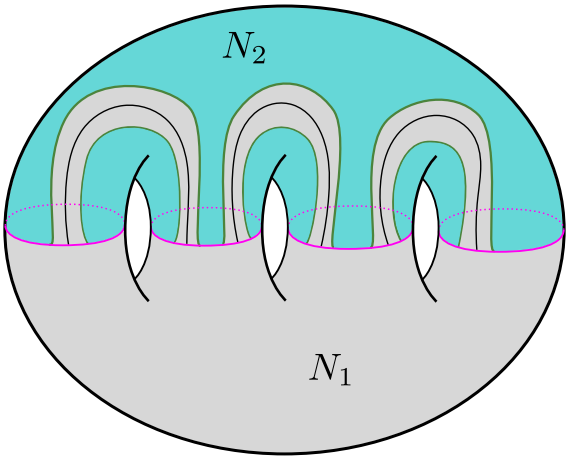

Figure 4.3.8: A schematic picture of the construction presented in the proof of *Step 3*.

embedded arcs $\alpha_1, \dots, \alpha_{2^k-1}$ in N_+ so that α_i connects the i-th and the $(i+1)$-th boundary components of N_+. If we denote with U a tubular neighbourhood of these arcs in N_+ we have that $N = N_1 \cup_\partial N_2$ where $N_1 = N_- \cup U$ and $N_2 = N_+ \setminus U$, and where $\partial N_1 = \partial N_2$ is exactly the connected sum M'. Since M is an L-space, M' is an L-space as a consequence of [86, Proposition 6.1]. See Figure 4.3.8 for a schematic picture of this construction. By studying the orientations induced on the copies of W embedded in N, one can state more precisely that

$$M' \cong 2^{k-1}M \# 2^{k-1}\overline{M},$$

even if we do not need this for our construction.

- *Step 4:* $b_2^+(N_1) = b_2^+(N_2) \geq 1$.

  By virtue of *Step 2*, to prove that

  $$b_2^+(N_1) = b_2^+(N_2) \geq 1$$

  it will be sufficient to show that $b_2^+(N_1) = b_2^+(N_-)$ and $b_2^+(N_2) = b_2^+(N_+)$. The manifold N_1 is obtained by gluing 4-dimensional 1-handles to N_-, that is to say, by gluing copies of $\mathbb{D}^1 \times \mathbb{D}^3$ to N_- along $\partial\mathbb{D}^1 \times \mathbb{D}^3$. Since the gluing regions have vanishing first and second homology groups, it is a consequence of the Mayer-Vietoris sequence that

  $$H_2(N_1, \mathbb{Z}) = H_2(N_-, \mathbb{Z})$$

  and that

  $$b_2^+(N_1) = b_2^+(N_-).$$

  We are left to prove that $b_2^+(N_2) = b_2^+(N_+)$ holds. To do this we notice that since N is obtained by gluing N_+ and N_- along a rational homology sphere, we can

apply the same reasoning of *Step 2* to deduce that

$$b_2^+(N) = b_2^+(N_1) + b_2^+(N_2),$$

and as a consequence of $b_2^+(N_1) = b_2^+(N_-)$ we have that

$$b_2^+(N_2) = b_2^+(N) - b_2^+(N_1) = b_2^+(N) - b_2^+(N_-) = b_2^+(N_+).$$

This concludes the proof. □

4.3.2 Some concrete examples

To conclude we now use the theory and the construction introduced in the previous section to present some explicit examples of hyperbolic 4-manifolds fulfilling the requirements of Question 2. Recall from Theorem E that we have six dodecahedral manifolds in the census $\mathscr{D}$ that are L-spaces. To produce our examples we want to apply Proposition 4.3.13 and to do this we need to find colourings of the manifols with corners containing our dodecahedral L-spaces. Before trying to find colourings, we have to check whether in the cases of our interests the construction of Proposition 4.3.5 yields manifolds with embedded facets (recall Example 4.3.7). Notice that by [43], the six manifolds in $\mathscr{D}$ that are L-spaces admit only one tessellation in right-angled dodecahedra up to combinatorial isomorphism. We have the following:

Proposition 4.3.14. *Let M be one of the six dodecahedral L-spaces in $\mathscr{D}$ (see Table 4.1.1). Then the manifold W built as in Remark 4.3.6 using its tessellation in dodecahedra has embedded facets if and only if M has index* 11 *or* 28*.*

Proof. The proof is computer-based. We build the manifolds following the instructions of Remark 4.3.6 starting with all the six dodecahedral L-spaces in $\mathscr{D}$ and we find non-embedded facets when performing this construction starting with the manifolds indexed with 0, 2, 8, 15. The code that we used can be found in [21]. □

Let W_{11} (resp. W_{28}) be the manifold with corners built as in Remark 4.3.6 starting with the dodecahedral manifold in $\mathscr{D}$ with index 11 (resp. 28). We have the following:

Lemma 4.3.15. *The manifolds with corners W_{11} and W_{28} admit a symmetric 6-colouring.*

Proof. The proof is computer-based. To search for a colouring of a manifold with corners W, we build a graph G_W in the following way: we take one vertex for each facet and we add one edge between two vertices if the corresponding facets are adjacent.

Once we have G_W, finding a colouring for the manifold with corners W is equivalent to finding a colouring of the graph G_W. The problem of colouring a graph is well known and Sage [109] provides a natural environment to search for minimal colouring of graphs.

In our cases, the graph $G_{W_{11}}$ is made out by two equivalent connected components with 334 vertices, one corresponding to the facets of W'_+ and one corresponding to the ones of W'_-. In order to find a symmetric colouring of W_{11} it is sufficient to colour only one of these two components and then extend the colouring as in the proof of Lemma 4.3.9. By using the Mixed Integer Linear Programming solver CPLEX [24] we find a 6-colouring in less than 5 minutes. We are also able to prove that $G_{W_{11}}$ is not 5-colourable.

The same holds also for $G_{W_{28}}$. We just point out that the fact that these graphs have the same number of vertices is not a casuality: this number in fact depends only on the number n of dodecahedra in the tessellation of the dodecahedral 3-manifold. Namely, the total number of vertices in G_W is

$$2 \cdot n \cdot \left(\frac{20}{8} + \frac{12}{2} + 30 + 12 + 20 + 12 + 1 \right),$$

where this formula descends from the discussion in [79, Proof of Lemma 7]. □

From now on we choose one specific 6-colouring for W_{11} (resp. W_{28}), that we denote by λ_{11} (resp. λ_{28}) and that can be found in [21]. We denote the hyperbolic 4-manifold obtained by this coloured manifold with corners (recall Proposition 4.3.2) with $\mathcal{N}_{11}$ (resp. $\mathcal{N}_{28}$). The following holds:

Theorem 4.3.16. *The manifold $\mathcal{N}_{11}$ (resp. $\mathcal{N}_{28}$):*

1. *is a connected, orientable, closed, hyperbolic 4-manifold;*
2. *is tessellated in 2^9 right-angled hyperbolic 120-cells;*
3. *can be written as $N_1 \cup_{M'} N_2$, where M' is an L-space and $b_2^+(N_i) \geq 1$ for $i = 1, 2$. In particular, its Seiberg-Witten invariants all vanish;*
4. *has Betti numbers with coefficients in $\mathbb{R}$ and $\mathbb{Z}_2$ as described in Table 4.3.1 (resp. Table 4.3.2).*

Proof. Point 1 is a direct consequence of Proposition 4.3.2. The same proposition also tells us that $\mathcal{N}_{11}$ (resp. $\mathcal{N}_{28}$) is tessellated in 2^6 copies of W_{11} (resp. W_{28}); since the latter is tessellated in 8 120-cells, we also obtain Point 2. We point out that this tesselation is explicit; in particular, in [21] there is the list of maps that describe the gluings of the facets of these 2^9 120-cells. Point 3 is a direct consequence of Proposition 4.3.13. The proof of Point 4 is computer-based. Using its tessellation in 120-cells, we obtain a description of $\mathcal{N}_{11}$ (resp. $\mathcal{N}_{28}$) as a CW-complex. In this way we can also check that the Euler characteristic is consistent with the one obtained from the formula described in the proof of Proposition 4.3.13, Step 1. We can now compute the Betti numbers using cellular homology. In particular:

- with $\mathbb{Z}_2$ coefficients, we write all the matrices that represent the boundary maps of the cellular chain complex in the standard bases (the ones given by the n-cells in degree n). Computing their rank we recover the Betti numbers;

- with $\mathbb{R}$ coefficients, we write two matrices that represent the boundary maps of the cellular chain complex in the standard bases: the one from the 1-cells to the 0-cells and the one from the 2-cells to the 1-cells. Computing the rank of these matrices we are able to verify that $b_0 = 1$ and to determine the b_1, and we recover the other Betti numbers using the Poincaré Duality and the Euler characteristic. Using these matrices and the Universal Coefficient Theorem, one should be able to find all the integral homology. However, the computation is too heavy for our computer resources.

The proof is complete. □

$\mathcal{N}_{11}$	b_0	b_1	b_2	b_3	b_4
$\mathbb{R}$	1	725	5800	725	1
$\mathbb{Z}_2$	1	746	5842	746	1

Table 4.3.1: The Betti numbers of $\mathcal{N}_{11}$.

$\mathcal{N}_{28}$	b_0	b_1	b_2	b_3	b_4
$\mathbb{R}$	1	741	5832	741	1
$\mathbb{Z}_2$	1	769	5888	769	1

Table 4.3.2: The Betti numbers of $\mathcal{N}_{28}$.

Generalised colourings

In this section we briefly describe a well-known generalisation of the notion of *colouring* (see [35] for a complete discussion). Let W be a compact n-manifold with corners. Let S be $\mathbb{Z}_2^m$, and let $e_1, \dots, e_m$ be its standard basis. We say that an element $v \in S$ is *odd* if it is a sum of an odd number of elements in the standard basis, and *even* otherwise.

Definition 4.3.17. A *generalised m-colouring* of W is a map $\rho\colon \mathcal{F}_W \to S$ such that:

- the elements in $\{\rho(F)\}_{F\in\mathcal{F}_W}$ generate S;

- if $F_{i_1}, \dots, F_{i_r}$ share a common subface, their images through ρ are linearly independent.

Given a generalised m-colouring ρ, we can define the topological space $\mathcal{M}_\rho = (W \times S)/_\sim$, where distinct $W \times \{u\}$, $W \times \{v\}$ are glued along the identity on a facet $F \in \mathcal{F}_W$ if $u - v = \rho(F)$. The analogous of Proposition 4.3.2 holds, and can be shown combining [79, Proposition 6] and [55, Lemma 2.4]:

Proposition 4.3.18. *The resulting $\mathcal{M}_\rho$ is a (possibly non-orientable) connected hyperbolic n-manifold tessellated into 2^m copies of W. If the elements in $\{\rho(F)\}_{F\in\mathcal{F}_W}$ are all odd, it is orientable.*

Remark 4.3.19. Given a k-colouring $\lambda\colon W \to \{1,\dots,k\}$, one can associate to it a generalised k-colouring ρ_λ by taking $S = \mathbb{Z}_2^k$ and defining $\rho(F) = e_{\lambda(F)}$. This is a generalised colouring because in a compact manifold with corners, facets that share a common subface are pairwise adjacent (see Example 4.3.3). The manifolds $\mathcal{M}_\lambda$ and $\mathcal{M}_\rho$ are naturally isometric.

Manifolds obtained by colourings are easier to visualize than those obtained by generalised colourings. On the other hand, generalised colourings often give the chance to obtain manifolds tessellated with a lower number of copies of W, as the following proposition shows (see also [34, Proposition 3.1.16]):

Proposition 4.3.20. *Let λ be a k-colouring of a compact n-manifold with corners W. Let $\rho_\lambda\colon \mathcal{F}_W \to \mathbb{Z}_2^{k-1}$ be the map:*

$$\rho(F) = \begin{cases} e_{\lambda(F)} & \text{if } \lambda(F) \neq k \\ e_1 + \ldots + e_{k-1} & \text{if } \lambda(F) = k \end{cases}. \tag{4.1}$$

If k is even and $k > n$, ρ_λ is a generalised $(k-1)$-colouring such that all the elements in $\{\rho_\lambda(F)\}_{F\in\mathcal{F}_W}$ are odd.

Proof. The set $\{\rho_\lambda(F)\}_{F\in\mathcal{F}_W}$ generates $\mathbb{Z}_2^{k-1}$ because it contains $e_1,\dots,e_{k-1}$. To finish the proof we just need to show that if $F_{i_1},\dots,F_{i_r}$ share a common subface, their images through ρ_λ are linearly independent. Since the dimension of W is n, we know that $r \leq n < k$. Since λ is a colouring, we know that the set $A = \{\lambda(F_{i_1}),\dots,\lambda(F_{i_r})\}$ contains r distinct elements. Then we can conclude that:

- if $k \notin A$, $\rho_\lambda(F_{i_1}),\dots,\rho_\lambda(F_{i_r})$ are independent because they are part of a basis, see also Remark 4.3.19;
- otherwise, there is an element of $\{1,\dots,k\}$ that is not in A. It is then easy to show that $\rho_\lambda(F_{i_1}),\dots,\rho_\lambda(F_{i_r})$ are independent.

The proof is complete. □

Using the previous proposition, it is easy to obtain a generalised 5-colouring of W_{11} (resp. W_{28}) starting with λ_{11} (resp. λ_{28}) that produces an orientable manifold $\mathcal{M}_{11}$ (resp. $\mathcal{M}_{28}$) that is double-covered by $\mathcal{N}_{11}$ (resp. $\mathcal{N}_{28}$) and satisfies:

Proposition 4.3.21. *The manifold $\mathcal{M}_{11}$ (resp. $\mathcal{M}_{28}$):*

1. *is a connected, orientable, closed, hyperbolic 4-manifold;*
2. *is tessellated in 2^8 right-angled hyperbolic 120-cells;*
3. *can be written as $N_1 \cup_{M'} N_2$, where M' is an L-space and $b_2^+(N_i) \geq 1$ for $i = 1, 2$. In particular, its Seiberg-Witten invariants all vanish;*
4. *has Betti numbers with coefficients in $\mathbb{R}$ and $\mathbb{Z}_2$ as described in Table 4.3.3 (resp. Table 4.3.4).*

Proof. Everything works exactly as in proof of Theorem 4.3.16. □

$\mathcal{M}_{11}$	b_0	b_1	b_2	b_3	b_4
$\mathbb{R}$	1	37	2248	37	1
$\mathbb{Z}_2$	1	707	3588	707	1

Table 4.3.3: The Betti numbers of $\mathcal{M}_{11}$.

$\mathcal{M}_{28}$	b_0	b_1	b_2	b_3	b_4
$\mathbb{R}$	1	53	2280	53	1
$\mathbb{Z}_2$	1	713	3600	713	1

Table 4.3.4: The Betti numbers of $\mathcal{M}_{28}$.

4.4 Questions and further developments

Applicability of the algorithm. Despite the potential problems that the algorithm described in Section 4.2 may encounter, in practice it was pretty fast in proving that the six manifolds of Theorem E are L-spaces. In some cases, it helped avoiding some curves at the beginning of the algorithm to converge faster (see [21] for more details).

It would be interesting to use it to study larger families of manifolds. The greatest bottleneck appears to be the computation of the Turaev torsion, whose complexity seems to grow very fast with the number of tetrahedra in the ideal triangulation of the $\mathbb{Q}HT$.

The authors were made aware by Nathan Dunfield in a mail exchange that by using a similar approach it was possible to show that the Seifert-Weber manifold is an L-space with bare hands. This is a hyperbolic manifold tessellated by one hyperbolic dodecahedron with $\frac{2}{5}\pi$ dihedral angles, and was proved to be an L-space in the context of the monopole Floer homology in [75] with completely different methods. Also our algorithm confirms that this is the case.

In [30, Remark 4.9], Dunfield points out that there are 118 rational homology solid tori in $\mathscr{C}$ that is not known whether they are Floer simple or not. We used the algorithm to search for L-space fillings of these manifolds and we were able to prove that at least 116 of these are Floer simple. The two remaining ones are $o9_{36740}$ and $o9_{41707}$.

Limitations of the algorithm. The first step of the algorithm consists in drilling a curve from the rational homology sphere that one wants to study hoping to find a rational homology solid torus that is Floer simple, but we do not know if such a curve exists, even when if we start with an L-space. So we leave here the following question:

Question 3. Let M be an L-space. Does there exist a Floer simple rational homology solid torus Y such that M is a Dehn filling on Y?

A more specific question that applies to our algorithm would be:

Question 4. Let M be a hyperbolic L-space. Does there exist a geodesic γ such that drilling γ out of M yields a Floer simple rational homology solid torus?

Appendix

4.A The algorithm

In this appendix we explain in detail how the algorithm described in Section 4.2 works. The code can be found in [21]. The pseudocode presented here is written to improve the readability, not the speed of the algorithm; the implemented version is slightly different. Whenever we have a rational homology solid torus Y, we suppose it is given with a chosen basis for $H_1(\partial Y, \mathbb{Z})$; for this reason we always identify $Sl(Y)$ with $\mathbb{Q} \cup \{\infty\}$.

The algorithm essentially goes back and forth alternating between these two functions:

- `is_certified_L_space(`M`)`: takes as input M, a hyperbolic $\mathbb{Q}HS$, and searches for a nice drilling: it returns Y and $\mathcal{I}$, where Y is a Turaev simple hyperbolic $\mathbb{Q}HT$ such that the $1/0$ filling on Y gives back M and $\mathcal{I}$ is an interval in $Sl(Y)$ that contains $1/0$ and whose endpoints are elements in $\iota^{-1}(D^{\tau}_{>0}(Y))$ (in the case $D^{\tau}_{>0}(Y) = \emptyset$ we take $\mathcal{I}$ as $Sl(Y) \setminus [l]$, where $[l]$ is the homological longitude of Y);
- `small_fillings`$(Y, \mathcal{I})$: takes as input Y, a Turaev simple hyperbolic $\mathbb{Q}HT$, and $\mathcal{I}$, an interval in $Sl(Y)$, and returns the two $\mathbb{Q}HS$ with smallest volume among the fillings $Y(\alpha)$ with $\alpha \in \mathcal{I}$.

While these two functions operate, they try to identify all the manifolds they work with, with the hope to obtain information about their L-space value using the Dunfield census $\mathscr{Y}$. If we discover that two fillings with coefficient in $\mathcal{I}$ are L-spaces, we use Theorem 1.2.2 to conclude that all the fillings with coefficients in $\mathcal{I}$ are L-spaces. Eventually, we hope we will conclude that the initial manifold is an L-space.

We need some globally-defined variables:

- `old_mnfds`: a list of the manifolds that we already found. We want to avoid them, because otherwise the algorithm would enter an infinite loop. Its starting value is the empty list;
- `M_C`: Max Coefficient, a positive integer. When we search for minimal volume fillings on Y, we search among the fillings h/k with $|h|, |k| \leq$ `M_C`.

Data: M a hyperbolic $\mathbb{Q}HS$.
Result: `True` if a proof that M is an L-space is found, `False` otherwise.

---

add M to `old_mnfds`;
C = finite collection of simple closed curves in M, provided by SnapPy;
$X = \{M \setminus$ the interior of a tubular neighborhood of $c\}_{c \in C}$;
`/* For every` Y `in` X`, we fix a peripheral basis such that the filling` $^1/_0$ `on` Y `gives back` M`.` `*/`
for $Y \in X$ **do**
  if *Y belongs to Dunfield census* **then**
    return "L-space value of M found using the census"
`found = False ;`
while *`found`* $==$ *`False`* **do**
  if *there is no hyperbolic Y in $X \setminus$ `old_mnfds`* **then**
    return `False`
  Y = smallest volume hyperbolic $Y \in X \setminus$`old_mnfds`;
  if *Y is Turaev simple* **then**
    `found = True ;`
  else
    $X = X \setminus \{Y\}$;
`Possible_intervals` = intervals in $Sl(Y)$ that contains $^1/_0$ and whose endpoints are elements in $\iota^{-1}(D^{\tau}_{>0}(Y))$ (in the case $D^{\tau}_{>0}(Y) = \emptyset$ we consider $Sl(Y) \setminus [l]$, where $[l]$ is the homological longitude of Y);
if *`Possible_intervals`* $== \{\mathcal{I}_1; \mathcal{I}_2\}$ **then**
  return (`small_fillings`$(Y, \mathcal{I}_1)$ **or** `small_fillings`$(Y, \mathcal{I}_2)$) ;
else if *`Possible_intervals`* $== \{\mathcal{I}\}$ **then**
  return `small_fillings`$(Y, \mathcal{I})$;

Algorithm 1: `is_certified_L_space`

Data: Y Turaev simple hyperbolic $\mathbb{Q}HT$; $\mathcal{I}$, an interval in $Sl(Y)$ that contains $1/0$ and whose endpoints are in $\iota^{-1}(D^{\tau}_{>0}(Y))$.
Result: `True` if a proof that $Y(1/0)$ is an L-space is found, `False` otherwise.

---

add Y to `old_mnfds`;
`pairs` $= \{(h,k) | h \in [-$`M_C`$,$`M_C`$], k \in [0,$`M_C`$], \gcd(h,k) = 1\}$;
$X = \{Y(h/k) | (h,k) \in$ `pairs`$, (h,k) \neq (-1,0), (h,k) \in \mathcal{I}\}$;
`/*` X `is a list more than a set: even if` $Y(h/k)$ `is diffeomorphic to` $Y(h'/k')$`, we count them as two elements in` X`. For this reason we avoid the case` $(h,k) = (-1,0)$`. */`
`L_space_found`=0;
for $M \in X$ **do**
  if *M is in Dunfield_QHS_Census* **then**
    if *"L-space value of M found using the census" == `False`* **then**
      return `False`
    else
      `L_space_found`=`L_space_found`+1;
      $X = X \setminus \{M\}$;
if *`L_space_found`* ≥ 2 **then**
  return `True`
if *`L_space_found`* $== 1$ **then**
  if *there is no hyperbolic M in $X \setminus$ `old_mnfds`* **then**
    return `False`
  $M =$ smallest volume hyperbolic $M \in X \setminus$`old_mnfds`;
  return `is_certified_L_space`(M)
if *`L_space_found`* $== 0$ **then**
  if *there are no two hyperbolic manifolds in $X \setminus$ `old_mnfds`* **then**
    return `False`
  $M_1, M_2 =$ two smallest volume hyperbolic manifolds in $X \setminus$`old_mnfds`;
  return (`is_certified_L_space`(M_1) **and** `is_certified_L_space`(M_2));

Algorithm 2: `small_fillings`

4.B Reading the output of the algorithm

Here we comment how to read the output of the function `is_certified_L_space`. Suppose we give the following commands:

```
M=CubicalOrientableClosedCensus(betti=0)[15]
val=is_certified_L_space(M, save_QHT=True, path_save_QHT=
"./proofs/RA_dod_15/")
print(val)
```

At line 2, we set the options

```
save_QHT=True, path_save_QHT="./proofs/RA_dod_15/";
```

they mean that we want to save the $\mathbb{Q}HT$s that we find while the algorithm is running as SnapPy triangulations. These will be saved in the directory `./proofs/RA_dod_15/` (remember to create the directory, otherwise nothing will be saved). The output we obtain is the following:

```
Inizializing...
: M has volume 17.2248... and homology Z/513
: Computing Turaev torsion drilling...
1: T(1, 2) has volume 14.2777... and homology Z/329
1: Computing Turaev torsion drilling...
11: The manifold T1 filled with (-1, 2) is [s345(-1,3)], its
L-space value is 1
12: T1(0, 1) has volume 8.96606... and homology Z/143
12: Computing Turaev torsion drilling...
121: The manifold T12 filled with (1, 1) is [v3245(1,2)], its
L-space value is 1
122: T12(3, 5) has volume 6.30690... and homology Z/59
122: T12(3, 5) is t12195(-1,-3), whose L-space value is known to be 1
2: T(1, 3) has volume 13.8548... and homology Z/237
2: Computing Turaev torsion drilling...
21: The manifold T2 filled with (0, 1) is [v2876(-1,2)], its
L-space value is 1
22: T2(-1, 3) has volume 9.69817... and homology Z/66
22: Computing Turaev torsion drilling...
221: T22(-2, 3) has volume 6.51216... and homology Z/87
221: T22(-2, 3) is o9_36980(1,2), whose L-space value is known to be 1
222: T22(-3, 4) has volume 6.38898... and homology Z/94
222: T22(-3, 4) is o9_34893(-3,2), whose L-space value is known to be 1

True
```

Since the value of `val` is `True`, we conclude that the given manifold is an L-space. The idea of the algorithm is the following: we start with the manifold M. We drill it

and we obtain T. By filling T we obtain $M1$ and $M2$. By drilling $M1$ we obtain $T1$. By filling $T1$ we obtain $M11$ and $M12$, and so on.

At the beginning of each line there is a number, which represents which $\mathbb{Q}HS$ we are referring to. For example, Line 7 starts with 12; this means we are referring to $M12$.

A *drilling-filling tree* is a tree where each node is either a $\mathbb{Q}HS$ or a $\mathbb{Q}HT$, and we have a labeled edge between A and B if B is obtained by Dehn-filling A, and the edge is labelled with the coefficients of the filling.

From this output we discover the existence of a drilling-filling tree as in Figure 4.B.1, that can be used to prove, through Theorem 1.2.2, that the given manifold is an L-space.

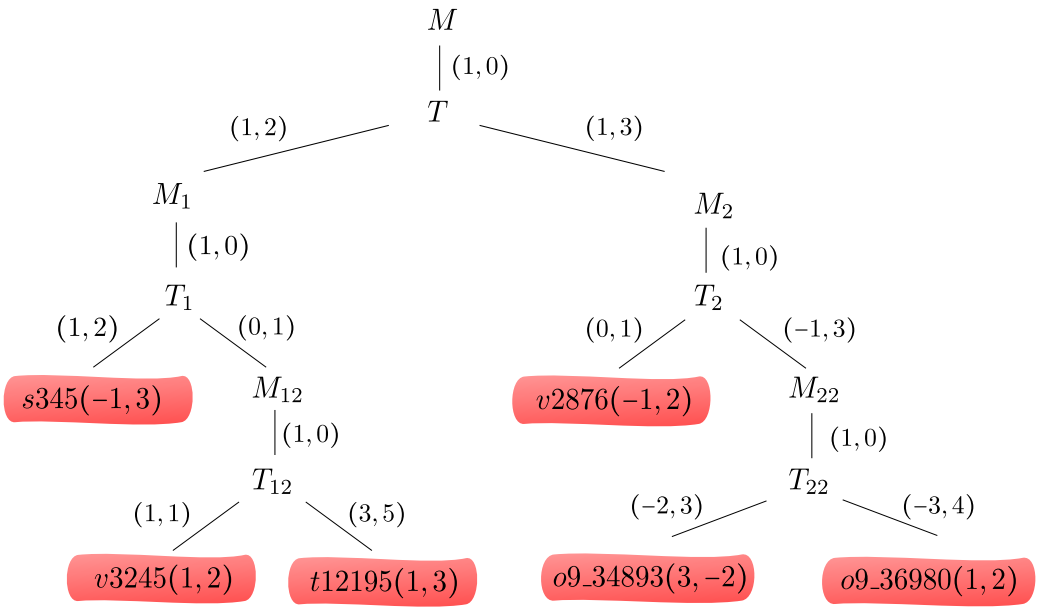

Figure 4.B.1: One example of drilling-filling tree. The manifolds that are L-spaces belonging to the Dunfield census are highlighted in red. In this case M=CubicalOrientableClosedCensus(betti=0)[15].

When $1/0$ is contained in $\iota^{-1}(D^{\tau}_{>0})$, we have two possible intervals to work with. In this case the output looks like the following (we extract some lines from a bigger output):

```
2211: T221(-2, 3) has volume 7.91082... and homology Z/2 + Z/2 + Z/12
2211: Computing Turaev torsion drilling...
22111: T2211(3, 4) has volume 7.32772... and homology Z/2 + Z/2 + Z/8
22111: Computing Turaev torsion drilling...
22111: Double interval..
22111A1: T22111(1, 2) has volume 9.49189... and homology Z/2 + Z/2 + Z/8
22111A1: Computing Turaev torsion drilling...
22111A11: T22111A1(2, 1) has volume 11.0403... and homology Z/2 + Z/42
22111A11: Computing Turaev torsion drilling...
```

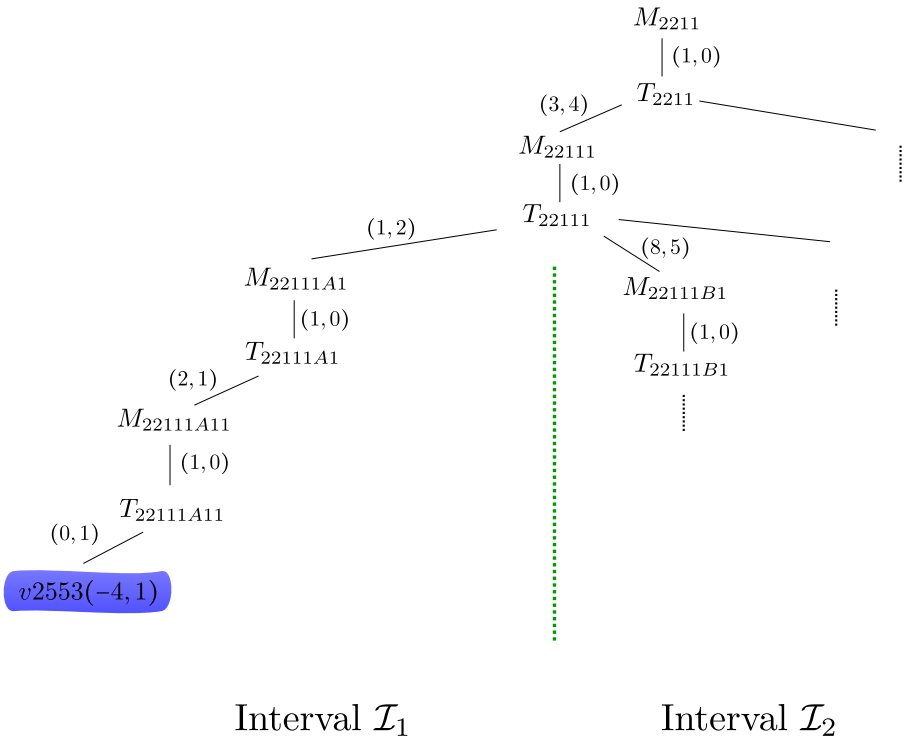

Figure 4.B.2: A portion of a drilling-filling tree. In this case the slope $1/0$ is contained in $\iota^{-1}(D^{\tau}_{>0})$ and therefore there are two intervals $\mathcal{I}_1$ and $\mathcal{I}_2$ in $Sl(T_{22111})$ to work with. The manifold $v2553(-4,1)$ is highlighted in blue since it belongs to the Dunfield census and it is not an L-space.

```
22111A111: The manifold T22111A11 filled with (0, 1) is
[v2553(-4,1)], its L-space value is -1
22111B1: T22111(8, 5) has volume 8.92932... and homology Z/4 + Z/24
22111B1: Computing Turaev torsion drilling...
22111B11: T22111B1(2, 3) has volume 9.26762... and homology Z/108
22111B11: Computing Turaev torsion drilling...
```

At Line 5, the code is telling us that $T22111$, obtained by drilling $M22111$, has two intervals we want to work with. The fillings on the first of these intervals will have labels starting with $22111A$ and the ones on the second one will have labels starting with $22111B$. From this output we discover the existence of a drilling-filling tree as in Figure 4.B.2. When we find a double interval, we have two possible intervals in $Sl(Y)$ where we can look for L-spaces. If for some filling in the first one the algorithm returns `False`, we go on looking in the other one.

Bibliography

[1] Ian Agol and Francesco Lin. Hyperbolic four-manifolds with vanishing Seiberg-Witten invariants. *Characters in Low-Dimensional Topology*, 760:1–8, 2020.

[2] Sebastian Baader and Christian Graf. Fibred links in S^3. *Expositiones Mathematicae*, 34(4):423–435, 2016.

[3] Ludovico Battista, Leonardo Ferrari, and Diego Santoro. Dodecahedral L-spaces and hyperbolic 4-manifolds. *arXiv preprint at arXiv:2208.01542.* Accepted for publication in Communications in Analysis and Geometry, 2022.

[4] Riccardo Benedetti and Carlo Petronio. *Lectures on hyperbolic geometry.* Springer Science & Business Media, 1992.

[5] Jonathan Bowden. Approximating C^0-foliations by contact structures. *Geometric and Functional Analysis*, 26(5):1255–1296, 2016.

[6] Steven Boyer and Adam Clay. Foliations, orders, representations, L-spaces and graph manifolds. *Advances in Mathematics*, 310:159–234, 2017.

[7] Steven Boyer, Cameron McA Gordon, and Liam Watson. On L-spaces and left-orderable fundamental groups. *Mathematische Annalen*, 356(4):1213–1245, 2013.

[8] Steven Boyer and Ying Hu. Taut foliations in branched cyclic covers and left-orderable groups. *Transactions of the American Mathematical Society*, 372(11):7921–7957, 2019.

[9] Steven Boyer, Dale Rolfsen, and Bert Wiest. Orderable 3-manifold groups. In *Annales de l'institut Fourier*, volume 55, pages 243–288, 2005.

[10] Mark Brittenham, Ramin Naimi, and Rachel Roberts. Graph manifolds and taut foliations. *Journal of Differential Geometry*, 45(3):446–470, 1997.

[11] Gerhard Burde and Heiner Zieschang. *Knots.* De Gruyter, 2003.

[12] Benjamin A Burton. The cusped hyperbolic census is complete. *arXiv preprint arXiv:1405.2695*, 2014.

[13] Benjamin A. Burton, Ryan Budney, William Pettersson, et al. Regina: Software for low-dimensional topology. `http://regina-normal.github.io/`, 1999–2021.

[14] Danny Calegari and Nathan M. Dunfield. Laminations and groups of homeomorphisms of the circle. *Inventiones mathematicae*, 152(1):149–204, 2003.

[15] A. Candel and L. Conlon. *Foliations I.* Number v. 1 in Foliations I. American Mathematical Society, 2000.

[16] Alberto Cavallo and Beibei Liu. Fibered and strongly quasi-positive L-space links. *Michigan Mathematical Journal*, 1(1):1–16, 2021.

[17] Shiing-Shen Chern. On curvature and characteristic classes of a Riemann manifold. In *Abhandlungen aus dem Mathematischen Seminar der Universität Hamburg*, volume 20, pages 117–126. Springer, 1955.

[18] Adam Clay, Tye Lidman, and Liam Watson. Graph manifolds, left-orderability and amalgamation. *Algebraic & Geometric Topology*, 13(4):2347–2368, 2013.

[19] Adam Clay and Dale Rolfsen. *Ordered groups and topology*, volume 176. American Mathematical Soc., 2016.

[20] Code available at https://sites.google.com/view/santoro/research.

[21] Code. Dodecahedral L-spaces and hyperbolic 4-manifolds. `https://doi.org/10.7910/DVN/A9WKAG`, 2022.

[22] Vincent Colin, Paolo Ghiggini, and Ko Honda. Equivalence of Heegaard Floer homology and embedded contact homology via open book decompositions. *Proceedings of the National Academy of Sciences*, 108(20):8100–8105, 2011.

[23] Vincent Colin, William H. Kazez, and Rachel Roberts. Taut foliations. *Communications in Analysis and Geometry*, 27(2):357–375, 2019.

[24] IBM ILOG Cplex. V20.1: User's manual for cplex. *International Business Machines Corporation*, 2021.

[25] Marc Culler and Nathan Dunfield. Orderability and Dehn filling. *Geometry & Topology*, 22(3):1405–1457, 2018.

[26] Marc Culler, Nathan M. Dunfield, Matthias Goerner, and Jeffrey R. Weeks. SnapPy, a computer program for studying the geometry and topology of 3-manifolds. Available at `http://snappy.computop.org` (28/06/2022).

[27] Nakul Dawra. On the link floer homology of L-space links. *arXiv preprint arXiv:1505.01100*, 2015.

[28] Charles Delman and Rachel Roberts. Taut foliations from double-diamond replacements. *Characters in Low-Dimensional Topology*, 760:123, 2020.

[29] Charles Delman and Rachel Roberts. Persistently foliar composite knots. *Algebraic & Geometric Topology*, 21(6):2761–2798, 2021.

[30] Nathan M. Dunfield. Floer homology, group orderability, and taut foliations of hyperbolic 3–manifolds. *Geometry & Topology*, 24:2075–2125, 2020.

[31] Nathan M Dunfield and Jacob Rasmussen. A unified Casson-Lin invariant for the real forms of $SL(2)$. *arXiv preprint arXiv:2209.03382*, 2022.

[32] David Eisenbud, Ulrich Hirsch, and Walter Neumann. Transverse foliations of Seifert bundles and self homeomorphism of the circle. *Commentarii Mathematici Helvetici*, 56(1):638–660, 1981.

[33] Yakov Eliashberg and William P. Thurston. *Confoliations*, volume 13. American Mathematical Soc., 1998.

[34] Leonardo Ferrari. *Hyperbolic Manifolds and Coloured Polytopes*. PhD thesis, Università di Pisa, 2021.

[35] Leonardo Ferrari, Alexander Kolpakov, and Leone Slavich. Cusps of hyperbolic 4-manifolds and rational homology spheres. *Proceedings of the London Mathematical Society*, 123(6):636–648, 2021.

[36] Ronald Fintushel and Ronald J Stern. Constructing lens spaces by surgery on knots. cl. *Math. Z*, 175:33–51, 1980.

[37] William Floyd and Ulrich Oertel. Incompressible surfaces via branched surfaces. *Topology*, 23(1):117–125, 1984.

[38] David Gabai. Foliations and the topology of 3-manifolds. *Journal of Differential Geometry*, 18(3):445 – 503, 1983.

[39] David Gabai. The Murasugi sum is a natural geometric operation II. *Contemp. Math*, 44:93–100, 1985.

[40] David Gabai and William H Kazez. Pseudo-Anosov maps and surgery on fibred 2-bridge knots. *Topology and its Applications*, 37(1):93–100, 1990.

[41] David Gabai and Ulrich Oertel. Essential laminations in 3-manifolds. *Annals of Mathematics*, 130(1):41–73, 1989.

[42] Paolo Ghiggini. Knot Floer homology detects genus-one fibred knots. *American journal of mathematics*, 130(5):1151–1169, 2008.

[43] Matthias Goerner. A census of hyperbolic Platonic manifolds and augmented knotted trivalent graphs. *arXiv preprint arXiv:1602.02208*, 2016.

[44] Eugene Gorsky, Beibei Liu, and Allison H Moore. Surgery on links of linking number zero and the Heegaard Floer d-invariant. *Quantum Topology*, 11(2):323–378, 2020.

[45] Eugene Gorsky and András Némethi. Links of plane curve singularities are L–space links. *Algebraic & Geometric Topology*, 16(4):1905–1912, 2016.

[46] André Haefliger. Structures feuilletées et cohomologie à valeur dans un faisceau de groupoïdes. *Commentarii Mathematici Helvetici*, 32(1):248–329, 1958.

[47] Jonathan Hanselman, Jacob Rasmussen, Sarah Dean Rasmussen, and Liam Watson. L-spaces, taut foliations, and graph manifolds. *Compositio Mathematica*, 156(3):604–612, 2020.

[48] Matthew Hedden. Notions of positivity and the Ozsváth–Szabó concordance invariant. *Journal of Knot Theory and its Ramifications*, 19(05):617–629, 2010.

[49] Craig D. Hodgson, G. Robert Meyerhoff, and Jeffrey R. Weeks. Surgeries on the Whitehead link yield geometrically similar manifolds. In *Topology'90*, pages 195–206. de Gruyter, 2011.

[50] Jennifer Hom. A survey on Heegaard Floer homology and concordance. *Journal of Knot Theory and Its Ramifications*, 26(02):1740015, 2017.

[51] Ying Hu. Euler class of taut foliations and Dehn filling. *arXiv preprint arXiv:1912.01645*, 2019.

[52] András Juhász. A survey of Heegaard Floer homology. In *New ideas in low dimensional topology*, pages 237–296. World Scientific, 2015.

[53] Tejas Kalelkar and Rachel Roberts. Taut foliations in surface bundles with multiple boundary components. *Pacific Journal of Mathematics*, 273(2):257–275, 2014.

[54] William Kazez and Rachel Roberts. C^0 approximations of foliations. *Geometry & Topology*, 21(6):3601–3657, 2017.

[55] Alexander Kolpakov, Bruno Martelli, and Steven Tschantz. Some hyperbolic three-manifolds that bound geometrically. *Proc. Amer. Math. Soc.*, 143:9:4103–4111, 2015.

[56] Alexander Kolpakov, Alan W. Reid, and Leone Slavich. Embedding arithmetic hyperbolic manifolds. *Mathematical Research Letters*, 25:1305–1328, 2018.

[57] David Krcatovich. The reduced knot floer complex. *Topology and its Applications*, 194:171–201, 2015.

[58] Siddhi Krishna. Taut foliations, positive 3-braids, and the L-space conjecture. *Journal of Topology*, 13(3):1003–1033, 2020.

[59] Peter Kronheimer and Tomasz Mrowka. Monopoles and three-manifolds. *(No Title)*, 2007.

[60] Peter Kronheimer, Tomasz Mrowka, Peter Ozsváth, and Zoltán Szabó. Monopoles and lens space surgeries. *Annals of mathematics*, pages 457–546, 2007.

[61] Peter B. Kronheimer and Tomasz Mrowka. *Monopoles and three-manifolds*, volume 10. Cambridge University Press Cambridge, 2007.

[62] Peter B Kronheimer and Tomasz S Mrowka. Monopoles and contact structures. *Inventiones mathematicae*, 130(2):209–256, 1997.

[63] Çağatay Kutluhan, Yi-Jen Lee, and Clifford Taubes. HF= HM, I: Heegaard Floer homology and Seiberg–Witten Floer homology. *Geometry & Topology*, 24(6):2829–2854, 2020.

[64] Çağatay Kutluhan, Yi-Jen Lee, and Clifford Taubes. HF= HM, II: Reeb orbits and holomorphic curves for the ech/Heegaard Floer correspondence. *Geometry & Topology*, 24(6):2855–3012, 2020.

[65] Çağatay Kutluhan, Yi-Jen Lee, and Clifford Taubes. HF= HM, III: holomorphic curves and the differential for the ech/Heegaard Floer correspondence. *Geometry & Topology*, 24(6):3013–3218, 2020.

[66] Çağatay Kutluhan, Yi-Jen Lee, and Clifford Taubes. HF= HM, IV: The Seiberg–Witten Floer homology and ech correspondence. *Geometry & Topology*, 24(7):3219–3469, 2021.

[67] Çağatay Kutluhan, Yi-Jen Lee, and Clifford Taubes. HF= HM, V: Seiberg–Witten Floer homology and handle additions. *Geometry & Topology*, 24(7):3471–3748, 2021.

[68] Marc Lackenby. The volume of hyperbolic alternating link complements. *Proceedings of the London Mathematical Society*, 88(1):204–224, 2004.

[69] Claude LeBrun. Hyperbolic manifolds, harmonic forms, and Seiberg–Witten invariants. *Geometriae Dedicata*, 91(1):137–154, 2002.

[70] Tao Li. Laminar branched surfaces in 3–manifolds. *Geometry & Topology*, 6(1):153–194, 2002.

[71] Tao Li. Boundary train tracks of laminar branched surfaces. In *Proceedings of symposia in pure mathematics*, volume 71, pages 269–286. Providence, RI; American Mathematical Society; 1998, 2003.

[72] Tao Li. Taut foliations of 3-manifolds with Heegaard genus two. *arXiv preprint arXiv:2202.00737*, 2022.

[73] Tao Li and Rachel Roberts. Taut foliations in knot complements. *Pacific Journal of Mathematics*, 269(1):149–168, 2014.

[74] William Bernard Raymond Lickorish. A foliation for 3-manifolds. *Annals of mathematics*, pages 414–420, 1965.

[75] Francesco Lin and Michael Lipnowski. Monopole Floer Homology, Eigenform Multiplicities, and the Seifert–Weber Dodecahedral Space. *International Mathematics Research Notices*, 2022(9):6540–6560, 2022.

[76] Paolo Lisca and András I Stipsicz. On the existence of tight contact structures on Seifert fibered 3-manifolds. *Duke Mathematical Journal*, 148(2):175–209, 2009.

[77] Yajing Liu. L-space surgeries on links. *arXiv:1409.0075*, 2014.

[78] Yajing Liu. L-space surgeries on links. *Quantum Topology*, 8(3):505–570, 2017.

[79] Bruno Martelli. Hyperbolic 3-manifolds that embed geodesically. *arXiv preprint https://arxiv.org/abs/1510.06325*.

[80] Bruno Martelli. Hyperbolic four-manifolds. In *Handbook of group actions, III*, pages 37–58. International Press of Boston, Inc., 2018.

[81] William Menasco. Closed incompressible surfaces in alternating knot and link complements. *Topology*, 23(1):37–44, 1984.

[82] Yi Ni. Knot Floer homology detects fibred knots. *Inventiones mathematicae*, 170(3):577–608, 2007.

[83] Sergei Petrovich Novikov. Topology of foliations. *Trans. Moscow Math. Soc*, 14:248–278, 1965.

[84] Ulrich Oertel. Incompressible branched surfaces. *Inventiones mathematicae*, 76(3):385–410, 1984.

[85] Peter Ozsváth and Zoltán Szabó. Holomorphic disks and genus bounds. *Geometry & Topology*, 8(1):311–334, 2004.

[86] Peter Ozsváth and Zoltán Szabó. Holomorphic disks and three-manifold invariants: properties and applications. *Annals of Mathematics*, pages 1159–1245, 2004.

[87] Peter Ozsváth and Zoltán Szabó. Holomorphic disks and topological invariants for closed three-manifolds. *Annals of Mathematics*, pages 1027–1158, 2004.

[88] Peter Ozsváth and Zoltán Szabó. On knot Floer homology and lens space surgeries. *Topology*, 44(6):1281–1300, 2005.

[89] Peter S Ozsváth and Zoltán Szabó. Knot Floer homology and rational surgeries. *Algebraic & Geometric Topology*, 11(1):1–68, 2010.

[90] Carlos Frederico Borges Palmeira. Open manifolds foliated by planes. *Annals of Mathematics*, pages 109–131, 1978.

[91] Robert C. Penner. A construction of pseudo-Anosov homeomorphisms. *Transactions of the American Mathematical Society*, 310(1):179–197, 1988.

[92] Robert C. Penner and John L. Harer. *Combinatorics of Train Tracks.(AM-125), Volume 125*. Princeton University Press, 2016.

[93] Jacob Rasmussen and Sarah Dean Rasmussen. Floer simple manifolds and L-space intervals. *Advances in Mathematics*, 322:738–805, 2017.

[94] Rachel Roberts. Taut foliations in punctured surface bundles, I. *Proceedings of the London Mathematical Society*, 82(3):747–768, 2000.

[95] Rachel Roberts. Taut foliations in punctured surface bundles, II. *Proceedings of the London Mathematical Society*, 83(2):443–471, 2001.

[96] Rachel Roberts, John Shareshian, and Melanie Stein. Infinitely many hyperbolic 3-manifolds which contain no reebless foliation. *Journal of the American Mathematical Society*, 16(3):639–679, 2003.

[97] Harold Rosenberg. Foliations by planes. *Topology*, 7(2):131–138, 1968.

[98] Diego Santoro. L-spaces, taut foliations and the Whitehead link. *arXiv preprint arXiv:2201.01211.* Accepted for publication in Algebraic and Geometric Topology, 2022.

[99] Diego Santoro. L-spaces, taut foliations and fibered hyperbolic two-bridge links. *arXiv preprint arXiv:2304.14914*, 2023.

[100] Horst Schubert. Knoten mit zwei brücken. *Mathematische Zeitschrift*, 65(1):133–170, 1956.

[101] Nathan Seiberg and Edward Witten. Electric-magnetic duality, monopole condensation, and confinement in n= 2 supersymmetric yang-mills theory. *Nuclear Physics B*, 426(1):19–52, 1994.

[102] Nathan Seiberg and Edward Witten. Monopoles, duality and chiral symmetry breaking in n= 2 supersymmetric QCD. *Nuclear Physics B*, 431(3):484–550, 1994.

[103] Clifford Henry Taubes. The Seiberg-Witten invariants and symplectic forms. *Mathematical Research Letters*, 1(6):809–822, 1994.

[104] Clifford Henry Taubes. Embedded contact homology and Seiberg–Witten Floer cohomology I. *Geometry & Topology*, 14(5):2497–2581, 2010.

[105] Clifford Henry Taubes. Embedded contact homology and Seiberg–Witten Floer cohomology II. *Geometry & Topology*, 14(5):2583–2720, 2010.

[106] Clifford Henry Taubes. Embedded contact homology and Seiberg–Witten Floer cohomology III. *Geometry & Topology*, 14(5):2721–2817, 2010.

[107] Clifford Henry Taubes. Embedded contact homology and Seiberg–Witten Floer cohomology IV. *Geometry & Topology*, 14(5):2819–2960, 2010.

[108] Clifford Henry Taubes. Embedded contact homology and Seiberg–Witten Floer cohomology V. *Geometry & Topology*, 14(5):2961–3000, 2010.

[109] The Sage Developers. *SageMath, the Sage Mathematics Software System*, 2022. `https://www.sagemath.org`.

[110] William P. Thurston. The geometry and topology of 3-manifolds. *Lecture notes*, 1978.

[111] William P. Thurston. A norm for the homology of 3-manifolds. *Memoirs of the American Mathematical Society*, 59(339):99–130, 1986.

[112] William P. Thurston. Hyperbolic structures on 3-manifolds, II: Surface groups and 3-manifolds which fiber over the circle. *arXiv preprint math/9801045*, 1998.

[113] Vladimir Turaev. *Torsions of 3-dimensional manifolds*, volume 208. Birkhäuser, 2002.

[114] Andrei Vesnin. Volumes and normalized volumes of right-angled hyperbolic polyhedra. *Atti del Seminario Matematico e Fisico dell' Università di Modena e Reggio Emilia*, 01 2010.

[115] Andrei Yurievich Vesnin. Three-dimensional hyperbolic manifolds of Löbell type. *Sibirskii Matematicheskii Zhurnal*, 28(5):50–53, 1987.

[116] Edward Witten. Monopoles and four manifolds. *Math. Res. Lett.*, 1:769–796, 1994.

[117] Jonathan Zung. Taut foliations, left-orders, and pseudo-Anosov mapping tori. *arXiv preprint arXiv:2006.07706*, 2020.